AD NUMBER

AD259026

NEW LIMITATION CHANGE

TO

Approved for public release, distribution unlimited

FROM

Distribution authorized to U.S. Gov't. agencies and their contractors; Administrative/Operational Use; 1 May 1961. Other requests shall be referred to the Naval Research Laboratory, Washington, DC 20375.

AUTHORITY

USNASC ltr, 6 Apr 1977

THIS REPORT HAS BEEN DELIMITED
AND CLEARED FOR PUBLIC RELEASE
UNDER DOD DIRECTIVE 5200.20 AND
NO RESTRICTIONS ARE IMPOSED UPON
ITS USE AND DISCLOSURE.

DISTRIBUTION STATEMENT A

APPROVED FOR PUBLIC RELEASE;
DISTRIBUTION UNLIMITED.

NOTICE: When government or other drawings, specifications or other data are used for any purpose other than in connection with a definitely related government procurement operation, the U. S. Government thereby incurs no responsibility, nor any obligation whatsoever; and the fact that the Government may have formulated, furnished, or in any way supplied the said drawings, specifications, or other data is not to be regarded by implication or otherwise as in any manner licensing the holder or any other person or corporation, or conveying any rights or permission to manufacture, use or sell any patented invention that may in any way be related thereto.

GOODYEAR

GOODYEAR AIRCRAFT CORPORATION

GER- 10052
CODE 25500
DATE May 1, 1961

GOODYEAR

GOODYEAR AIRCRAFT CORPORATION

AKRON, OHIO

THE KITING MOTION OF A MASTED AIRSHIP AS DETERMINED BY ANALYTIC EVALUATION OF WATER MODEL TESTS

Contract NOw 60-029c

MIL & GOVT
BuWeps DLI-302

REVISIONS

REV	DATE	MADE BY	APPD BY	PAGES AFFECTED	REMARKS

13-51 (1-50)M

TABLE OF CONTENTS

INTRODUCTION

The frequency and severity of damage to masted airships caused by kiting requires that an effective means of prevention be sought out. Analysis of the problem requires accurate knowledge of the airship mass and aerodynamic characteristics as well as a realistic knowledge of critical wind gustiness. Due primarily to insufficient and inaccurate data, establishment of these necessary parameters accurately has been at best rather difficult.

With the aim of acquiring better knowledge, two experimental investigations were conducted in the General Development Corporation towing tank. In the first, the steady aerodynamic forces and moments acting on a model of a kiting airship were measured. In the second the motions of a masted airship model, when released from predetermined angles of yaw and pitch, were recorded as a function of time.

It is the purpose of this report, in fulfillment of Contract No. NOw 60-0296C, to analyze these data so that specific recommendations concerning effective means and techniques for the preventation of damage due to kiting may be made.

SUMMARY

To establish the necessary parameters by which the problem of damage due to kiting of a masted airship may be analyzed, data resulting from two experimental investigations utilizing airship models were analyzed. As a result both the aerodynamic and the aerodynamic damping characteristics of a kiting airship were determined with sufficient accuracy to permit a mathematical description of the motions of a kiting airship.

The feasible means by which a reduction of the likelihood of damage due to kiting were reviewed. Having considered each of these schemes, the most promising single solution appeared in the employment of a weight attached to the stern handling lines of the airship. Then, the equations of motion were written and solved on the GEDA electric analogue computer for an airship configured with weights fixed to the airship stern. From the resulting solutions it was concluded that although this anti-kiter design did reduce kiting appreciably, large and impractical weights were required to reduce contact velocities to acceptable values. To remedy this, a redesign of the anti-kiter attachment system which keeps the anti-kiting unit close to the ground was studied. With this modification, both the kiting and the contact velocities were reduced appreciably at all wind speeds with practical anti-kiter weights. Consequently, it was recommended that an anti-kiting unit with the suggested design changes to the attachment system be employed to reduce the likelihood of damage due to kiting of masted airships.

LIST OF SYMBOLS

Geometric

a	-	distance from the bow to the center of buoyancy (ft)
a_1	-	distance from the model bow attachment point to the center of buoyancy (ft)
a_2	-	distance from the model stern attachment point to the center of buoyancy (ft)
b	-	distance from the bow to the landing gears (ft)
c	-	distance from the bow to the stern handling lines (ft)
d	-	distance from the bow to the dynamic center (ft)
h	-	elevation above the ground (ft)
h_m	-	metacentric height (ft)
k	-	radius of gyration about the bow (ft)
$\forall$	-	displaced volume (ft^3)
x	-	distance along x - x axis
y	-	distance along the y - y axis
η	-	distance along the η - η axis

Angular

θ	-	kiting angle (rad)
$\dot{\theta}$	-	kiting velocity (rad/sec)
$\ddot{\theta}$	-	kiting acceleration (rad/sec^2)
θ_o	-	static trim angle (rad)
θ_i	-	initial model kiting release angle (rad or degrees)
ψ	-	yaw angle (rad)
$\dot{\psi}$	-	yawing velocity (rad/sec)

LIST OF SYMBOLS - continued

Angular (continued)

$\ddot{\psi}$ - yawing acceleration (rad/sec^2)

ψ_i - initial model yaw release angle (rad or degrees)

χ - wind shift angle (rad)

$\dot{\chi}$ - wind shift velocity (rad/sec)

χ_i - equivalent sudden wind shift (rad or degrees)

ϕ - roll angle (rad)

δ_e - elevator deflection (degrees) (up-positive)

ω - angular velocity (rad/sec)

Mooring Loads

M_x - axial mast reaction (lb)

M_y - transverse mast reaction (lb)

M_z - vertical mast reaction (lb)

P - anti-kiter attachment line loads (lb)

R - wheel reaction (lb)

R_1 thru R_5 - water model balance system reactions (lb)

Aerodynamic forces, moments and coefficients

X - axial force (lb)

Y - transverse force (lb)

Z - vertical force (lb)

LIST OF SYMBOLS - continued

Aerodynamic forces, moments and coefficients (continued)

M	-	kiting moment (ft-lb)
N	-	yawing moment (ft-lb)
F	-	zonal force (lb)
C_x	-	axial force coefficient ($C_x = X/_{2q}\ \forall^{2/3}$)
C_y	-	transverse force coefficient ($C_y = Y/_{2q}\ \forall^{2/3}$)
C_z	-	vertical force coefficient ($C_z = Z/_{2q}\ \forall^{2/3}$)
C_m	-	kiting moment coefficient ($C_m = M/_{2q}\ \forall$)
C_n	-	yawing moment coefficient ($C_n = N/_{2q}\ \forall$)
C_F	-	zonal force coefficient ($C_F = \dfrac{dF/dx}{\rho\ \omega\ x^2 y}$)

Miscellaneous

t	-	time (sec)
τ	-	time ratio
λ	-	length ratio
g	-	acceleration due to gravity (ft/sec^2)
ρ	-	density of immersion fluid (# sec^2/ft^4)
σ	-	fluid density ratio
V_{200}	-	prevailing wind speed measured at 200 ft elevation (knots)
V_{75}	-	prevailing wind speed measured at 75 ft elevation (knots)
v	-	model towing speed (ft/sec)
q	-	dynamic pressure (lb/ft^2)
U_v	-	vertical component of contact velocity (ft/sec)
U_a	-	transverse component of contact velocity (ft/sec)

LIST OF SYMBOLS - continued

Miscellaneous - continued

W - basic equilibrium design gross weight (lbs)

W_{SH} - airship heaviness (lb)

I - mass moment of inertia about the mooring attachment point (ft-lb-sec^2)

C_I - moment of inertia coefficient ($C_I = I/\rho\ V^{5/3}$)

AKM - anti kiting moment (ft lb)

K - correction factor

μ - absolute viscosity (lb sec/ft^2)

GEDA Computer Symbols


Resistor


Capacitor

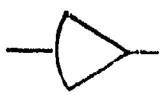
Operational Amplifier
(No Feed Back Component)


Sign Change


Coefficient Potentiometer
(Bottom of Pot, Grounded)

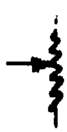
Voltage Divider
(Both Ends of Pot Open)

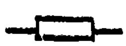
Limiter

GEDA Computer Symbols (continued)

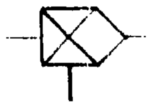
Electronic Multiplier

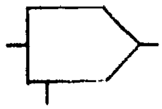
Diode Function Generator


Ground


Constant Multiplier

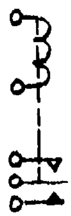
Relay Coil

Relay

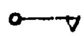 Normally Open Contact

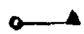 Normally Closed Contact


Switch

Hand Sw. - Handswitch

"H.-O." Sw - Open In Hold and I.C.
- Closed in Operate

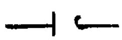
Diode

Interconnection, N = Number
(All Connections with Same Number are Hooked Together)

LIST OF FIGURES

LIST OF FIGURES - continued

LIST OF FIGURES - continued

I DISCUSSION

A. The Kiting Phenomenon

An airship moored at the bow and free to swing about the mast is highly stable and will point directly into any steady wind. Any shifting of the prevailing wind sets up a yaw angle which produces aerodynamic forces which cause the airship to weathervane and tends to kite the airship as well. If the wind shift is slow enough, the airship will weathervane without appreciable lag, and kiting will not occur. It is only when the wind shifts at a rate much faster than the airship is able to follow that kiting occurs.

If the maximum yaw angle experienced is less than one hundred thirty degrees, the kiting angle, kiting velocity, yawing velocity, metacentric moment, and static heaviness produce anti-kiting moments which oppose the kiting tendency due to yaw and limit the maximum kiting angle. Then as the yaw angle is reduced by weathervaning these anti-kiting moments, damped only by the moment due to the negative kiting velocities, force the airship to the ground.

If the maximum yaw angle experienced is more than one hundred thirty degrees (a tail-to-wind condition) the kiting tendency due to yaw is augmented by a kiting tendency due to the kiting angle causing the airship to kite to larger angles limited only by damping, metacentric and heaviness moments. Then, once the airship has weathervaned substantially into the wind it is again forced to the ground.

If the wind shifts and velocities are severe enough, high vertical and transverse impact velocities may result on contact with the ground. The kinetic energy accompanying these impact velocities must be absorbed by the landing gear and its supporting structure. When the ultimate capacity of the landing gear is exceeded, kiting damage is incurred.

B. The Prevention of Kiting Damage

In the interest of preventing kiting damage, the following alternatives appear feasible:

1. Application of an anti-kiting moment of a magnitude sufficient to either prevent kiting completely or at least to limit its magnitude to tolerable values for all weather conditions in which the airship is expected to be moored. Some of the means by which this may be attempted are:

   (a) Increase the static heaviness by adding ballast to the car.

   (b) Attach a weight to the stern handling lines leaving the airship free to weathervane by rolling on the ground until the airship kites.

(c) Apply up elevator control

(d) Trim the airship tail-heavy with ballonet.

2. After a kiting peak is reached reduce vertical impact velocities by deflecting the elevator control down.

3. Increase the load capacity of the landing gear and its supporting structure to withstand all impact loads which might be experienced.

4. Moor the airship to a high mast.

The anti-kiting moment applied by adding ballast to the car is limited to something less than the design load capacity of the landing gear. Should kiting occur, static heaviness will reduce the maximum kiting angles experienced, however, once a kiting peak is reached, it serves only to accelerate the airship towards the ground.

As compared to static heaviness, a weight attached to the stern handling lines represents an improved anti-kiting system. First, because the weight which can be added is limited only by the strength of the handling lines and their attachment points. If necessary, these lines may be strengthened without incurring a large weight penalty. Second, because a weight attached to the stern lines has nearly half again as much leverage as does ballast placed in the car and third, should the airship kite, on impact the stern weight will contact the ground shortly before the landing gear. Consequently, the energy due to motion of its mass would not be absorbed by the airship landing gear.

In winds greater than 25 knots, proper use of the elevator controls can be quite effective both to prevent or limit kiting and to reduce impact velocities should kiting occur. By deflecting the elevator full up, kiting can be delayed and reduced. However, in high winds, in order not to impose large sustained loads on the landing gear, the elevator control should not be deflected full up until the airship actually kites. Then, after the maximum kiting angle is attained, by deflecting the elevator full down, the impact velocity on contact with the ground can be reduced. As a result of these considerations, it can be concluded that effective use of the elevator controls requires that they should be manipulated either manually or automatically during kiting. Limited by their ineffectiveness in winds of low intensity, however, the elevator contol is not sufficient in itself to prevent kiting damage. Instead, it should be considered a most valuable aid.

The anti-kiting moment obtained by trimming the airship tail heavy is small. Somewhat similar to the effect of static heaviness, it will reduce the maximum kiting angles, however, after a kiting peak is reached, the tail heavy trim condition accelerates the airship towards the ground.

Although, kiting damage can be eliminated with certainty by increasing the load capacity of the landing gear, the added weight consequental with this modification would detract noticeably from the performance of the airship in flight. The weight penalty may be reduced somewhat by the installation of an auxiliary landing gear which can be removed for flight.

The aerodynamic forces which cause the airship to kite in shifting winds are due basically to ground interference effects. Consequently, by mooring the airship to a high mast, kiting tendencies may be reduced if not eliminated. The kiting which does occur while moored high, moreover, is less likely to result in damage. However, the present utility and mobility of the low mast must be retained. Therefore, a mast of new design (convertible from a low to a high mast) would be necessary.

C. Dynamics of a Kiting Airship

The masted airship has freedom to roll, to kite, and to weathervane. Neglecting any coupling effects of roll, the mooring loads, the kiting, and the weathervaning motions may be described by the following generalized simultaneous differential equations:

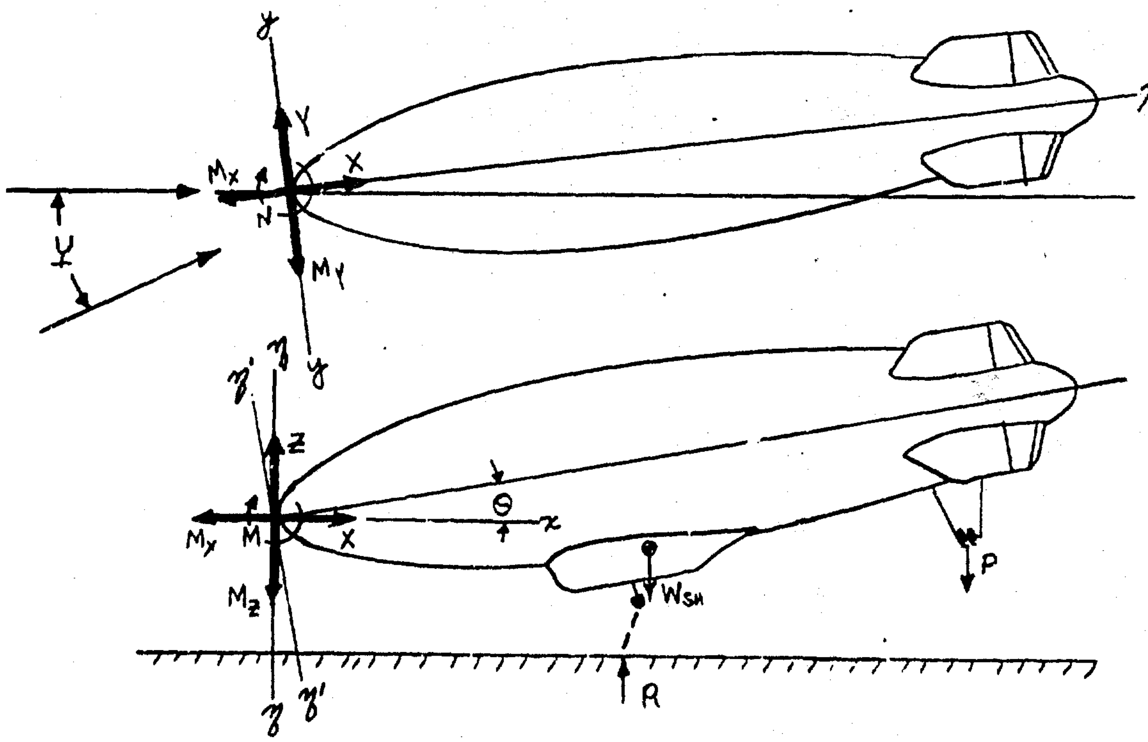

$$\Sigma F_x = \frac{\partial X}{\partial(\dot{\Psi}-\dot{\psi})}(\dot{\Psi}-\dot{\psi}) + \frac{\partial X}{\partial(\Psi-\psi)}(\Psi-\psi) + \frac{\partial X}{\partial\dot{\theta}}(\dot{\theta}) + \frac{\partial X}{\partial\theta}(\theta) - M_X = 0 \qquad (1)$$

$$\Sigma F_y = -\left(\frac{d}{k^2} I_{z\text{-}z}\right)(\ddot{\psi}) + \frac{\partial Y}{\partial(\dot{\Psi}-\dot{\psi})}(\dot{\Psi}-\dot{\psi}) + \frac{\partial Y}{\partial(\Psi-\psi)}(\Psi-\psi) + \frac{\partial Y}{\partial\dot{\theta}}(\dot{\theta}) + \frac{\partial Y}{\partial\theta}(\theta) - M_Y = 0 \qquad (2)$$

$$\Sigma F_z = -\left(\frac{d}{k^2} I_{y\text{-}y}\right)(\ddot{\theta}) + \frac{\partial Z}{\partial\dot{\theta}}(\dot{\theta}) + \frac{\partial Z}{\partial\theta}(\theta) + \frac{\partial Z}{\partial\delta_e}(\delta_e) + \frac{\partial Z}{\partial(\dot{\Psi}-\dot{\psi})}(\dot{\Psi}-\dot{\psi}) + \frac{\partial Z}{\partial(\Psi-\psi)}(\Psi-\psi)$$
$$- P + R - M_z = 0 \qquad (3)$$

$$\Sigma M_{z\text{-}z} = -I_{z\text{-}z}(\ddot{\psi}) + \frac{\partial N}{\partial(\dot{\Psi}-\dot{\psi})}(\dot{\Psi}-\dot{\psi}) + \frac{\partial N}{\partial(\Psi-\psi)}(\Psi-\psi) + \frac{\partial N}{\partial\dot{\theta}}(\dot{\theta}) + \frac{\partial N}{\partial\theta}(\theta) = 0 \qquad (4)$$

$$\Sigma M_{y\text{-}y} = -I_{y\text{-}y}(\ddot{\theta}) + \frac{\partial M}{\partial\dot{\theta}}(\dot{\theta}) + \frac{\partial M}{\partial\theta}(\theta) + \frac{\partial M}{\partial\delta_e}(\delta_e) + \frac{\partial M}{\partial(\dot{\Psi}-\dot{\psi})}(\dot{\Psi}-\dot{\psi}) + \frac{\partial M}{\partial(\Psi-\psi)}(\Psi-\psi) - PC\cos\theta$$
$$- W h_m \sin(\theta-\theta_o) = 0 \qquad (5)$$

If the airship is kiting $R = 0$; if not, $R > 0$ and $\theta = \dot{\theta} = \ddot{\theta} = 0$. The inertia and the aerodynamic characteristics may be expressed in terms of non-dimensional coefficients which are independent of displaced volume, wind speed, and fluid density as follows:

$$I_{y\text{-}y} = C_{I_{y\text{-}y}}\,\rho\,\forall^{5/3}$$

$$I_{z\text{-}z} = I_{z'\text{-}z'}\cos^2\theta + I_{x\text{-}x}\sin^2\theta = \left(C_{I_{z'\text{-}z'}}\cos^2\theta + C_{I_{x\text{-}x}}\sin^2\theta\right)\rho\,\forall^{5/3} = C_{I_{z\text{-}z}}\,\rho\,\forall^{5/3}$$

$\frac{\partial X}{\partial(\dot{\Psi}-\dot{\psi})} = C_{X_{\dot{\psi}}}\rho v \forall$	$\frac{\partial Y}{\partial(\dot{\Psi}-\dot{\psi})} = C_{Y_{\dot{\psi}}}\rho v \forall$	$\frac{\partial Z}{\partial(\dot{\Psi}-\dot{\psi})} = C_{Z_{\dot{\psi}}}\rho v \forall$	$\frac{\partial M}{\partial(\dot{\Psi}-\dot{\psi})} = C_{M_{\dot{\psi}}}\rho v \forall^{4/3}$	$\frac{\partial N}{\partial(\dot{\Psi}-\dot{\psi})} = C_{N_{\dot{\psi}}}\rho v \forall^{4/3}$
$\frac{\partial X}{\partial\dot{\theta}} = C_{X_{\dot{\theta}}}\rho v \forall$	$\frac{\partial Y}{\partial\dot{\theta}} = C_{Y_{\dot{\theta}}}\rho v \forall$	$\frac{\partial Z}{\partial\dot{\theta}} = C_{Z_{\dot{\theta}}}\rho v \forall$	$\frac{\partial M}{\partial\dot{\theta}} = C_{M_{\dot{\theta}}}\rho v \forall^{4/3}$	$\frac{\partial N}{\partial\dot{\theta}} = C_{N_{\dot{\theta}}}\rho v \forall^{4/3}$
$\frac{\partial X}{\partial(\Psi-\psi)} = C_{X_{\psi}}\rho v^2 \forall^{2/3}$	$\frac{\partial Y}{\partial(\Psi-\psi)} = C_{Y_{\psi}}\rho v^2 \forall^{2/3}$	$\frac{\partial Z}{\partial(\Psi-\psi)} = C_{Z_{\psi}}\rho v^2 \forall^{2/3}$	$\frac{\partial M}{\partial(\Psi-\psi)} = C_{M_{\psi}}\rho v^2 \forall$	$\frac{\partial N}{\partial(\Psi-\psi)} = C_{N_{\psi}}\rho v^2 \forall$
$\frac{\partial X}{\partial\theta} = C_{X_{\theta}}\rho v^2 \forall^{2/3}$	$\frac{\partial Y}{\partial\theta} = C_{Y_{\theta}}\rho v^2 \forall^{2/3}$	$\frac{\partial Z}{\partial\theta} = C_{Z_{\theta}}\rho v^2 \forall^{2/3}$	$\frac{\partial M}{\partial\theta} = C_{M_{\theta}}\rho v^2 \forall$	$\frac{\partial N}{\partial\theta} = C_{N_{\theta}}\rho v^2 \forall$
		$\frac{\partial Z}{\partial\delta_e} = C_{Z_{\delta_e}}\rho v^2 \forall^{2/3}$	$\frac{\partial M}{\partial\delta_e} = C_{M_{\delta_e}}\rho v^2 \forall$	

Substituting these values into equations (1) thru (5) and dividing thru by the moments of inertia we have:

$$-\ddot{\psi}+\left[C_{N_{\dot{\psi}}}(\dot{\Psi}-\dot{\psi})+C_{N_{\dot{\theta}}}\dot{\theta}\right]\left[\frac{V}{\Psi^{2/3}C_{I_{z\cdot z}}}\right]+\left[C_{N_{\psi}}(\Psi-\psi)+C_{N_{\theta}}\theta\right]\left[\frac{V^{2}}{\Psi^{2/3}C_{I_{z\cdot z}}}\right]=0 \qquad (6)$$

$$-\ddot{\theta}+\left[C_{M_{\dot{\theta}}}\dot{\theta}+C_{M_{\dot{\psi}}}(\dot{\Psi}-\dot{\psi})\right]\left[\frac{V}{\Psi^{2/3}C_{I_{y\cdot y}}}\right]+\left[C_{M_{\theta}}\theta+C_{M_{\psi}}(\Psi-\psi)+C_{M_{\delta_e}}\delta_e\right]\left[\frac{V^{2}}{\Psi^{1/3}C_{I_{y\cdot y}}}\right]-\frac{Pc\cos\theta}{\rho\Psi^{5/3}C_{I_{y\cdot y}}}-\frac{Wh_{a}\sin(\theta-\theta_{a})}{\rho\Psi^{5/3}C_{I_{y\cdot y}}}=0 \qquad (7)$$

$$M_x=\rho\Psi^{2/3}\left\{\left[C_{X_{\dot{\psi}}}(\dot{\Psi}-\dot{\psi})+C_{X_{\dot{\theta}}}\dot{\theta}\right]V\Psi^{1/3}+\left[C_{X_{\psi}}(\Psi-\psi)+C_{X_{\theta}}\theta\right]V^{2}\right\} \qquad (8)$$

$$M_Y=\rho\Psi^{2/3}\left\{-C_{I_{z\cdot z}}\frac{d\Psi}{h^{2}}\ddot{\psi}+\left[C_{Y_{\dot{\psi}}}(\dot{\Psi}-\dot{\psi})+C_{Y_{\dot{\theta}}}\dot{\theta}\right]V\Psi^{1/3}+\left[C_{Y_{\psi}}(\Psi-\psi)+C_{Y_{\theta}}\theta\right]V^{2}\right\} \qquad (9)$$

$$M_Z=\rho\Psi^{2/3}\left\{-C_{I_{y\cdot y}}\frac{d\Psi}{h^{2}}\ddot{\theta}+\left[C_{Z_{\dot{\psi}}}(\dot{\Psi}-\dot{\psi})+C_{Z_{\dot{\theta}}}\dot{\theta}\right]V\Psi^{1/3}+\left[C_{Z_{\psi}}(\Psi-\psi)+C_{Z_{\theta}}\theta+C_{Z_{\delta_e}}\delta_e\right]V^{2}+\right.$$

$$\left.R-P\cos\theta\right\} \qquad (10)$$

With accurate knowledge of the mass and aerodynamic characteristics, solution of these simultaneous differential equations yields a time history of the motion, angular velocities, and angular accelerations experienced by a mast moored airship for selected kiting conditions. From these time histories, then, the vertical and transverse components of contact velocity may be observed for any anti-kiting scheme being considered.

II ANALYSIS

A. Geometric & Inertia Characteristics

The model used to measure the force and moment coefficients reported in reference 1, the model used to measure the motions of a kiting airship model as reported in reference 2, and the ZPG-2/2W/3W airships have the following pertinent mass and geometric characteristics:

Characteristics	1/75 Scale ZPN-1 Water Model(Ref.1)	1/75 Scale ZPN-2 Water Model(Ref.2)	ZPG-2/2W	ZPG-3W
a	2.03	2.14	157.9	185.6
a_1	2.27	2.71	-	-
a_2	2.50	-	-	-
b	-	-	150.0	187.0
c	-	-	290.0	344.0
d	-	2.20	162	193
h_m	-	0	29.0	26.3
I_M	-	42.76	143×10^6	308×10^6
I_N	-	$(42.76 \cos^2\theta + .82 \sin^2\theta)$	$(143 \cos^2\theta + 2.78 \sin^2\theta)10^6$	$[308 \cos^2\theta + 5.45 \sin^2\theta]10^6$
W	-	150.5	64,000	112,000
k		2.34	176.5	207

B. Aerodynamic Characteristics of a Kiting Airship

The motion of a kiting airship is caused by moments produced by aerodynamic pressure forces acting on it. Since the kiting airship is free to yaw, to kite, and to roll, knowledge of the changes which take place in these moments as a function of each degree of freedom is necessary. An experimental investigation of the aerodynamic characteristics of a kiting airship was conducted in the General Development Corporation towing basin using a 1/75th scale model of the ZPN-1 airship. Tests were run at yaw angles ranging from 0 to 180 degrees and at pitch angles ranging from 0 to 60 degrees with the elevator set neutral, 5, and 15 degrees up. The resulting data expressed in the form of calculated force and moment coefficients were reported in reference 1. A schematic diagram of the model test set up is shown below:

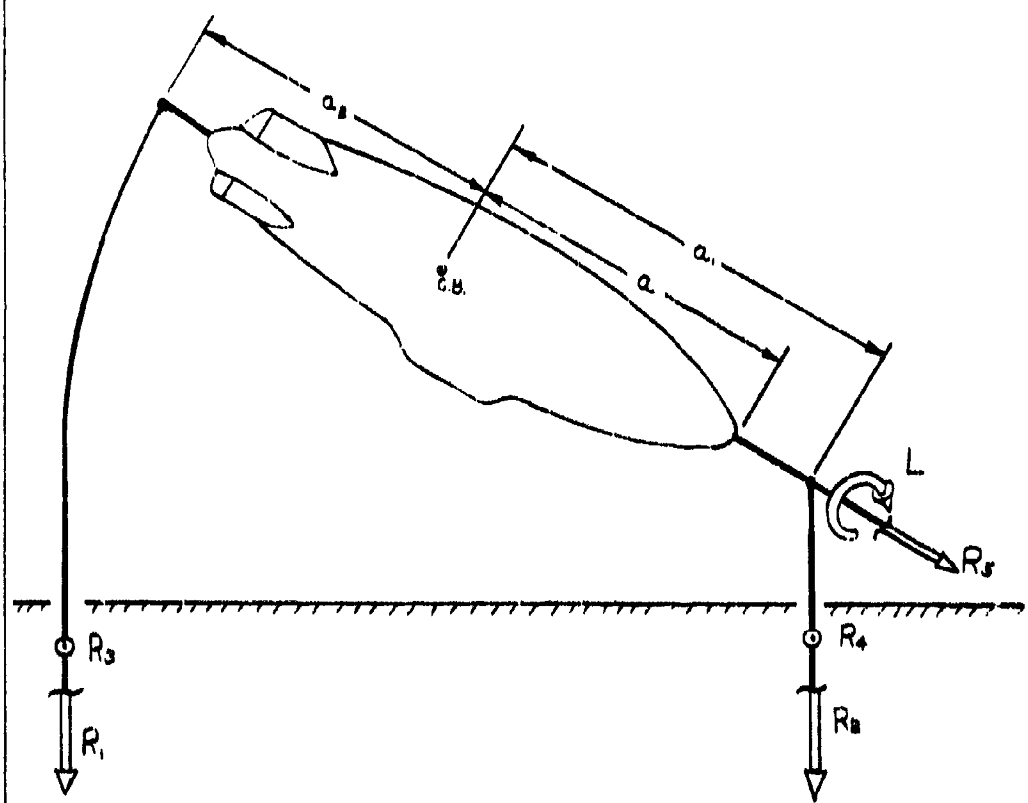

The axial force coefficient, $C_x = \frac{X}{\rho V^2 \forall^{2/3}} = \frac{R_3 \cos\theta}{\rho V^2 \forall^{2/3}}$ (11)

The transverse force coefficient, $C_Y = \frac{Y}{\rho V^2 \forall^{2/3}} = \frac{R_3 + R_4}{\rho V^2 \forall^{2/3}}$ (12)

The vertical force coefficient, $C_Z = \frac{Z}{\rho V^2 \forall^{2/3}} = \frac{R_1 + R_2 + R_3 \sin\theta}{\rho V^2 \forall^{2/3}}$ (13)

The kiting moment coefficient, $C_M = \frac{M}{\rho V^2 \forall} = \frac{(a + a_2) R_1}{\rho V^2 \forall}$ (14)

The weathervaning moment coefficient $C_N = \frac{N}{\rho V^2 \forall} = \frac{(a + a_2) R_3 + L \sin\theta}{\rho V^2 \forall}$ (15)

The force and moment coefficients reported in reference 1 are given in terms of coefficients at the center of buoyancy calculated as follows:

The cross force coefficient, $C_y = \frac{R_3 + R_4}{q \forall^{2/3}}$ (16)

The lift coefficient, $C_z = \frac{R_1 + R_2}{q \forall^{2/3}}$ (17)

The rolling moment coefficient, $C_l = \frac{L}{q \forall}$ (18)

The pitching moment coefficient, $C_m = \frac{R_1 a_2 - R_2 a_1}{q \forall}$ (19)

The yawing moment coefficient, $C_n = \frac{R_3 a_2 - R_4 a_1}{q \forall}$ (20)

Solving these equations for R_1, R_2, and R_3 and substituting these values into equations (11) thru (1) the forces and moments at the bow are:

$$C_x = \frac{R_3 \cos\theta}{2 q \forall^{2/3}} \quad (21)$$

$$C_Y = \frac{C_y}{2} \quad (22)$$

$$C_Z = \frac{C_z}{2} + \frac{R_3 \sin\theta}{2 q \forall^{2/3}} \quad (23)$$

$$C_M = \frac{1}{2}\left(\frac{a}{\forall^{1/3}} C_z - C_m\right)\left(\frac{a + a_2}{a_1 + a_2}\right) = .755\, C_z - .475\, C_m \quad (24)$$

$$C_N = \frac{1}{2}\left[\frac{a}{\forall^{1/3}} C_y - C_n + C_l \sin\theta\right]\left[\frac{a + a_2}{a_1 + a_2}\right] = .755\, C_y - .475(C_n - C_l \sin\theta) \quad (25)$$

Neither R_5 nor coefficients based on R_5 were reported in reference 1. Therefore numerical values of C_x and C_z cannot be established from these data. Utilizing the data reported in reference 1, numerical calculations of equations 22, 24, and 25 were made. The results were plotted vs the yaw angle at constant pitch angles, then crossplotted. Both the plots and cross plots were faired smooth and orderly to minimize the effects of test inaccuracies. The resulting curves are plotted on figure 1 and 2. With kiting restrained ($\Theta = 0$), the kiting moment coefficients are positive at all yaw angles. With $\psi = 0$, the kiting moments are negative for the entire range of pitch angles tested. As the yaw angle increases, the negative kiting moments due to pitch decrease becoming zero at $\psi = 133^\circ$ then become positive at the higher yaw angles. The weathervaning moment coefficients are always positive proving that an airship moored at the bow is highly stable and will point directly into any steady wind.

The model was towed at a speed of 1.75 ft/sec at all yaw angles except $\psi = 90^\circ$ where the towing velocity was 1.18 ft/sec. The Reynolds numbers associated with these test conditions were nearly identical with Reynolds Numbers developed while testing the 1/75 scale dynamic airship model. However, the possibility of extrapolating these results to the Reynolds Numbers of an airship moored in high winds must be investigated. As most of the tests were made at only one towing speed, a direct extrapolation is not possible. However, by examining the nature of the flow, for any critical changes throughout the range of Reynolds Numbers involved, we may determine the maximum wind speeds for which these data are applicable.

We may consider the flow pattern over the airship as divided into a flow pattern due to flow along the longitudinal axis and one due to flow transverse to longitudinal axis. The flow pattern due to flow along the longitudinal axis is similar to the flow patterns experienced during airship take-off runs and landing roll outs. Analysis of drag coefficients during these maneuvers indicate that there are no marked transitions in the flow pattern over the range of Reynolds Numbers being considered. The flow pattern due to flow transverse to the longitudinal axis is similar to the flow patterns of circular cylinders in normal flow. Two stable types of flow over circular sections may occur with the transition occuring at Reynolds Numbers between 400,000 and 500,000 based on the cross section diameter. The maximum model Reynolds Number based on the maximum cross sectional diameter was only 120,000 which is less than critical. Based on the maximum cross sectional diameter of the airship, the transverse flow becomes supercritical at wind speeds of approximately one-half knot. Therefore, the flow over the model will not, in general, be similar to the flow over an airship, and the numerical values of the force and moment coefficients may be somewhat in error at yaw angles, near 90°. As the flow pattern due to the transverse components of the wind velocity at or above critical Reynolds Numbers is characterized by delayed separation with an associated drag reduction as compared to the flow patterns at less than critical Reynolds Numbers, it is expected that the force and moment coefficients at yaw angles near 90° will be somewhat less than those shown on Figures 1 and 2.

C. Aerodynamic Damping Characteristics of a Kiting Airship

To simulate the motion of a kiting airship it is required that the yaw and kiting angles of the model be the same as those of the airship. Where the prime (') designates the model characteristics,

we have: $\Theta = \Theta'$, $\Theta_0 = \Theta_0'$, $\psi = \psi'$, $\Upsilon = \Upsilon'$

let: $\frac{t}{t'} = \tau$ and $\left(\frac{\Psi}{\Psi'}\right)^{1/3} = \lambda$

then: $\frac{d\theta}{dt} = \frac{d\theta'}{d\tau t'} = \frac{1}{\tau}\frac{d\theta'}{dt'}$ or $\dot\theta = \frac{1}{\tau}\dot\theta'$

and, $\frac{d\dot\theta}{dt} = \frac{1}{\tau}\frac{d\dot\theta'}{dt} = \frac{1}{\tau^2}\frac{d\dot\theta'}{dt'}$ or $\ddot\theta = \frac{1}{\tau^2}\ddot\theta'$

similarly, $\dot\psi = \frac{1}{\tau}\dot\psi'$, $\ddot\psi = \frac{1}{\tau^2}\ddot\psi'$, and $\dot\Upsilon = \frac{1}{\tau}\dot\Upsilon'$

Substituting these values for Θ, ψ, Υ, and their derivatives with respect to time into equations (6) and (7) and multiplying thru by τ^2 we have:

$$-\ddot\psi' + \tau\left(\frac{C_{n\dot\psi}}{C_{I_{y-y}}}\right)\left(\frac{V}{\Psi^{1/3}}\right)(\dot\Upsilon'-\dot\psi') + \tau^2\left(\frac{C_{n\psi}}{C_{I_{y-y}}}\right)\left(\frac{V}{\Psi^{1/3}}\right)^2(\Upsilon'-\psi') + \tau\left(\frac{C_{n\dot\theta}}{C_{I_{y-y}}}\right)\left(\frac{V}{\Psi^{1/3}}\right)(\dot\theta')$$
$$+\tau^2\left(\frac{C_{n\theta}}{C_{I_{y-y}}}\right)\left(\frac{V}{\Psi^{1/3}}\right)^2(\theta') = 0 \qquad (26)$$

$$-\ddot\theta' + \tau\left(\frac{C_{m\dot\theta}}{C_{I_{y-y}}}\right)\left(\frac{V}{\Psi^{1/3}}\right)(\dot\theta') + \tau^2\left(\frac{C_{m\theta}}{C_{I_{y-y}}}\right)\left(\frac{V}{\Psi^{1/3}}\right)^2(\theta') + \tau^2\left(\frac{C_{m\psi}}{C_{I_{y-y}}}\right)\left(\frac{V}{\Psi^{1/3}}\right)^2(\Upsilon'-\psi') + \tau^2\left(\frac{C_{m\delta_e}}{C_{I_{y-y}}}\right)\left(\frac{V}{\Psi^{1/3}}\right)^2(\delta_e')$$
$$+\tau\left(\frac{C_{m\dot\psi}}{C_{I_{y-y}}}\right)\left(\frac{V}{\Psi^{1/3}}\right)(\dot\Upsilon'-\dot\psi') - \tau^2\left(\frac{PC\cos\Theta'}{C_{I_{y-y}}\rho\Psi^{4/3}}\right) - \tau^2\left(\frac{W h_m \sin(\Theta'-\Theta_0')}{C_{I_{y-y}}\rho\Psi^{4/3}}\right) = 0 \qquad (27)$$

Writing these equations for the model, however, we have:

$$-(\ddot\psi') + \left(\frac{C'_{n\dot\psi}}{C'_{I_{y-y}}}\right)\left(\frac{V'}{\Psi'^{1/3}}\right)(\dot\Upsilon'-\dot\psi') + \left(\frac{C'_{n\psi}}{C'_{I_{y-y}}}\right)\left(\frac{V'}{\Psi'^{1/3}}\right)^2(\Upsilon'-\psi') + \left(\frac{C'_{n\dot\theta}}{C'_{I_{y-y}}}\right)\left(\frac{V'}{\Psi'^{1/3}}\right)(\dot\theta') + \left(\frac{C'_{n\theta}}{C'_{I_{y-y}}}\right)\left(\frac{V'}{\Psi'^{1/3}}\right)^2(\theta') = 0 \qquad (28)$$

$$-(\ddot\theta') + \left(\frac{C'_{m\dot\theta}}{C'_{I_{y-y}}}\right)\left(\frac{V'}{\Psi'^{1/3}}\right)(\dot\theta') + \left(\frac{C'_{m\theta}}{C'_{I_{y-y}}}\right)\left(\frac{V'}{\Psi'^{1/3}}\right)^2(\theta') + \left(\frac{C'_{m\psi}}{C'_{I_{y-y}}}\right)\left(\frac{V'}{\Psi'^{1/3}}\right)^2(\Upsilon'-\psi') + \left(\frac{C'_{m\delta_e}}{C'_{I_{y-y}}}\right)\left(\frac{V'}{\Psi'^{1/3}}\right)^2(\delta_e')$$

$$+\left(\frac{C'_{m\dot\psi}}{C'_{I_{y-y}}}\right)\left(\frac{V'}{\Psi'^{1/3}}\right)(\dot\Upsilon'-\dot\psi') + \left(\frac{P'C'\cos\Theta'}{C'_{I_{y-y}}\rho'\Psi'^{4/3}}\right) + \frac{W'h'_m\sin(\Theta'-\Theta_0')}{C'_{I_{y-y}}\rho'\Psi'^{4/3}} = 0 \qquad (29)$$

Comparing equation (26) with (28) and (27) with (29), it follows that for similitude of motion, the coefficients of those differential equations must have the same value for the airship and for the model. It is most convenient to set $(\lambda \mathcal{V}'/\tau \mathcal{V}) = 1$ by letting $\tau = 1$ and $\mathcal{V}/\mathcal{V}' = \lambda$. By symmetry $C_{I'_{y-y}} = C_{I'_{z-z}}$. Then letting $(\rho/\rho') = \sigma$, the laws of similitude are defined by:

$$\left[\frac{C_{N\dot\psi}}{C'_{N\dot\psi}} = \frac{C_{N\dot\phi}}{C'_{N\dot\phi}} = \frac{C_{M\dot\theta}}{C'_{M\dot\theta}} = \frac{C_{M\dot\psi}}{C'_{M\dot\psi}} = \frac{C_{N\psi}}{C'_{N\psi}} = \frac{C_{N\theta}}{C'_{N\theta}} = \frac{C_{M\theta}}{C'_{M\theta}} = \frac{C_{M\psi}}{C'_{M\psi}} = \frac{C_{M\delta_e}\,\delta_e}{C'_{M\delta_e}\,\delta'_e}\right] = \left[\frac{C_{I_{z-z}}}{C'_{I_{z-z}}} = \frac{C_{I_{y-y}}}{C'_{I_{y-y}}}\right] \quad (30)$$

$$\text{and} \quad \frac{P c}{P' c'} = \frac{W h_m}{W' h'_m} = \sigma \lambda^4 \left(\frac{C_{I_{y-y}}}{C'_{I_{y-y}}}\right) \quad (31)$$

The first equation (30) may be satisfied by simply requiring that the model be geometrically similar, that the Reynolds Number effect be accountable, and that the distribution of mass be somewhat similar.

As reported in reference 2, the 1/75th scale water model of the ZPN-2 airship was tested in an inverted position. Consequently, the effects of hydrostatic heaviness (W'_{SH}), hydrostatic stability ($W' h'_m$), static trim (Θ'_o) and a stern weight (P') are opposite to that of a model tested in an upright position, and to simulate static heaviness by static lightness, etc would distort the ratio of these static effects to the mass effects. Therefore, it was necessary that the model floated in static equilibrium ($W_{SH}' = 0$ and $W' = W/\sigma\lambda^3$), that the center of gravity and the center of buoyancy coincided on the longitudinal axis ($\Theta'_o = 0$ and $h'_m = 0$), and that the stern weight was removed ($P' = 0$). The model was moored by a boom extending 4.5 inches or approximately 8% of the model length forward of the bow. By assuming an additional mass equal to the physical mass, the virtual moment of inertia coefficient of the model was:

$$C'_{I_{Bow}} = \frac{2 I'}{\rho' \mathcal{V}'^{5/3}} = 5.45 \text{ about the bow}$$

$$\text{and} \quad C'_I = \left(C'_{I_{Bow}} + \frac{d_1^2 - d_2^2}{\mathcal{V}'^{2/3}}\right) = 7.48 \text{ about the mooring point.}$$

For similitude, the model should have been tested upright, the metacentric height (h') should have been to scale with the airship, the model should have been moored at the bow, and the virtual moment of inertia coefficient about the bow should have been identical to that of the ZPN-2 airship ($\text{e.i.}\ C'_{I_{Bow}} = C_{I_{Bow}} = 2I/\rho \mathcal{V}^{5/3} = 6.90$). Because of these dissimilarities, the angular motions of the motions of the model were not the same as the motions of a kiting airship in static trim and equilibrium. To correct for these dissimilarities, and because of the need for a method by which the merit of various anti-kiting schemes may be evaluted, making the simplifying assumption that the aerodynamic loads are such that they depend on the instantaneous position and motion of the airship and not on how it displaced into that position, the data reported in reference 2 was used to predict the magnitude of the rotary damping characteristics in order that the equation of motion for a kiting airship may be written, modified to account for the anti-kiting scheme being considered, then solved for the resulant motions as affected by selected atmospheric disturbances; an explanation follows:

The data reported in reference 2 simulated the effect of a sudden wind shift by towing the model at a steady speed, then releasing it from initial selected angles of yaw and pitch, and allowing the model to kite and weathervane freely while these angular motions were recorded. Comparing the nomenclature used to present the data with the nomenclature used in the generalized equations of motion it is seen that $\psi' = (\Psi - \psi)$, $\dot{\psi}' = (\dot{\Psi} - \dot{\psi})$, and $\ddot{\psi}' = -\ddot{\psi}$ as stated above, $\theta' = h' = P' = 0$. Substituting these into equations (6) and (7) the equations of motion for the model with the elevator held neutral ($\delta e = 0$) reduce to:

$$\ddot{\psi}' + \left(\frac{C'_{N\dot{\psi}}\, v'}{C'_{N_I}\, \forall'^{1/3}}\right)\dot{\psi}' + \left(\frac{C'_{N\dot{\theta}}\, v'}{C'_{N_I}\, \forall'^{1/3}}\right)\dot{\theta}' + \left(\frac{C_N'\, v'^2}{C'_{N_I}\, \forall'^{2/3}}\right) = 0 \qquad (32)$$

$$-\ddot{\theta}' + \left(\frac{C'_{M\dot{\theta}}\, v'}{C'_{M_I}\, \forall'^{1/3}}\right)\dot{\theta}' + \left(\frac{C'_{M\dot{\psi}}\, v'}{C'_{M_I}\, \forall'^{1/3}}\right)\dot{\psi}' + \left(\frac{C_M'\, v'^2}{C'_{M_I}\, \forall'^{2/3}}\right) = 0 \qquad (33)$$

and

$$\theta' \cong 0 \qquad (34)$$

where: $C'_{M_I} = 7.48$, $C'_{N_I} = 7.48 \cos^2\theta' + .11 \sin^2\theta'$, $\forall' = 2.31$, and $v' = .5, 1.0,$ and 1.6 ft/sec.

The weathervaning and the kiting moment coefficients (C_N' and C_M') may be expressed in terms of the force data measured used to calculate the force and moment coefficients presented in reference 1 as follows:

$$C_N' = \frac{N'}{\rho v'^2 \forall} = \frac{\left[\left(\frac{\forall'}{\forall}\right)^{1/3} a_1' + a_2\right] R_3 + L \sin\theta}{\rho v'^2 \forall} \qquad (35)$$

$$C_M' = \frac{M'}{\rho v'^2 \forall} = \frac{\left[\left(\frac{\forall'}{\forall}\right)^{1/3} a_1' + a_2\right] R_1}{\rho v'^2 \forall} \qquad (36)$$

By substituting the force and moment coefficients for R_1 and R_3 as defined by equations (16) thru (20) we have:

$$C_N' = \frac{1}{2}\left[\left(\frac{\forall^{1/3} a_1'}{\forall^{1/3}} C_y - C_m\right) + C_\ell \sin\theta\right]\left(\frac{a_1' + a_2}{a_1 + a_2}\right)$$

$$C_N' = \frac{1}{2}\left[\left(\frac{1.32 \times 2.71}{1.28^2} C_y - C_m\right) + C_\ell \sin\theta\right]\left(\frac{2.71 + 2.50}{2.27 + 2.50}\right)$$

$$C_N' = 1.19 C_y - .546 (C_m - C_\ell \sin\theta) \tag{37}$$

$$C_M' = \frac{1}{2}\left[\frac{\forall^{1/3} a_1'}{\forall^{1/3}} C_y - C_m\right]\left(\frac{a_1' + a_2}{a_1 + a_2}\right)$$

$$C_M' = \frac{1}{2}\left[\frac{1.32 \times 2.71}{1.28^2} C_y - C_m\right]\left(\frac{2.71 + 2.50}{2.27 + 2.50}\right)$$

$$C_M' = 1.19 C_y - .546 C_m \tag{38}$$

Numerical calculations of equations (37) and (38) were made. The results were plotted, crossplotted, and faired smooth as shown on figure 3.

Now, with reference to equations (32) and (33), it is seen that there remains four unknown damping coefficients $C_{N\dot\psi}$, $C_{N\dot\theta}$, $C_{M\dot\theta}$, and $C_{M\dot\psi}$. Each of these non-dimensional coefficients are functions of undetermined form and may be dependent on the non-dimensional variables (ψ and θ) or the dimensionless group of variables (RN = $\rho V \forall^{1/3}/\mu$). The Reynolds Numbers for these tests were nearly identical with the Reynolds Numbers developed while measuring the static aerodynamic characteristics. Therefore, in the two differential equations there remains in effect eight unknowns. Solution of these unknown coefficients lies in establishing a relationship between the two simultaneous differential equations (32 & 33) and the motions of the 1/75th scale water model of a kiting airship as presented in reference 2. For any one test, an infinite number of solutions exist. The most convenient solutions, are ones which are not only simple but ones which satisfy a large number of individual tests as well. Before such solutions can be effected, however, familarity with the implications of assigning arbitrary values to any of the unknowns must be gained - otherwise agreement with the data would be at best only a highly improbable coincidence. Simplicity was attained by restracting the assigned values first to zero; then constant; then varying linearly, as a quadratic,as a cubic etc. The most advantageous procedure for evaluating these unknown functions lies in arranging the order in which the data is analyzed such that the number of variables which must be investigated at one time is reduced by selecting data which contained only one unknown coefficient as a function of one non-dimensional variable. This procedure was then repeated, where possible, for each of the remaining variables in turn.

The characteristics, equations (32 and 33), were set up on a GEDA electric analogue computer which is effectively a dissimilar model of the mechanical system duplicated in electric current. The elements in the computer electrical circuitry which simulated the unknown damping coefficients ($C'_{N\dot\psi}$, $C'_{N\dot\theta}$, $C_{M\dot\theta}$, and $C'_{M\dot\psi}$) were set up such that the values of these coefficients were readily adjustable. Then, data was selected in which the model weathervaned but did not kite substantially. (Reference 2, Appendix Volume II, page 52; and Appendix Volume III, pages 91, 111, and 116). Thus $\theta' = \dot\theta' = \ddot\theta' = 0$ and equation 32 reduces to:

$$\ddot\psi' + \frac{C'_{N\dot\psi}\, V'}{C'_{N_z}\, \psi'_3}\,\dot\psi' + \frac{C'_{N}\, V'^2}{C'_{N_z}\, \psi' K_3} = 0 \qquad (39)$$

This differential equation containing one unknown coefficient $C'_{N\dot\psi}\,\rho(\psi')$ was solved for ψ' using the GEDA electric analogue computer equipped with an (X-Y) plotter for arbitrary constant values of $C'_{N\dot\psi}\,\rho(\psi')$ and compared with the data for each of these tests. An example of this procedure is shown by the comparison of the data with the GEDA traces as plotted on figure 4.

With reference to the upper plot on figure 4, it is seen that yaw angle ψ' calculated with $C'_{N\dot\psi}\,\rho(\psi) = 4$ satisfies the data quite well at the higher yaw angles, but at the lower yaw angles the damping was nearly critical. Subsequently, trial and error solutions were made with $C'_{N\dot\psi}\,\rho(\psi)$ varying between 4 and 8 with ψ to the first, second, and third degree. From this it was concluded that $C'_{N\dot\psi}\,\rho(\psi)$ varied with (ψ') to approximately the third degree as shown by the center plot on figure 4. An example of the accuracy with which this function satisfied the data is shown on the lower plot of figure 4.

When $\theta' = \dot\theta' = \ddot\theta' = 0$ equation 33 reduces to:

$$C_{M\dot\psi}\,\rho(\psi) = \frac{C'_M\, V'}{\dot\psi'\, \psi K_3} \qquad (40)$$

Then, using the functions just derived to determine ψ as a function of time, the GEDA electric analogue computer was set up to make direct solutions of equations (40) for initial yaw angles which did not produce substantial kiting. The results are shown on the upper plot of figure 5. When a model was released from an initial yaw angle, time was required for the model to accelerate to a finite angular velocity; thus, when $\psi' = \psi_i$, $\dot{\psi}' = 0$. Similarly when the weathervaning motion ceased $\dot{\psi}' = 0$ again. Now, with reference to equation (40), it is seen that $C_{M\dot{\psi}}\, f(\psi)$ becomes indeterminate at $\psi = \psi_i$ and $\psi = 0$ as shown on the upper plot of figure 5. As the damping derivative $C_{M\dot{\psi}}$ must be a periodic function of ψ with a period of 2π radians, the solutions were corrected in the indeterminate regions and faired as shown on the lower plot of figure 5.

Next, data was selected in which the model was released from initial kiting angles at zero yaw (Reference 2, appendix Volume II pages 25 and 26, appendix volume III pages 89 and 90, and appendix Volume IV pages 1 and 3). Thus $\psi' = \dot{\psi}' = \ddot{\psi}' = 0$ and equation 33 reduces to:

$$-\ddot{\theta}' + \frac{C'_{M\dot{\theta}}\, v'}{C'_{M_r}\, \psi'^{1/3}}\, \dot{\theta}' + \frac{C_M'}{C_{M_r}}\frac{v'^2}{\psi'^{(1/3)}} = 0 \qquad (41)$$

Then, the GEDA electric analogue computer was set up to solve this equation for θ' (which was observed on the (X-Y) plotter) for arbitrary constant values of $C_{M\dot{\theta}}\, f(\theta')$ and compared with the data for each of these tests. As a result it was concluded that $C_{M\dot{\theta}}\, f(\theta') \cong 4$. The accuracy with which this numerical value satisfied the data is shown on figure 6.

Next using the derived values of $C'_{N\dot{\psi}}\, f(\psi)$, $C'_{M\dot{\psi}}\, f(\psi)$ and $C'_{M\dot{\theta}}\, f(\theta)$ the GEDA electric analogue computer was set up to solve equations (32) and (33), for both ψ and θ for an additional seventy two data plots with all combinations of yaw angles including ψ_i = 30, 60, 90, 120, 150, and 175 degrees; initial pitch angles of θ_i = 0, 10, 15, and 20 degrees and at model towing speeds of v = .5, 1.0, and 1.6 ft/sec. With $C_{N\dot{\psi}}\, f(\psi)$ and $C_{N\dot{\theta}}\, f(\psi, \theta)$ set equal to zero, trial and error adjustments of $C_{M\dot{\psi}}$ and $C_{M\dot{\theta}}$ were made until agreement was achieved between the computer solutions and the data for each of the 72 model test runs analyzed. As a result, it was concluded that $C_{N\dot{\psi}}\, f(\psi) = 0$, that $C_{N\dot{\theta}}\, f(\psi, \theta) = 0$, and that $C_{M\dot{\psi}}\, f(\theta)$ was approximately linear with the slope dependent on ψ as shown by the family of curves for $C_{M\dot{\psi}}\, f(\psi, \theta')$ plotted on figure 7. The accuracy with which these coefficients predicted the measured motions of the model are shown on figure 8. In general, the agreement is good, but the particular runs which are not satisfied, do indicate that error is present-either in the numerical values assigned to the damping coefficients or in the test data itself.

An approximate correction (K) for the dissimilarity imposed by the boom extending forward from the bow was applied to these rotary damping coefficients by comparing the integrated moments due to zonal forces (F) over the length of the model for pure rotation about the bow and for rotation about the boom mooring point. For an angular velocity (ω), the ratio of moments due to zonal forces for rotation about the bow as compared to rotation about the boom mooring point is:

$$K = \frac{\int_x x \, dF}{\int_x (x + a') \, dF} = \frac{\int_x C_F \rho \omega^2 x^3 y \, dx}{\int_x C_F \rho \omega^2 (x + a')^3 y \, dx}$$

Now, by assuming a constant sectional force coefficient (C_F) this expression reduces to:

$$K = \frac{\int_{x=0}^{x=L} x^3 y \, dx}{\int_{x=0}^{x=L+a'} (x + a_i' - a')^3 y \, dx} \qquad (42)$$

The planform of the model with the fins rotated 45° is shown on figure 9 and both ($X^3 y$) and $[(X + a')^3 y]$ are plotted vs X on figure 9 also. By graphical integration of these plots it was determined that K = .69. Then, this correction was applied to the rotary damping coefficients as previously derived and plotted on figure 10. It is believed that these coefficients are directly applicable to both the ZPG-2 and the ZPG-3 airships.

D. Anti-Kiting Study

Substituting the areodynamic and aerodynamic damping coefficients plotted on figures 1 and 10 along with the appropriate mass and geometric characteristics into equations 4 and 5, equations sufficiently accurate to describe the angular response of a mast moored airship to shifting winds are established.

The motions of a mast moored airship are dependent not only on its mass and aerodynamic properties but on the nature of the shifting winds as well. If the winds shift slowly, the airship weathervanes without appreciable lag and kiting tendencies remain small. Similarly, the yaw angles produced by high frequency shifting of the winds to both port and starboard will not cause kiting-first because time is required to build up the aerodynamic forces and second because the inertia of the airship must be overcome before kiting actually takes place. It is only when the winds shift much faster then the airship is able to follow and then stay in this new direction that kiting occurs. There is, at the present time a serious lack of knowledge concerning both the magnitude and character of wind shifts which must be anticipated while the airship is moored in winds of varying intensities.

To permit a study of the motions of a kiting airship for a elected kiting condition from which the relative merits of various anti-kiter designs may be compared, somewhat similar to the concept of the "effective sharp-edged gust" used to define in-flight gust load criteria, the concept of an "equivalent sudden wind shift" is introduced. The equivalent sudden wind shift is a theoretical wind shift which is assumed to strike the airship instantaneously over its whole length at the original wind speed.

Actually, it is impossible for the wind to shift suddenly. Absolute sudden changes in wind velocity or direction simply do not occur in the free atmosphere. There is always a finite interval of time required for the shifted wind to sweep gradually over the airship. In regard to the magnitude of shifting winds, it is obvious that a prevailing wind of high velocity cannot strike the airship broadside or from the stern. On the other hand when the wind is near calm a breeze may spring quite suddenly from any direction. Consequently, it appears reasonable that some statistical relationship exists between the equivalent sudden wind shift, the average wind speed, and the nature of the actual wind shifts which do occur. Realistic knowledge concerning this relationship is of first importance in determining the specific requirements for an effective anti-kiting device.

One of the important variables affecting the motion of a mast moored airship is the gradient of wind velocity with elevation (h) above the ground. This velocity gradient depends largely on the local terrain and the prevailing weather conditions. The calculated force and moment coefficients reported in reference 1 and the motions of a kiting airship model reported in reference 2 were based on a relative velocity measured 2-2/3 ft below the ground board with a velocity gradient approximately proportional to the 1/7 power of the distance below the ground board. This is equivalent to a wind speed measured at a full scale elevation of 200 ft with a wind velocity proportional to the 1/7 power of the elevation. In the field it is not practical to measure the wind speed at 200 ft elevations; therefore, the wind speeds upon which the anti-kiting study was based were corrected for a wind speed measured at a median height of aerology measuring stations (approximately 75 ft) for an assumed 1/7 power velocity gradient. That is:

$$V_{75} = \left(\frac{75}{200}\right)^{1/7} V_{200} = .869\ V_{200} \qquad (43)$$

To study the influence of anti-kiter design as tested on the ZPM-4 airship and described in reference 3, solutions of these equations, modified to account for the characteristics of this anti-kiting device were made for the ZPG-3W airship on the GEDA electric analogue computer for combinations of wind speeds from 0 to 70 knots, step function input wind shifts from 0 to 180 degrees, and for applied anti-kiting moments as may be imposed by the anti-kiter or static heaviness from 0 to the anti-kiting moment necessary to prevent kiting completely. A schematic of the GEDA computer wiring set up is shown on figure 11. Examples of the solutions obtained are shown on figure 12. From these solutions the maximum kiting angles, and the angular velocities at ground contact were noted. Then the vertical and Transverse components of contact velocity were calculated by the expressions:

$$u_{v} = b\ \dot{\theta} \quad \text{(impact)} \qquad (44)$$

$$\text{and} \quad u_{h} = b\ \dot{\psi} \quad \text{(impact)} \qquad (45)$$

then plotted vs the applied anti-kiting moment for wind speeds of 0, 20, 40, 60, and 80 knots and for equivalent sudden wind shifts of 0, 30, 60, 90, 120, 150, and 180 degrees as shown on figures 13 thru 18. The influence of any combination of anti-kiter weight and static heaviness may be determined by referring to the scales provided by summing the anti-kiting moments imposed by each. For the ZPG-3W airship, the anti-kiting moment of the anti-kiter is 344 times the anti-kiter weight (AKM = CP = 344P), and static heaviness imposes on anti-kiting moment 185.6 times the static heaviness (AKM = C W_{SH} = 185.6 W_{SH}).

When the airship kites, this anti-kiter is designed such that it is lifted to a height which for all practical purposes is directly proportional to the kiting angle. With reference figures 13 thru 18, it is seen that although this anti-kiter does reduce kiting appreciably, the anti-kiter weight necessary to reduce contact velocities to acceptable values appears impractical and yet, unless extremely heavy anti-kiters are employed, when the airship does kite the anti-kiter seems only to accelerate the airship to higher contact velocities than those experienced by an airship moored in static equilibrium and no anti-kiter attached. Consequently, the likelihood of damage due to kiting is increased.

This suggests that an improvement might be realised by a redesign of the anti-kiter attachment system such that when the attachment lines support the entire weight of the anti-kiter, instead of lifting it up, cable is reeled out sufficient to hold it just in contact with the ground until the maximum kiting angle is reached. Then the unit rests on the ground and cable is reeled in at reduced tension.

To study the influence of this redesign of the anti-kiter attachment system, the GEDA electric analogue computor was rewired to include a circuit which automatically switched the anti-kiter weight effect to zero when the angular kiting velocity became negative and restored it when the kiting velocity became positive. Then solutions were made for the ZPG-3W airship for the same combinations of wind speed, step function input wind shifts, and anti-kiting moments. Examples of the solutions obtained are shown on figures 19. The maximum kiting angles and the vertical and transverse components of contact velocity are plotted on figures 20 thru 25. With reference to these figures, it is seen that by a redesign of the anti-kiter attachment system, as just described, contact velocities are reduced appreciably at all wind speeds up to and including the design limit wind speed for mast mooring with practical anti-kiter weights. Thus, the likelihood of kiting damage is decreased appreciably.

These results were applied to the ZPG-2 type ai[illegible] [illegible] comparing the equations of motion for the ZPG-2 type airship with the equations of motion for the ZPG-3W.

By substitutin[illegible] [illegible] mass and geometric characteristics of the ZPG-2 type airship into e[illegible]ations 6 and 7 we have;

$$-\ddot{\psi} + \left(\frac{C_{N\dot{\psi}}\, V}{C_{I_{y\text{-}y}} + \psi^{k_3}}\right)_{2N} (\dot{\Psi} - \dot{\psi}) + \left(\frac{C_N\, V^2}{C_{I_{y\text{-}y}} + \psi^{k_3}}\right)_{2N} = 0 \qquad (46)$$

and
$$-\ddot{\theta} + \left(\frac{C_{m\dot{\theta}}\, V}{C_{I_{y\text{-}y}} + \psi^{k_3}}\right)_{2N} \dot{\theta} + \left(\frac{C_m\, V^2}{C_{I_{y\text{-}y}} + \psi^{k_3}}\right)_{2N} + \left(\frac{C_{m\dot{\psi}}\, V}{C_{I_{y\text{-}y}} + \psi^{k_3}}\right)_{2N} (\dot{\Psi} - \dot{\psi}) - \left(\frac{AKM}{C_{I_{y\text{-}y}} + \psi^{k_3}}\right)_{2N} = 0 \qquad (47)$$

and for the ZPG-3W type airship we have;

$$-\ddot{\psi} + \left(\frac{C_{N\dot{\psi}}\, V}{C_{I_{y\text{-}y}} + \psi^{k_3}}\right)_{3W} (\dot{\Psi} - \dot{\psi}) + \left(\frac{C_N\, V^2}{C_{I_{y\text{-}y}} + \psi^{k_3}}\right)_{3W} = 0 \qquad (48)$$

and
$$-\ddot{\theta} + \left(\frac{C_{m\dot{\theta}}\, V}{C_{I_{y\text{-}y}} + \psi^{k_3}}\right)_{3W} \dot{\theta} + \left(\frac{C_m\, V^2}{C_{I_{y\text{-}y}} + \psi^{k_3}}\right)_{3W} + \left(\frac{C_{m\dot{\psi}}\, V}{C_{I_{y\text{-}y}} + \psi^{k_3}}\right)_{3W} (\dot{\Psi} - \dot{\psi}) - \left(\frac{AKM}{C_{I_{y\text{-}y}} + \psi^{k_3}}\right)_{3W} = 0 \qquad (49)$$

For similar kiting and weathervaning motions for both the ZPG-2 and ZPG-3W airships, the coefficients of these differentials must be equal. Comparing equation (46) with (48) and (47) with (49), and assuming the mass and aerodynamic coefficients are the same for both airship types we have:

$$\frac{\left(\frac{V}{\forall^{1/3}}\right)_{2W}}{\left(\frac{V}{\forall^{1/3}}\right)_{3W}} = 1 \quad \text{therefore} \quad \frac{V_{2W}}{V_{3W}} = \left(\frac{\forall_{2W}}{\forall_{3W}}\right)^{1/3} = .872 \qquad (50)$$

$$\frac{\left(\frac{V}{\forall^{1/3}}\right)_{2W}}{\left(\frac{V}{\forall^{1/3}}\right)_{3W}} = 1 \quad \text{therefore} \quad \frac{(AKM)_{2W}}{(AKM)_{3W}} = \left(\frac{\forall_{2W}}{\forall_{3W}}\right)^{5/3} = \left(\frac{V_{2W}}{V_{3W}}\right)\left(\frac{\forall_{2W}}{\forall_{3W}}\right)^{4/3} = .583\left(\frac{V_{2W}}{V_{3W}}\right) \qquad (51)$$

$$\text{or} \quad \frac{P_{2W}}{P_{3W}} = .583\left(\frac{V_{2W}}{V_{3W}}\right)\left(\frac{C_{3W}}{C_{2W}}\right) = .692\,\frac{V_{2W}}{V_{3W}} \qquad (52)$$

$$\text{and} \quad \frac{(W_{3H})_{2W}}{(W_{3H})_{3W}} = .583\left(\frac{V_{2W}}{V_{3W}}\right)\left(\frac{b_{3W}}{b_{2W}}\right) = .728\left(\frac{V_{2W}}{V_{3W}}\right) \qquad (53)$$

The vertical and transverse contact velocities may be expressed as

$u_h = b\dot{\psi}_{\text{impact}}$ and $u_v = b\dot{\theta}_{\text{impact}}$. Therefore:

$$\frac{(u_v)_{2W}}{(u_v)_{3W}} = \frac{(u_h)_{2W}}{(u_h)_{3W}} = \frac{b_{2W}}{b_{3W}} = \frac{150}{187} = .802$$

Therefore, the results of the foregoing analysis of the mast moored ZPG-3W airship as plotted on figures 13 thru 25 were applied to the ZPG-2 type airship by:

1. increasing the wind speed by a factor of 1.15
2. decreasing the anti-kiting moment scale by a factor of .583
3. decreasing the anti-kiter weight scale by a factor .692
4. decreasing the static heaviness scale by a factor of .728
5. decreasing the contact velocities by a factor of .802

The results of these transformations are shown on figures 26 thru 37.

Conclusions and Recommendations

Based on water model test data, the aerodynamic and aerodynamic damping characteristics of a kiting airship were determined. Then, by substituting these coefficients along with the appropriate mass and geometric characteristics into the generalized equations of motion, equations sufficiently accurate to describe the angular response of a mast moored airship for selected kiting conditions were established.

Then, as a result of a study of the motions of a masted airship subjected to sudden wind shifts and configured with an anti-kiting weight fixed to the airship stern or ballasted at the car, it is concluded that although an anti-kiting device which is lifted to a height proportional to the kiting angle does reduce kiting appreciably, once a kiting peak is reached, the anti-kiter weight or car ballast serves only to accelerate the airship to higher contact velocities with the ground as shown on figures 13 thru 18 and 26 thru 31. Thus, the likelihood of damage due to kiting is increased. As the anti-kiter weight necessary to reduce contact velocities to acceptable values are large and impractical this design cannot be recommended. Furthermore, it is recommended that the airship be moored in static equilibrium. It is recommended also as a means of further reducing the possibilities of kiting damage that the elevators be controlled whether an anti-kiting weight is used or not.

However, as a result of further study, the results of which are plotted on figures 20 thru 25 and 32 thru 37, it is concluded that a considerable improvement may be realized by a redesign of the anti-kiter attachment system such that when the attachment cables nearly support the entire weight of the anti-kiting unit, instead of lifting it, cable is reeled out sufficient to hold the unit just in contact with the ground until a maximum kiting angle is reached. Then the unit rests on the ground and cable is reeled in at reduced tension. An anti-kiting device incorporating this attachment system design is recommended as a practical and an effective means of reducing the likelihood of damage due to kiting.

References

1. Hydrodynamic Nose-To-Wind and Tail-To-Wind Mooring Investigation of a 1/75th Scale Airship Model with Inverted "V" and "X" Type Empennage, General Development Corporation Report No. R 179B-1, dated April 1958.

2. Hydrodynamic Investigation of a 1/75 Scale Airship Model in A Free "Kiting" State and Equipped with an "X" Type Empennage, General Development Corporation Report No. R-235B-1 (Revised), Appendix Volumes I, II, III and IV dated 15, June 1958 and 27 August 1959.

3. Aerodynamic Evaluation of Kiting Prevention as Determined from the ZPM-4 Airship Anti-Kiting Tests, GER-8458 Rev. B, dated 17 January 1958.

PREPARED BY [illegible]
CHECKED BY [illegible]
DATE May [illegible]
REVISED

GOODYEAR AIRCRAFT

PAGE 36
MODEL ZPG-2/2W/3W
GER- 10052
REF NO. Code 25500

FIGURE 1
ZPG-2/2W/3W AIRSHIPS
AERODYNAMIC MOMENT COEFFICIENTS

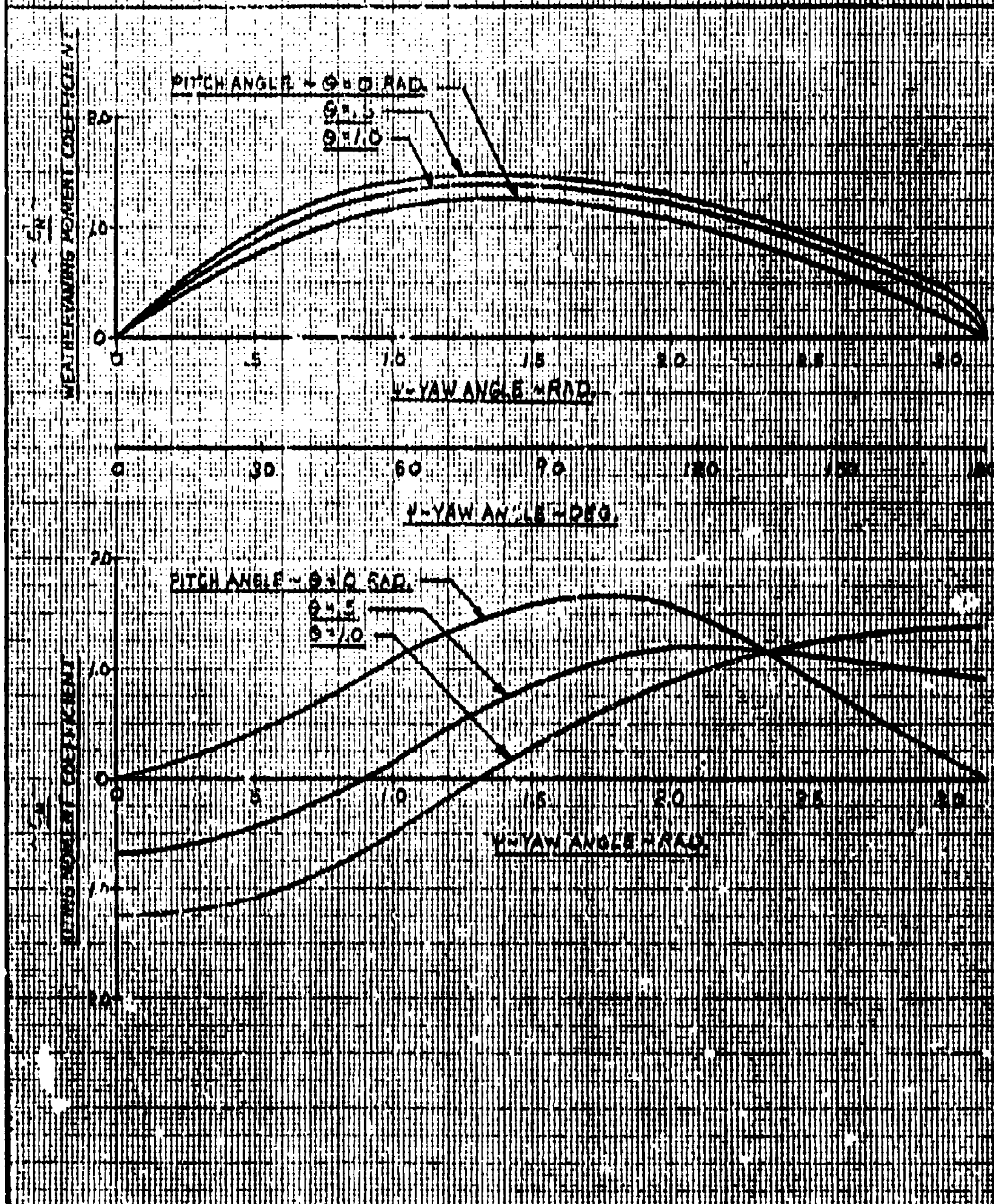

PREPARED BY
CHECKED BY
DATE
REVISED

GOODYEAR AIRCRAFT

PAGE 37
MODEL ZPG-2/2W/3W
GER- 10052
REF NO. Code 25500

FIGURE 2
ZPG-2/2W/3W AIRSHIPS
AERODYNAMIC FORCE COEFFICIENTS

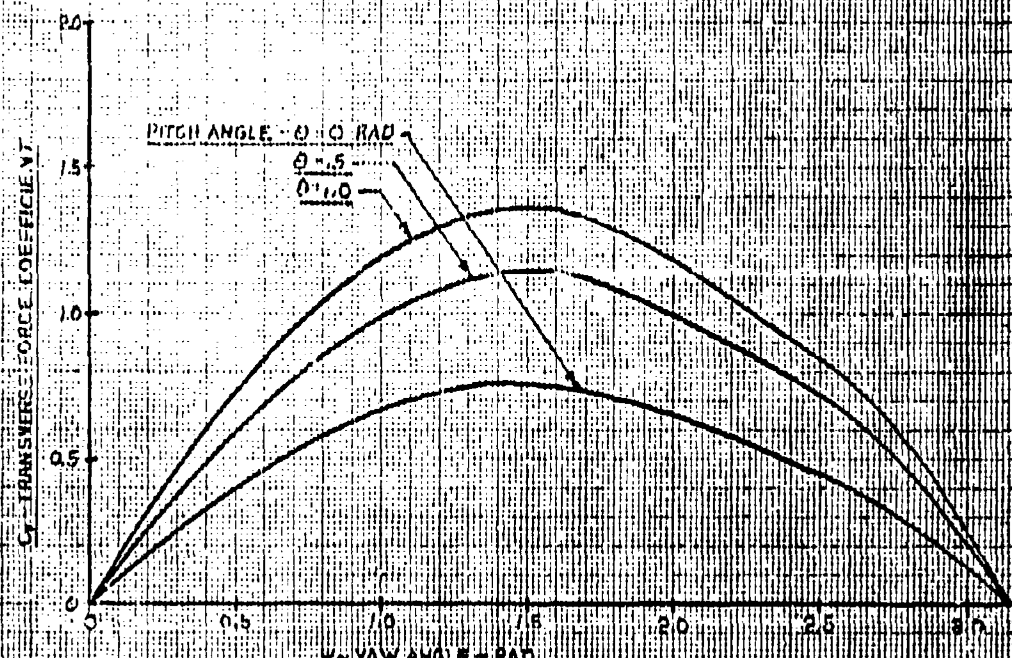

PREPARED BY ______

CHECKED BY ______

DATE ______

REVISED ______

GOODYEAR AIRCRAFT

PAGE 18

MODEL ZPG-2/2W/3W

GER- 10052

REF NO. Code 25500

FIGURE 3

1/75TH SCALE ZPN-2 AIRSHIP WATER MODEL (RUN 2)

AERODYNAMIC MOMENT COEFFICIENTS

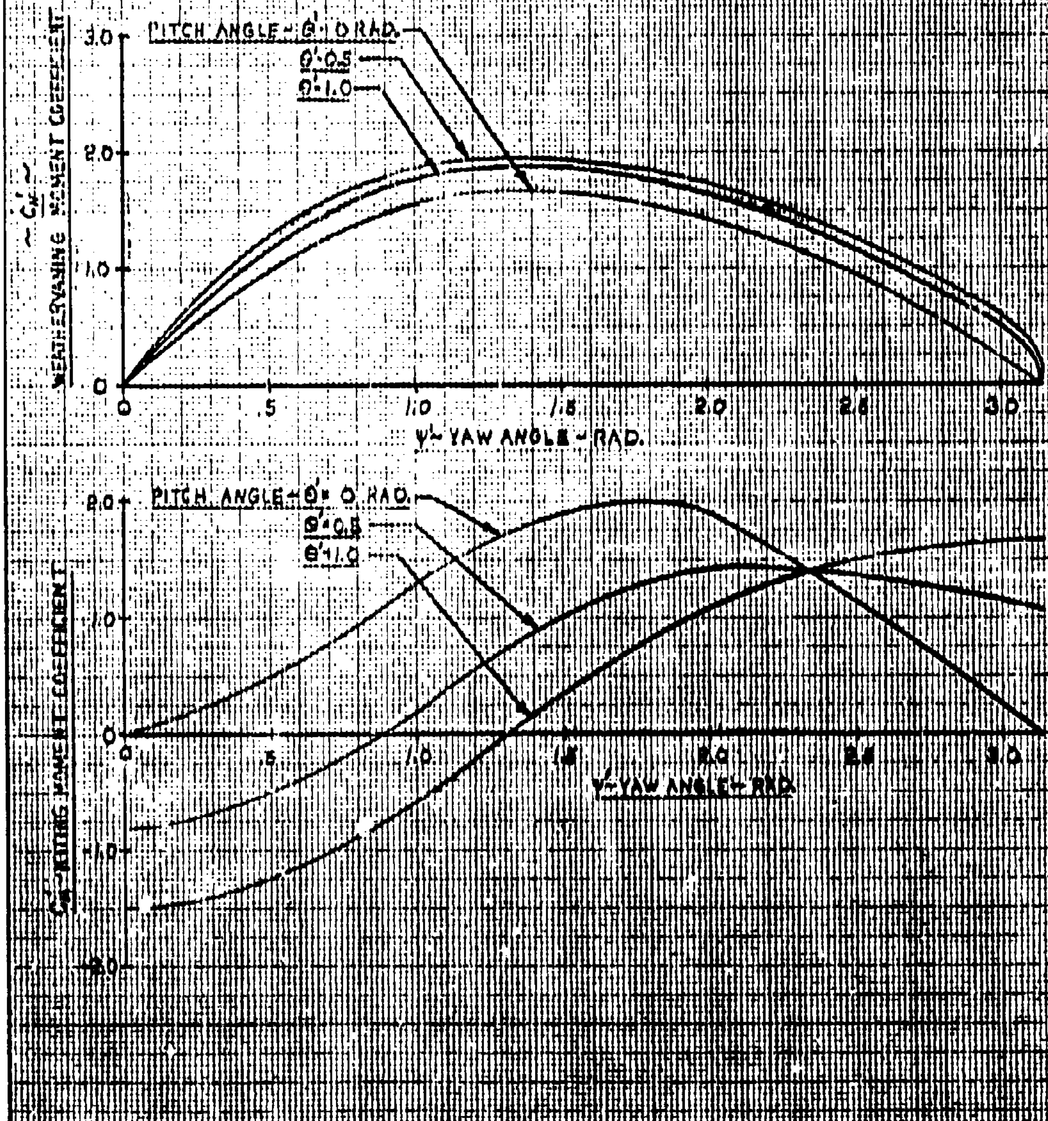

FIGURE 4
1/78TH SCALE ZPN-1 AIRSHIP WATER MODEL (REF 2)
DERIVATION OF DAMPING MOMENT COEFFICIENT $C_{N\psi}$ VS $f(\psi)$

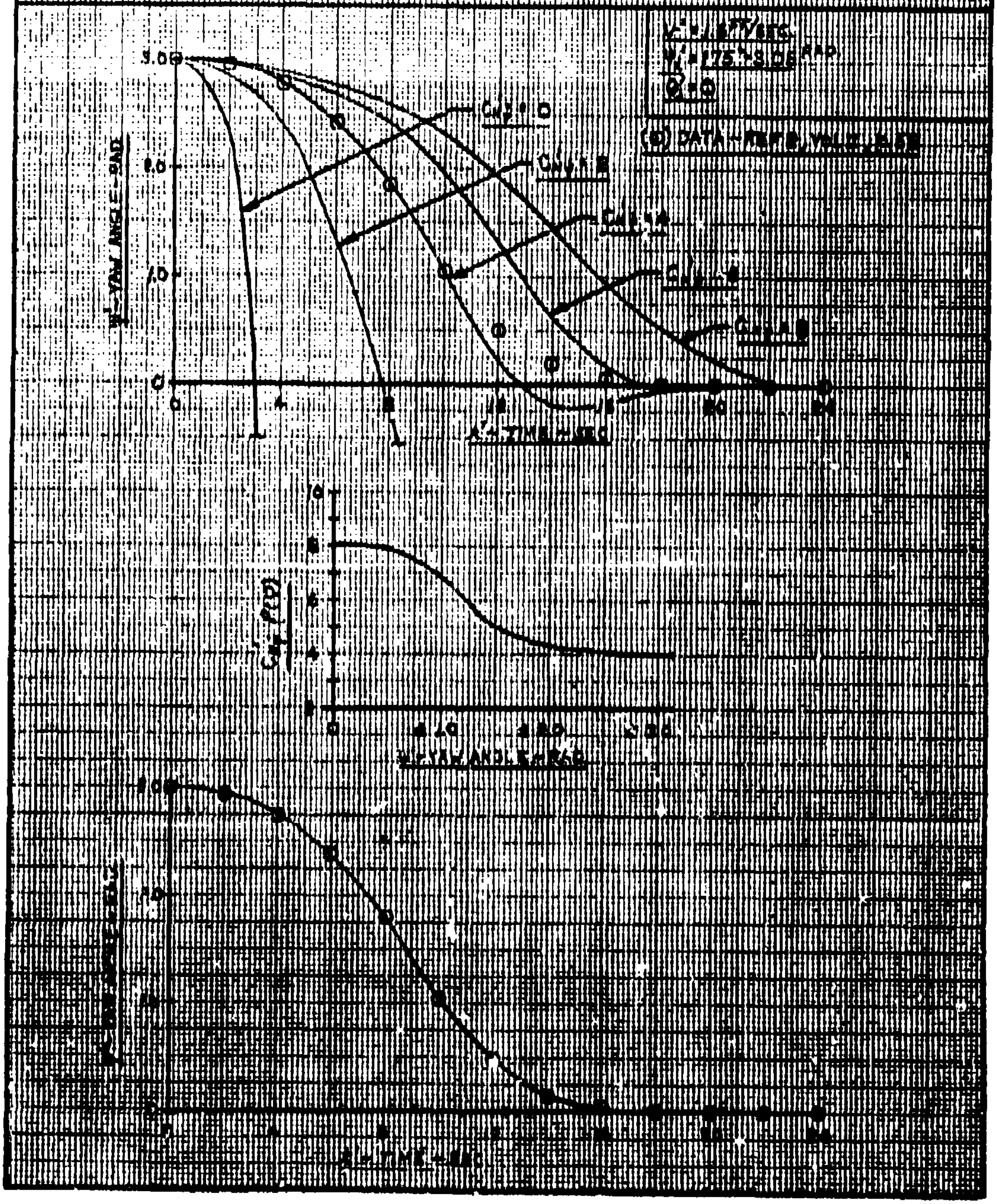

GOODYEAR AIRCRAFT

FIGURE 5
1/75TH SCALE ZPN-2 AIRSHIP WATER MODEL (APP.B)
DERIVATION OF DAMPING MOMENT COEFFICIENT $C'_{N_r} f(\psi)$

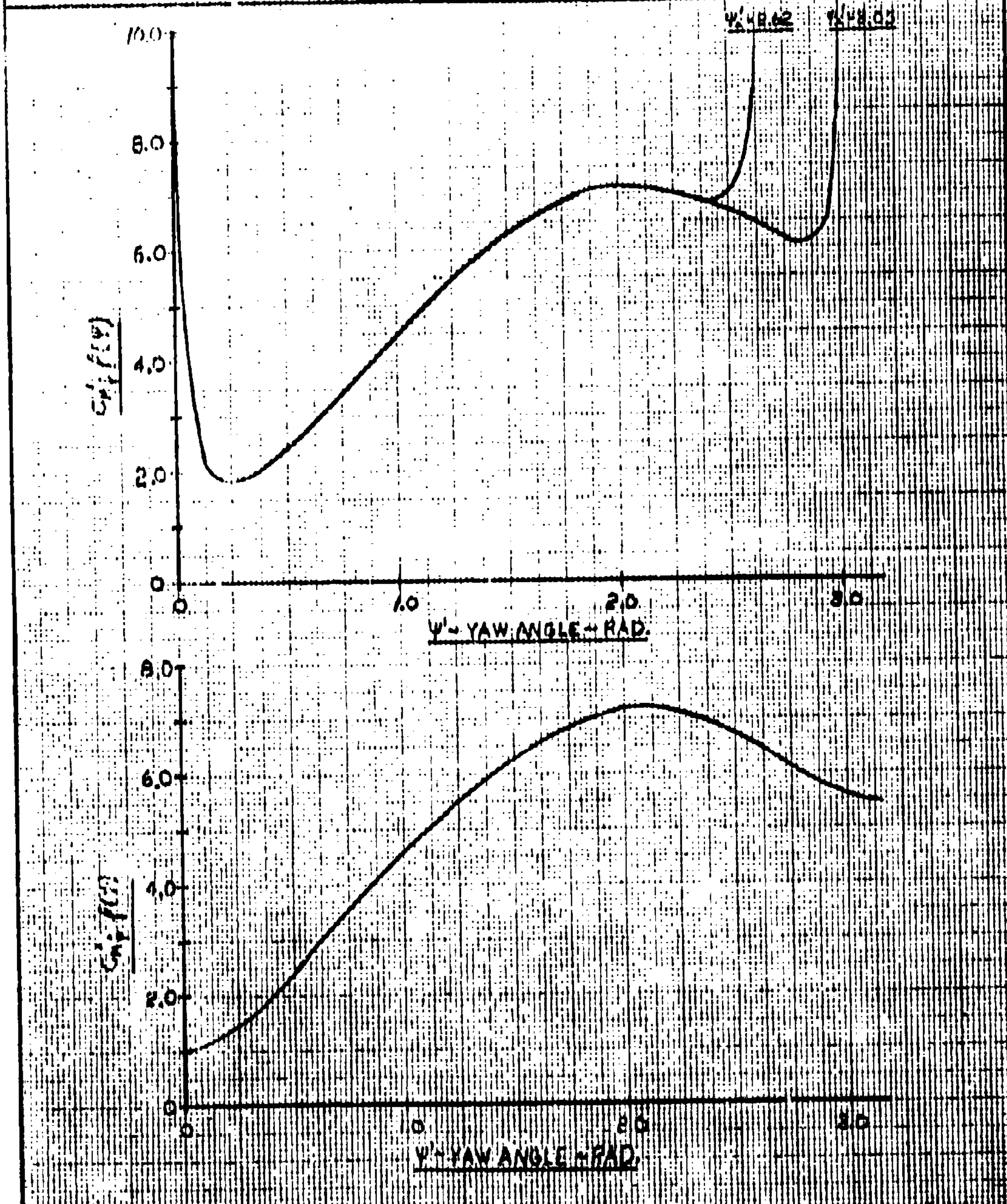

FIGURE 6
1/78TH SCALE ZPN-2 AIRSHIP WATER MODEL (REF. 2)
DERIVATION OF DAMPING MOMENT COEFFICIENT

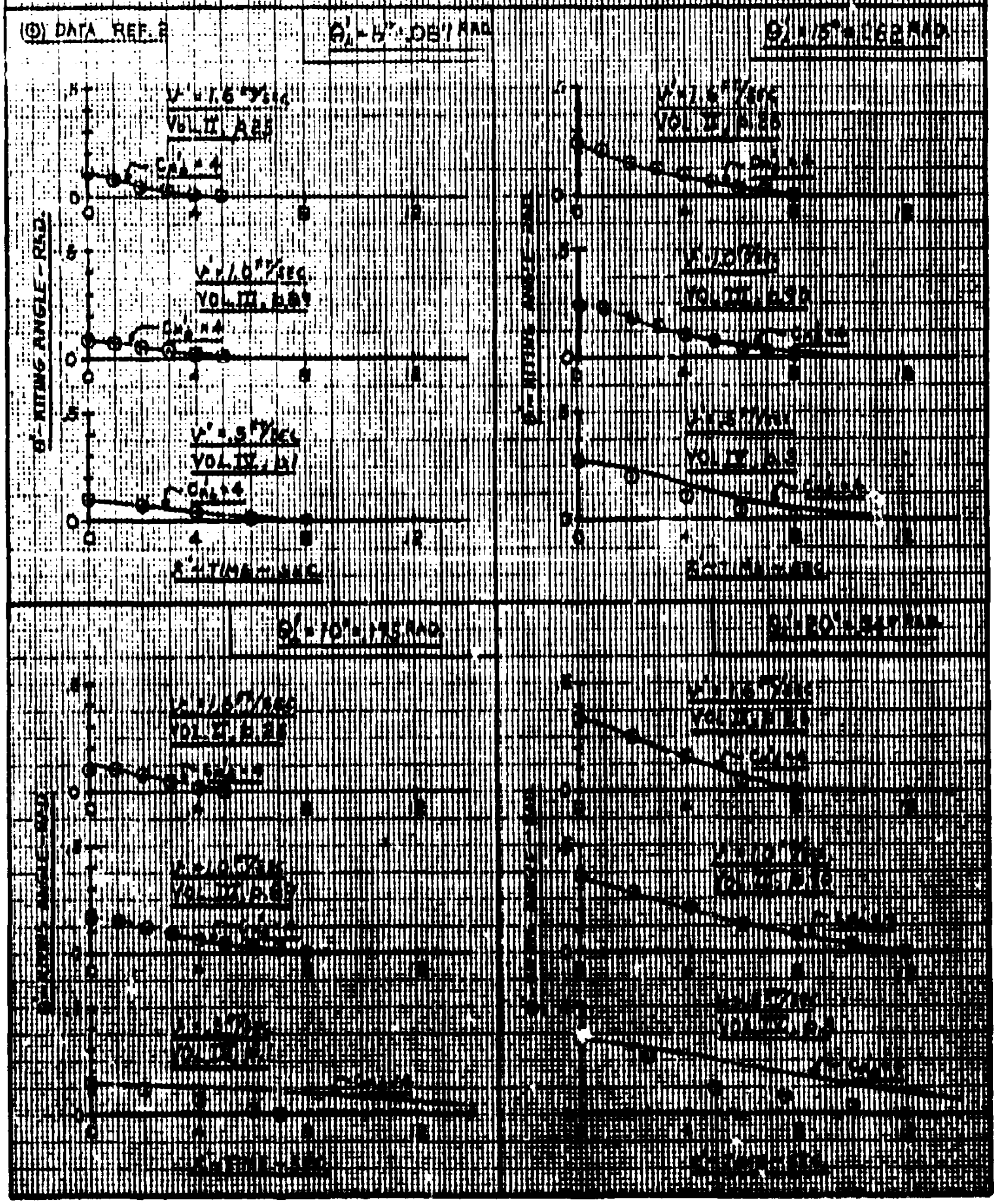

PREPARED BY J.D.M.
CHECKED BY J.W.B.
DATE May , 1961
REVISED

GOODYEAR AIRCRAFT

PAGE 42
MODEL ZPG-2/2W/2
SER— 10052
REF NO. Code 25500

FIGURE 7

(1/48 SCALE) ZPN-2 AIRSHIP WATER MODEL (REF)

DERIVATION OF DAMPING MOMENT COEFFICIENT

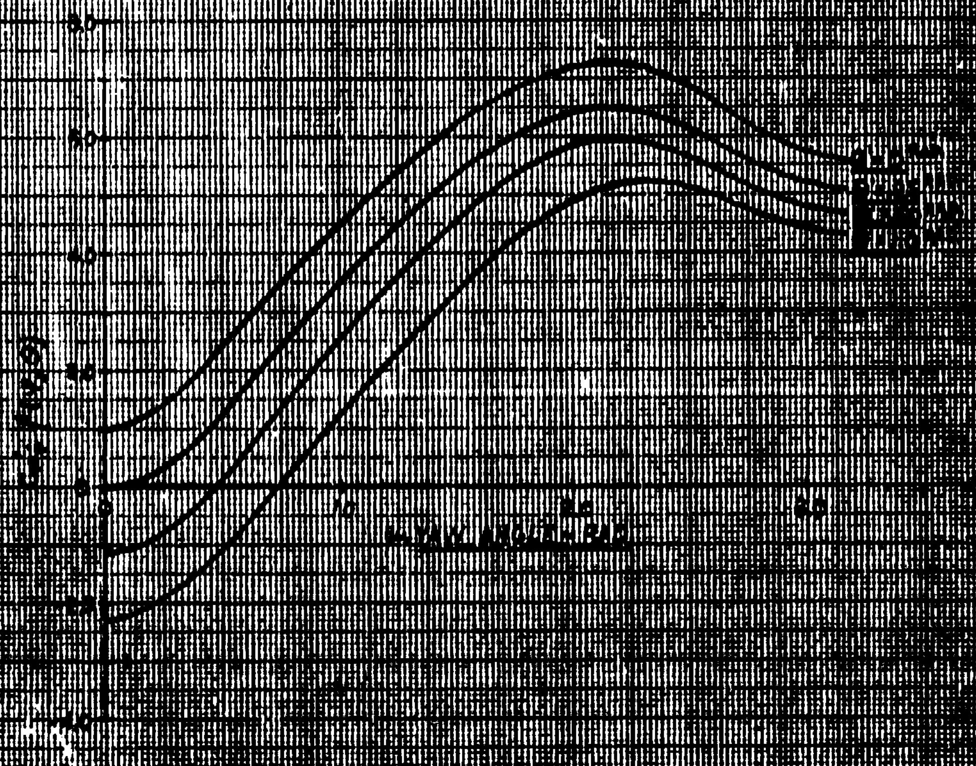

FIGURE 8
1/75TH SCALE WATER MODEL OF THE ZPGW AIRSHIP
COMPARISON BETWEEN MEASURED & CALCULATED MOTIONS

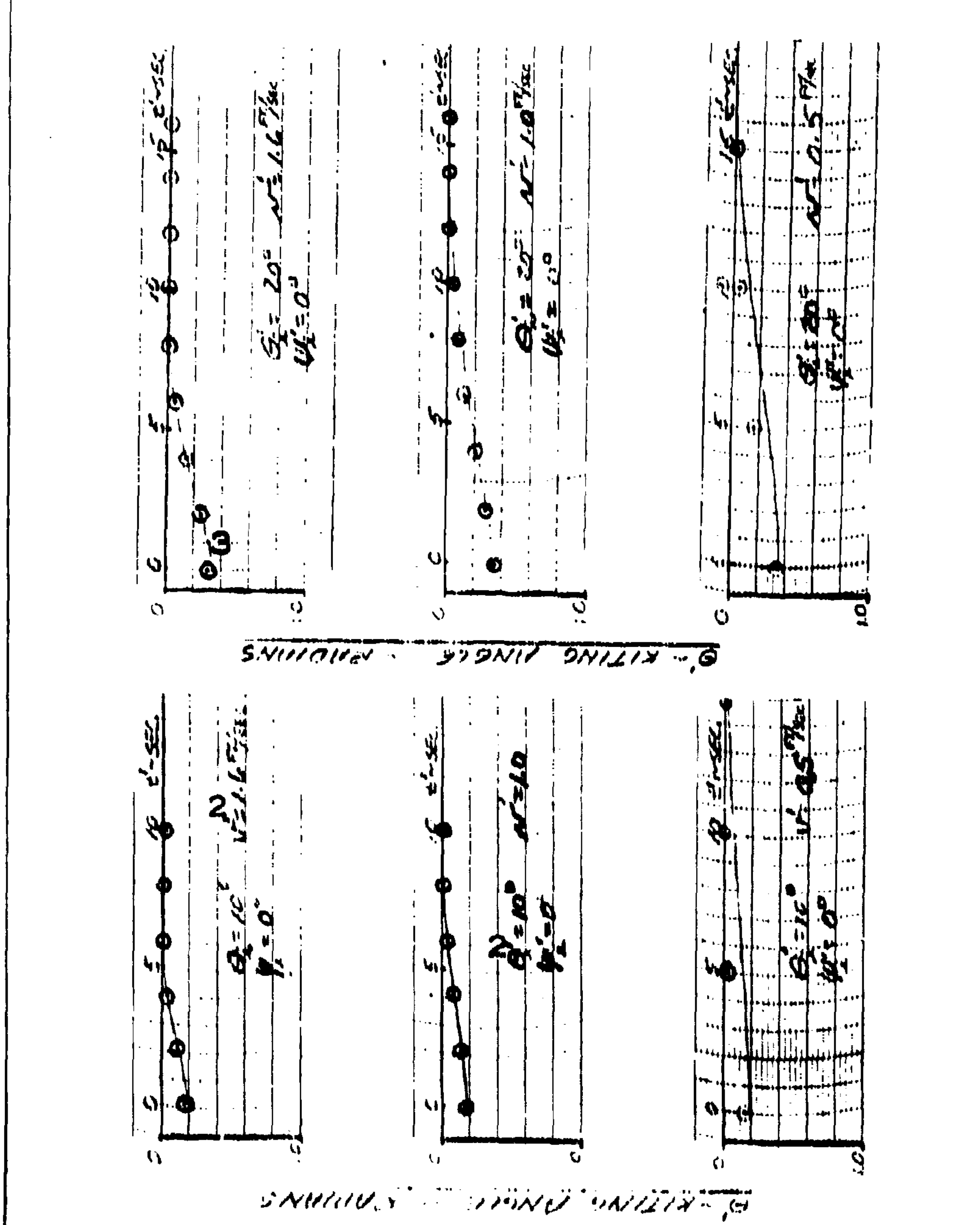

PREPARED [illegible]
CHECKED [illegible]
DATE May 1, 1961
REV DATE

GOODYEAR
GOODYEAR AIRCRAFT CORPORATION

PAGE 44
MODEL [illegible]
GER- 10052
CODE [illegible]

FIGURE 8
1/75TH SCALE WATER MODEL OF THE ZPGW AIRSHIP
COMPARISON BETWEEN MEASURED & CALCULATED MOTIONS

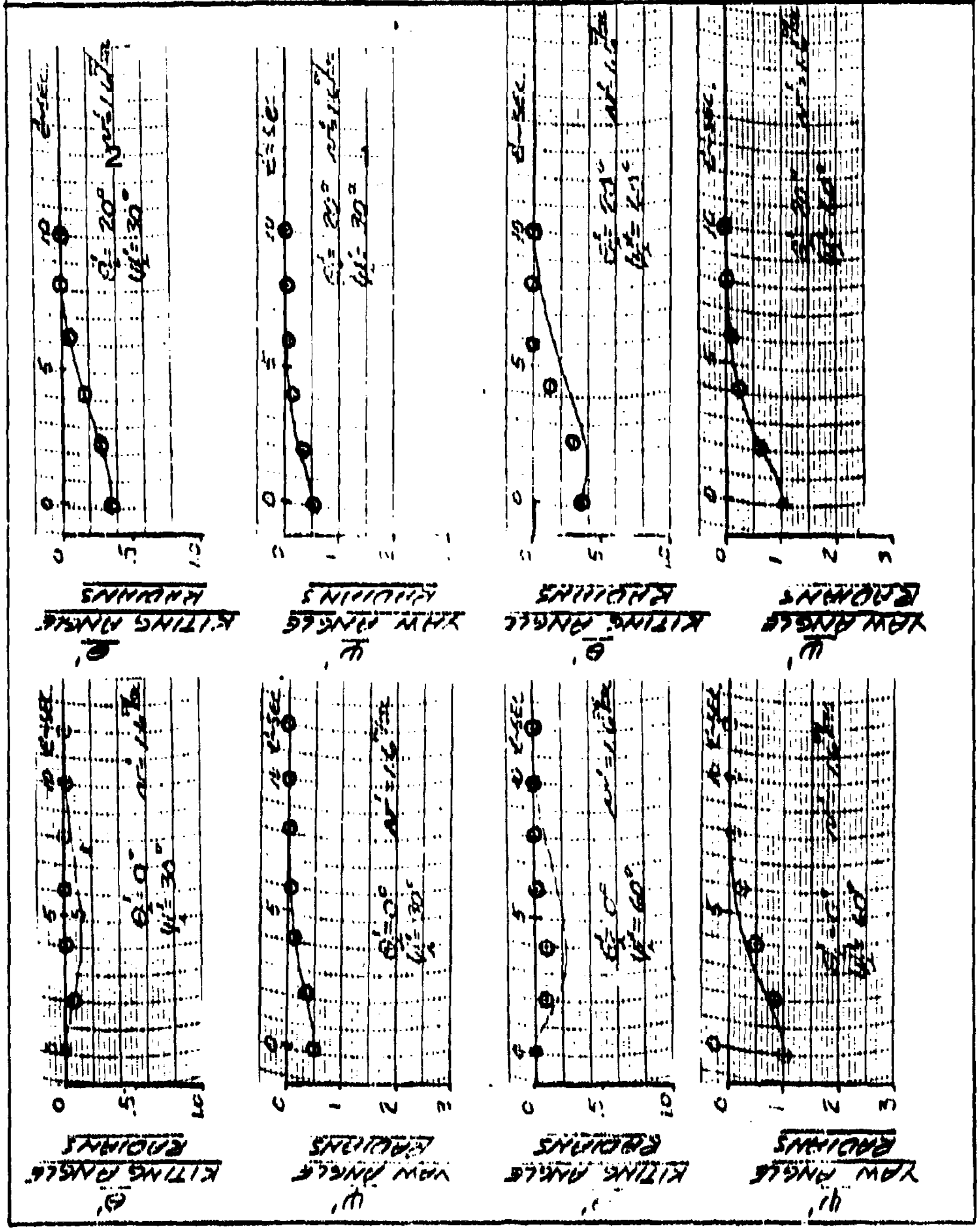

FIGURE 8

1/75TH SCALE WATER MODEL OF THE ZPGW AIRSHIP

COMPARISON BETWEEN MEASURED & CALCULATED MOTIONS

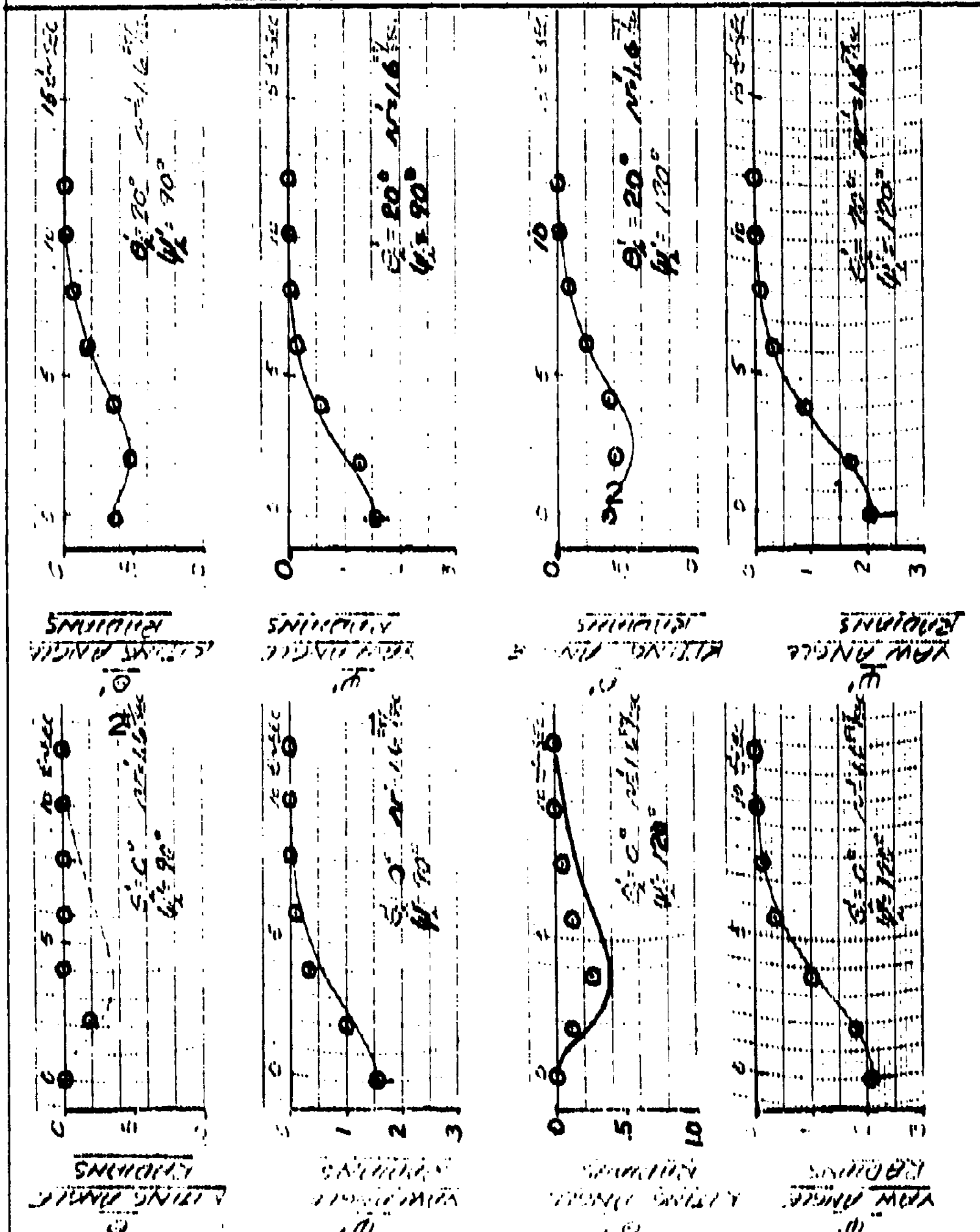

PREPARED	J. D. [illegible]	PAGE	46
CHECKED	J. [illegible]	MODEL	ZPG-3/2W/[illegible]
DATE	May 1, 1961	GER-	10052
REV DATE		CODE	25500

GOODYEAR
GOODYEAR AIRCRAFT CORPORATION

FIGURE 8:
1/75TH SCALE WATER MODEL OF THE ZPZW AIRSHIP
COMPARISON BETWEEN MEASURED & CALCULATED MOTIONS

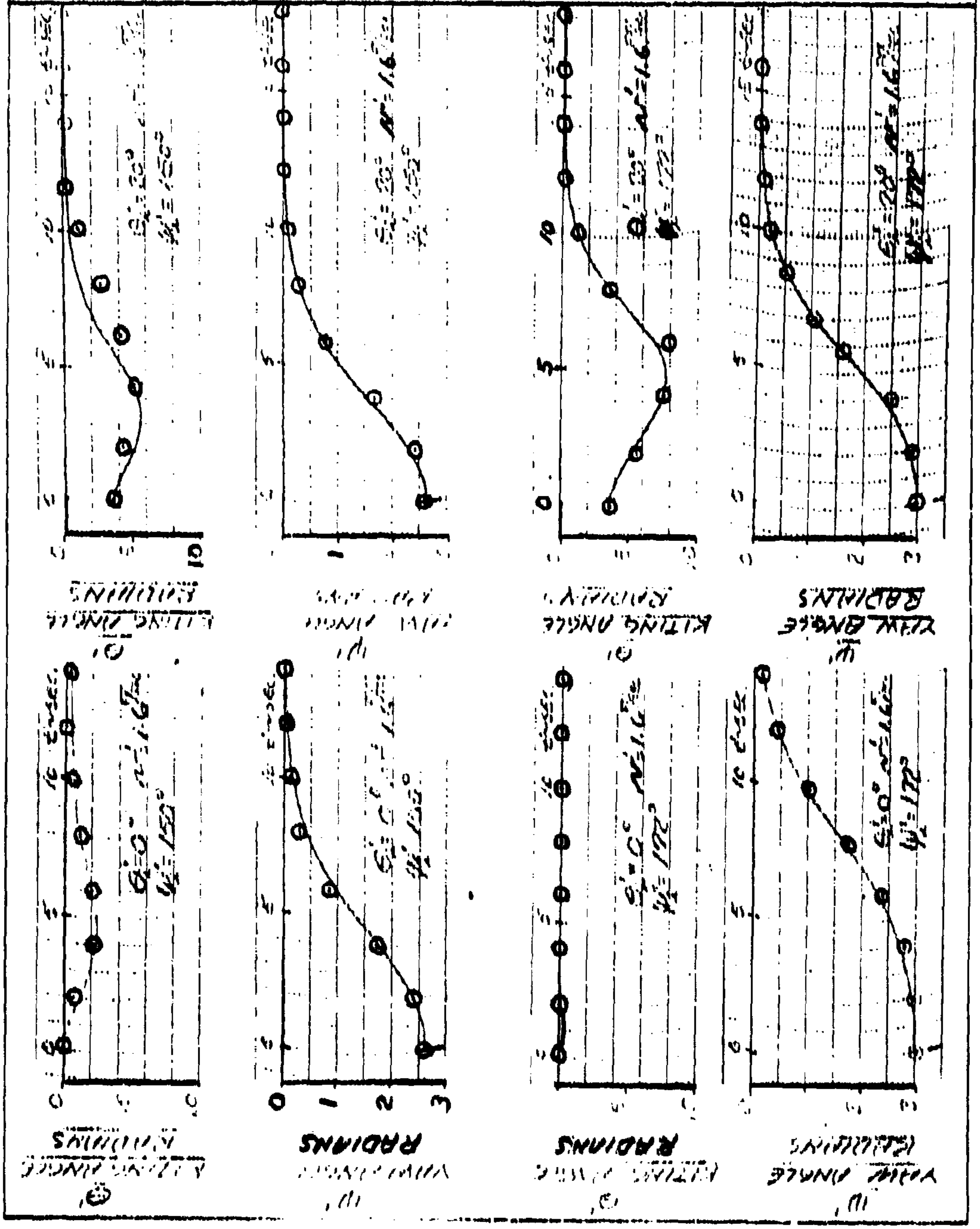

PREPARED J.D.M.
CHECKED
DATE May 1, 1961
REV DATE

GOODYEAR
GOODYEAR AIRCRAFT CORPORATION
AKRON OHIO

PAGE
MODEL
GER-
CODE 25500

FIGURE

1/75TH SCALE WATER MODEL OF THE ZPGW AIRSHIP
COMPARISON BETWEEN MEASURED & CALCULATED MOTIONS

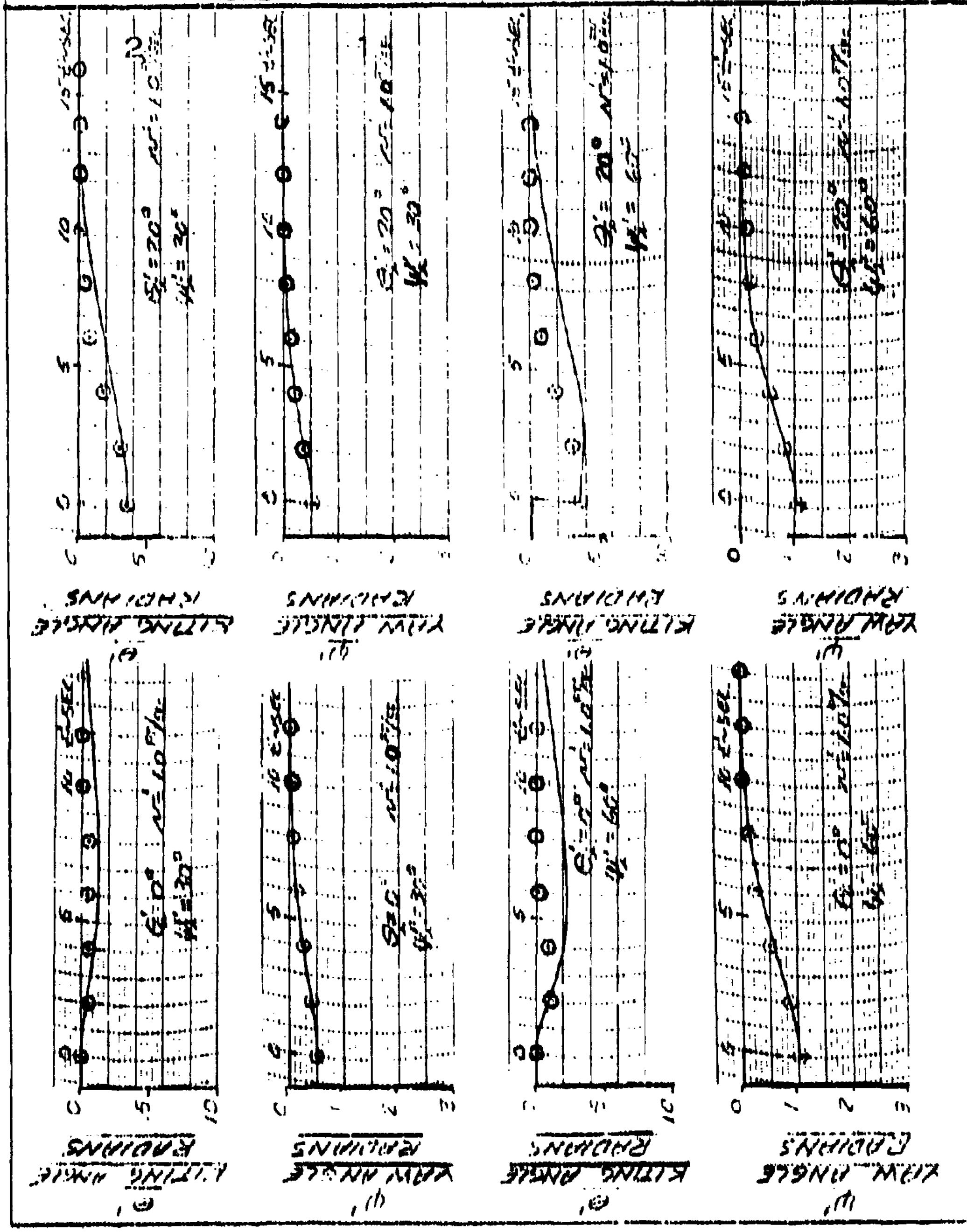

PREPARED J.D.M.
CHECKED J.W.B.
DATE May 1, 1961
REV DATE

GOODYEAR
GOODYEAR AIRCRAFT CORPORATION

PAGE 48
MODEL ZPG-2/2W/3W
REP. 10052
CODE 25500

FIGURE 8
1/75TH SCALE WATER MODEL OF THE ZPGW AIRSHIP
COMPARISON BETWEEN MEASURED & CALCULATED MOTIONS

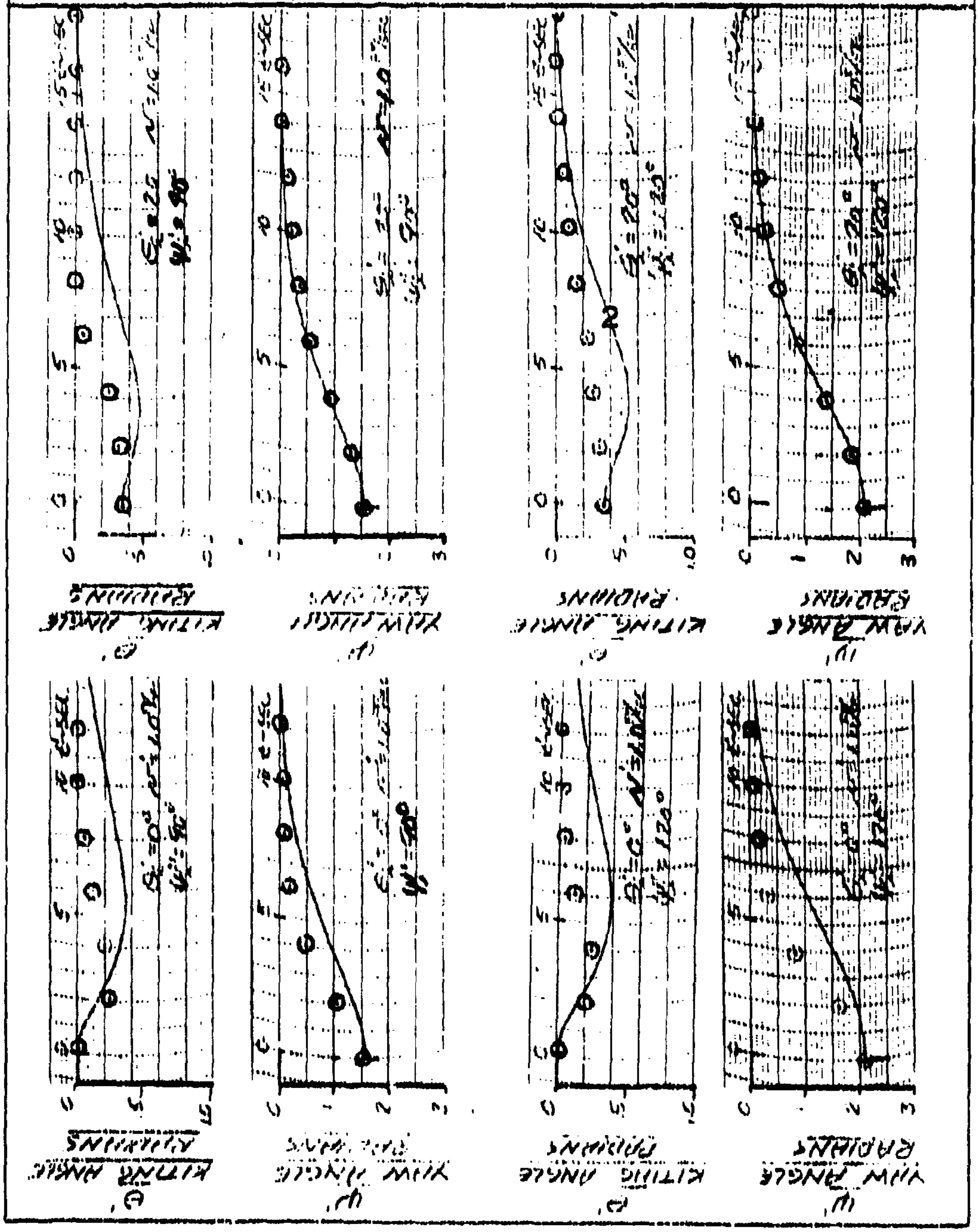

PREPARED J.D.M.
CHECKED J.W.B.
DATE May 1, 1961
REV DATE

GOODYEAR
GOODYEAR AIRCRAFT CORPORATION
AKRON OHIO

MODEL ZPG-2/2W/
GER- 10052
CODE 23500

FIGURE 8
1/75TH SCALE WATER MODEL OF THE ZP2W AIRSHIP
COMPARISON BETWEEN MEASURED & CALCULATED MOTIONS

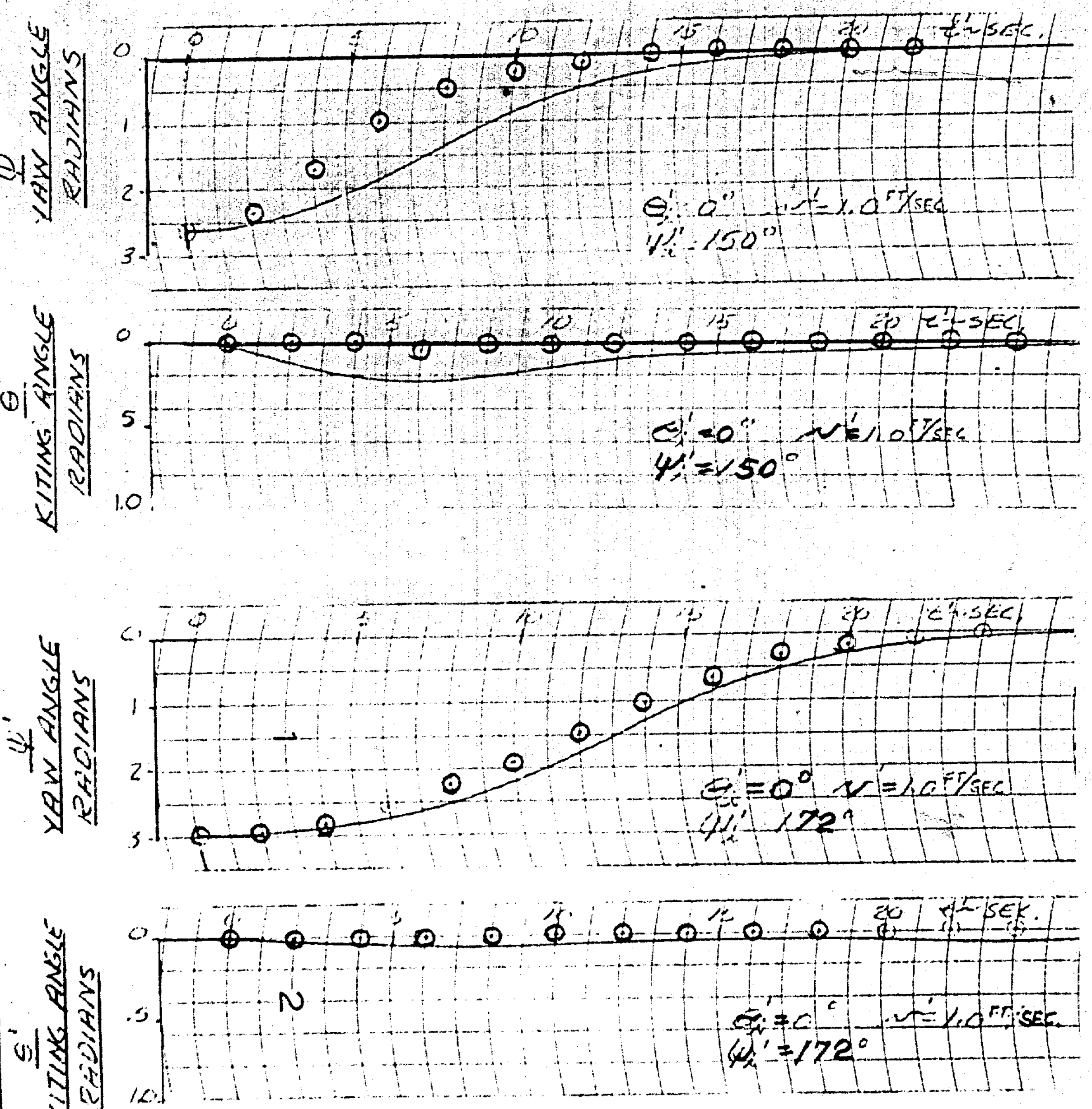

FIGURE 8

1/75TH SCALE WATER MODEL OF THE ZP2W AIRSHIP

COMPARISON BETWEEN MEASURED & CALCULATED MOTIONS

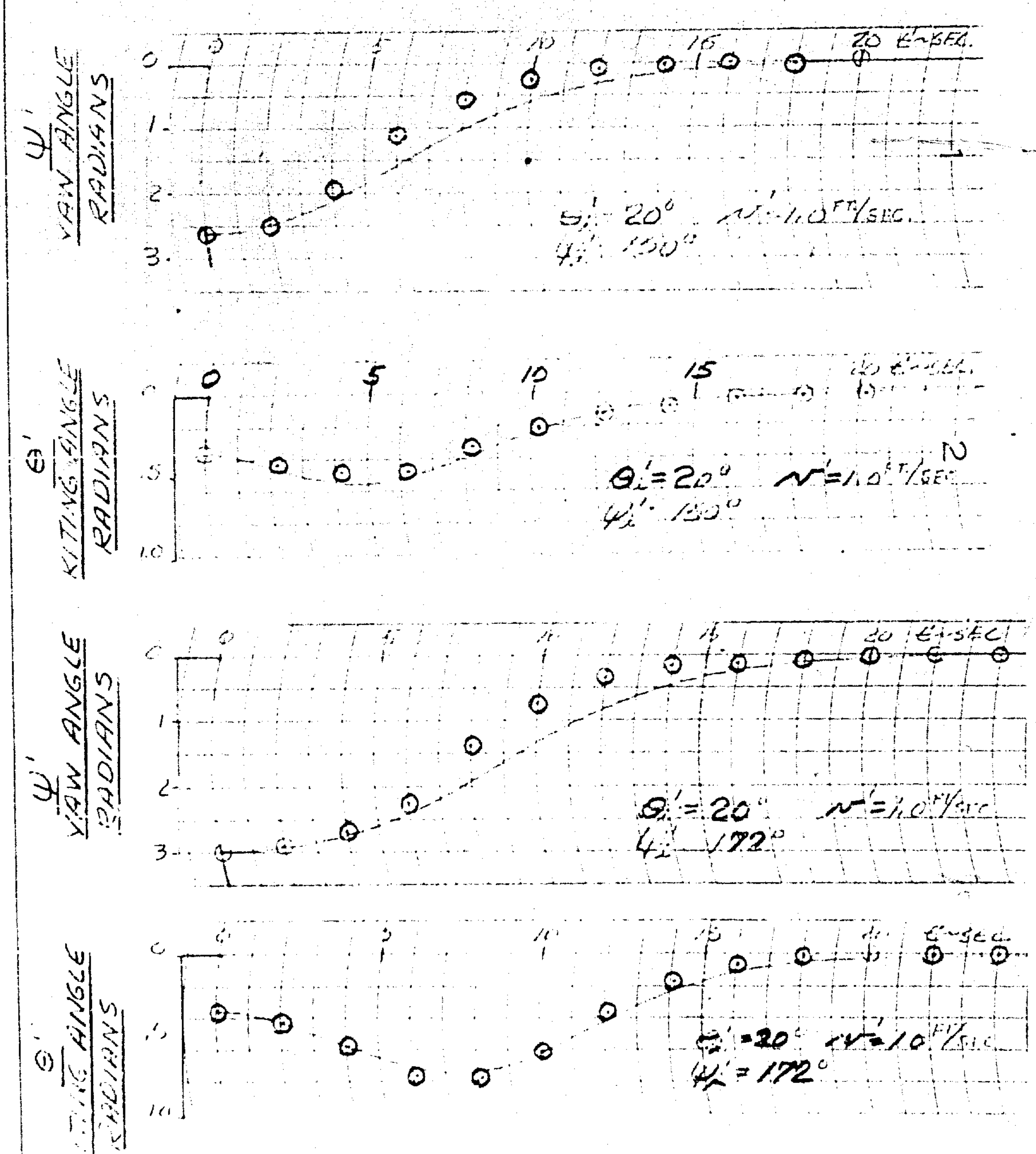

PREPARED J. D. M.
CHECKED J. W. B.
DATE May 1, 1961
REV DATE

GOODYEAR
GOODYEAR AIRCRAFT CORPORATION

PAGE 52
MODEL ZPG-2/2W/3W
GER- 10052
CODE 25500

FIGURE 8b
1/75TH SCALE WATER MODEL OF THE ZP2W AIRSHIP
COMPARISON BETWEEN MEASURED & CALCULATED MOTIONS

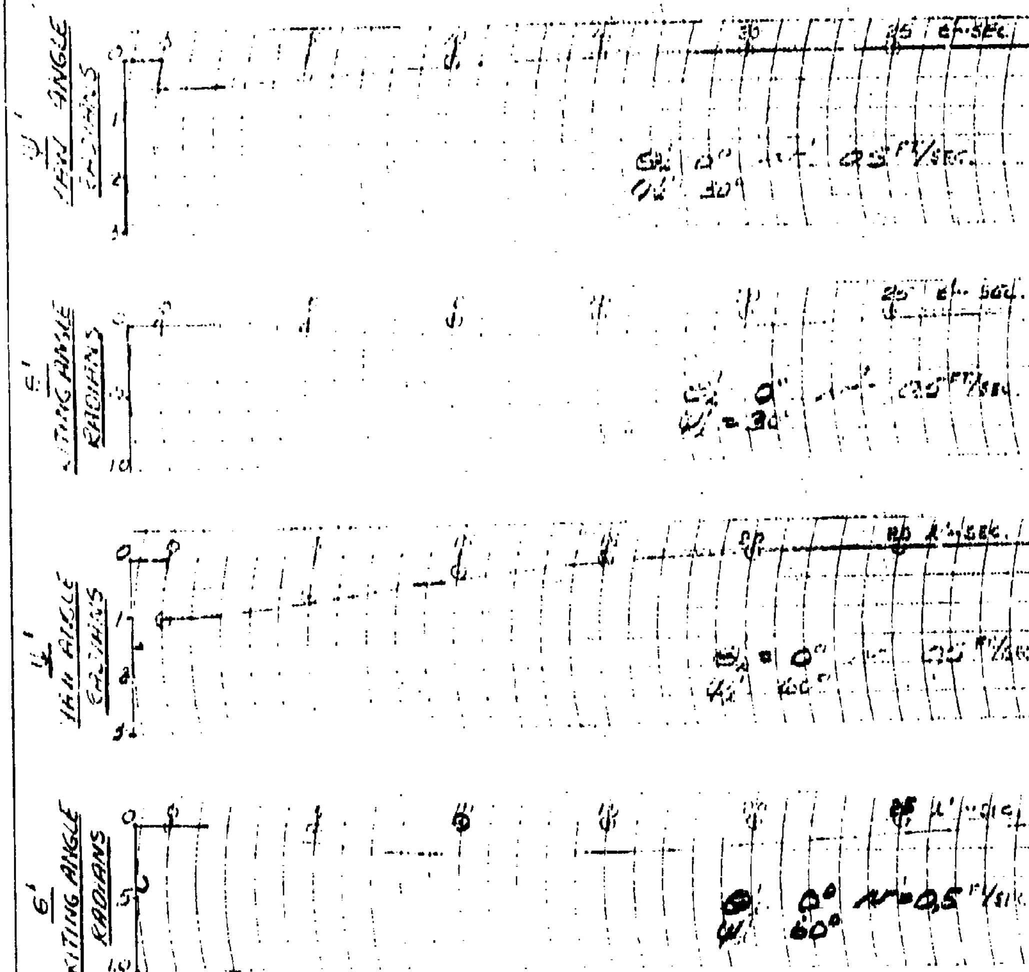

FIGURE [illegible]

1/75TH SCALE WATER MODEL OF THE ZPGW AIRSHIP

COMPARISON BETWEEN MEASURED & CALCULATED MOTIONS

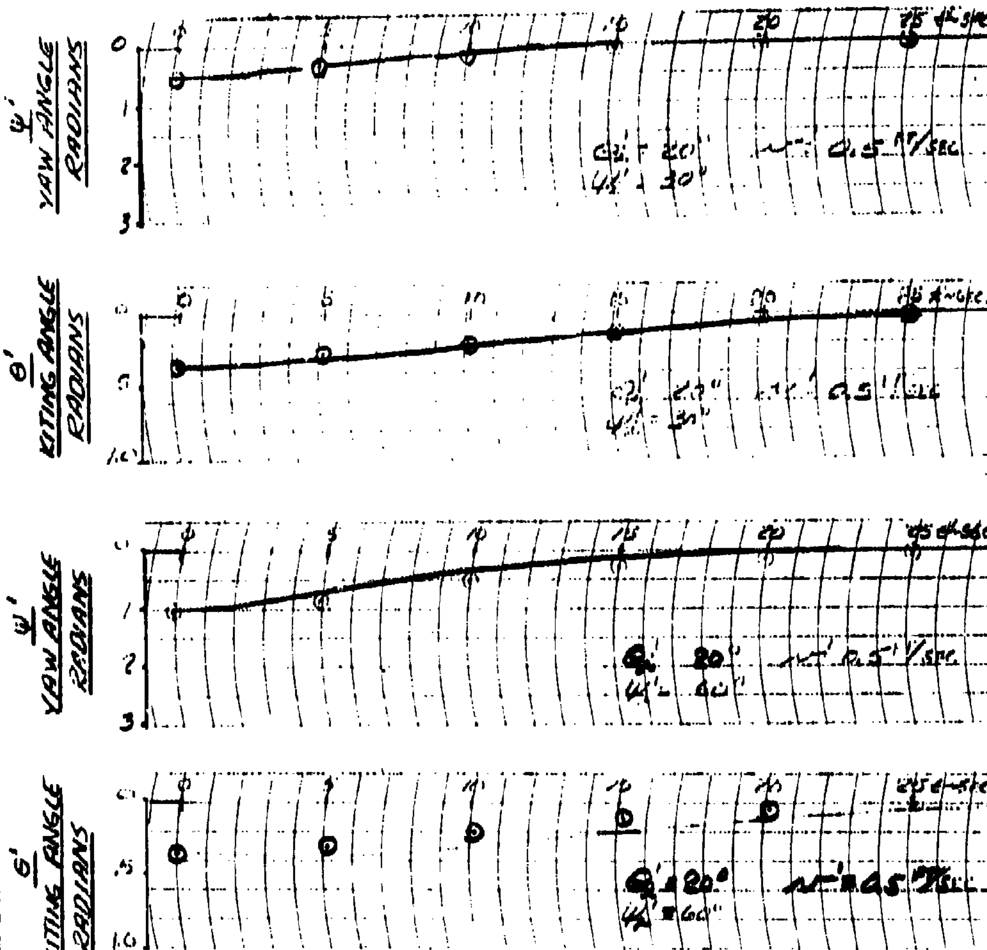

FIGURE #8
1/75TH SCALE WATER MODEL OF THE ZP2W AIRSHIP
COMPARISON BETWEEN MEASURED & CALCULATED MOTIONS

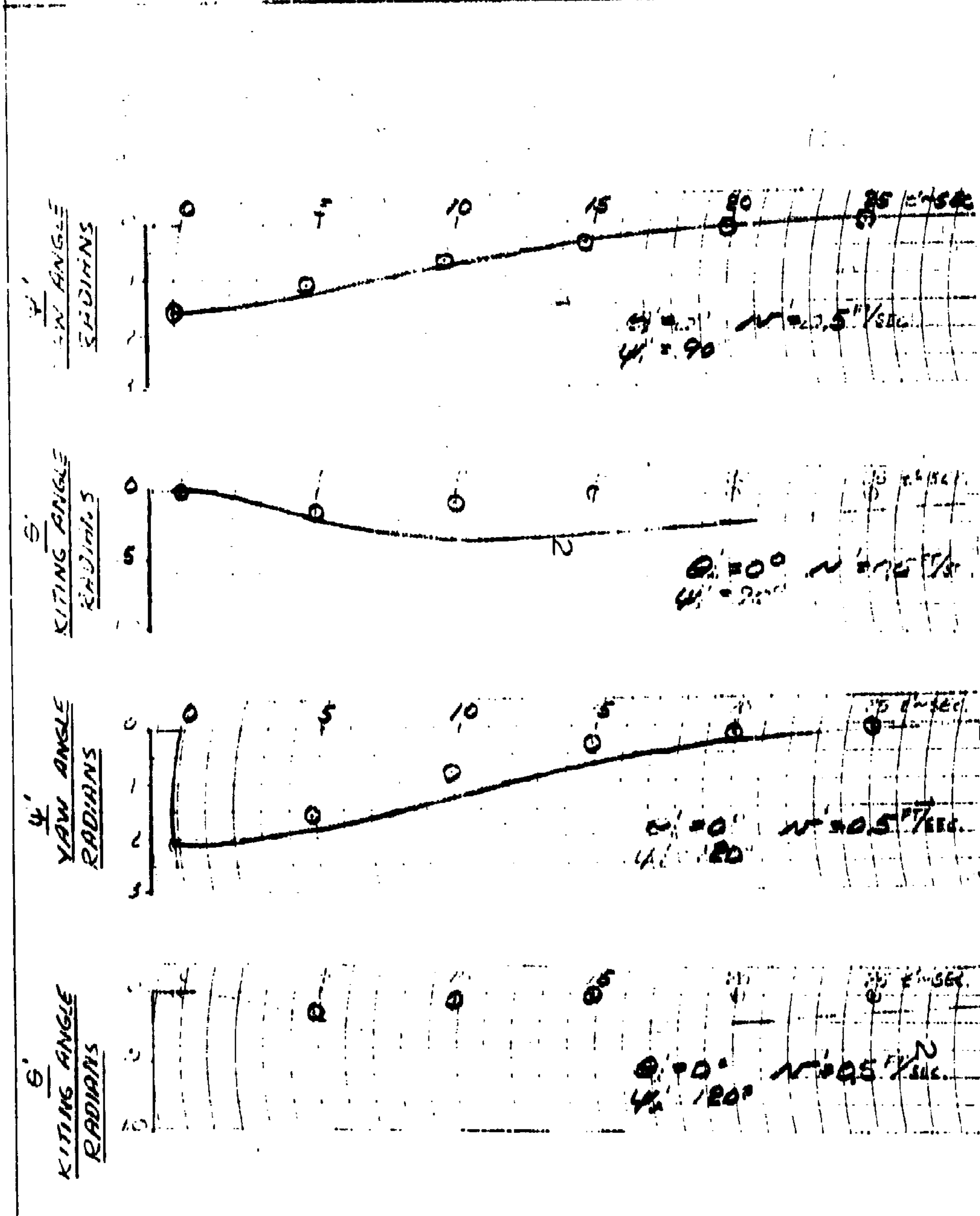

PREPARED J.D.L.
CHECKED J.W.B.
DATE May 1, 1961
REV. DATE

GOODYEAR
GOODYEAR AIRCRAFT CORPORATION
AKRON OHIO

PAGE 54
MODEL 2PG-2/2W/3W
GER- 10052

FIGURE 8
1/75TH SCALE WATER MODEL OF THE ZPGW AIRSHIP
COMPARISON BETWEEN MEASURED & CALCULATED MOTIONS

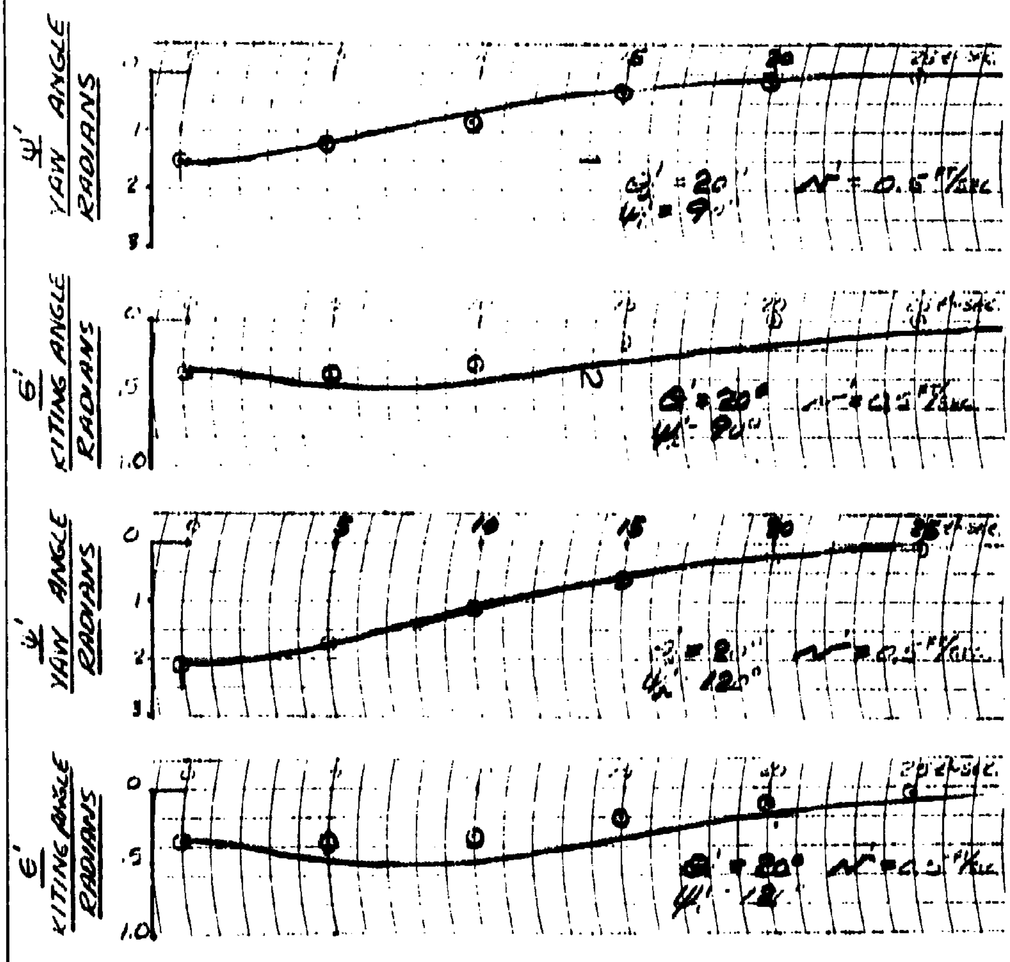

PREPARED J.D.M.
CHECKED J.W.B.
DATE May 1, 1961
REV DATE

GOODYEAR
GOODYEAR AIRCRAFT CORPORATION
AKRON OHIO

PAGE 55
MODEL ZPG-2/2W/3W
GER- 10052
CODE 25500

FIGURE [illegible]
1/75TH SCALE WATER MODEL OF THE ZP2W AIRSHIP
COMPARISON BETWEEN MEASURED & CALCULATED MOTIONS

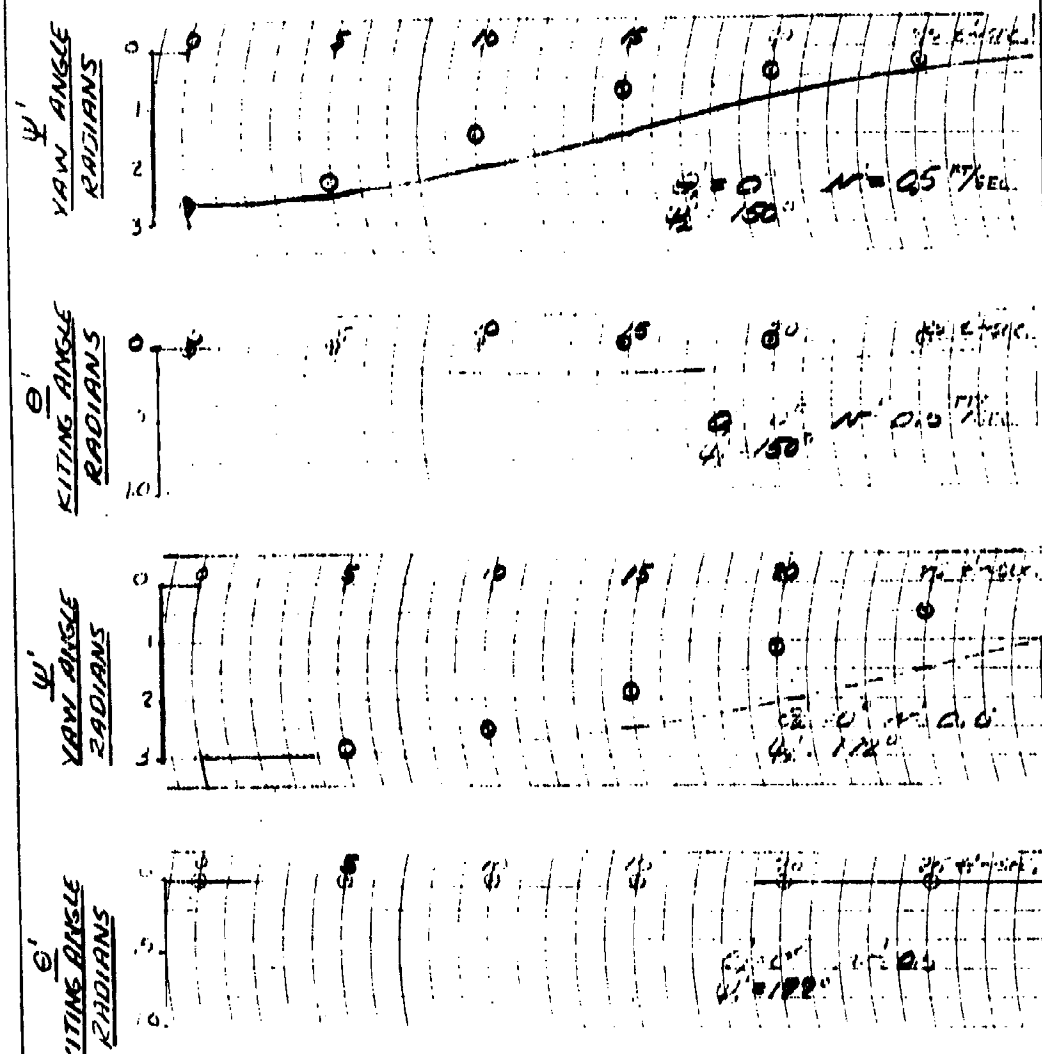

FIGURE [illegible]

1/75TH SCALE WATER MODEL OF THE ZP2W AIRSHIP

COMPARISON BETWEEN MEASURED & CALCULATED MOTIONS

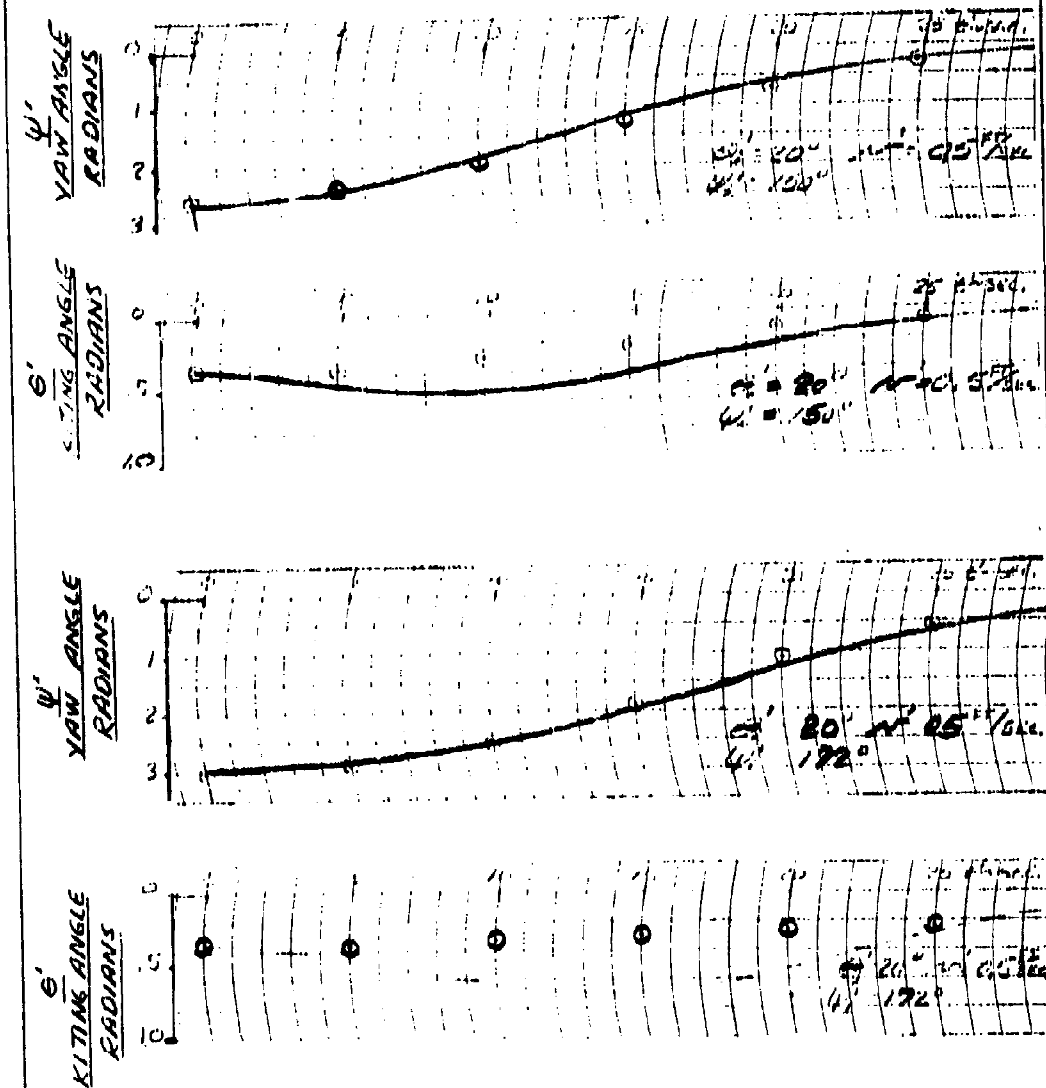

PREPARED BY J. D. M.
CHECKED BY J. W. B.
DATE May 1, 1961
REVISED

GOODYEAR AIRCRAFT

PAGE [illegible]
MODEL 2PC-[illegible]
GER- 100[illegible]
REF NO.

FIGURE 9

1/75TH SCALE ZPN-2 AIRSHIP WATER MODEL (REF [illegible])

CORRECTION FOR DISSIMILARITY IMPOSED BY THE BOOM

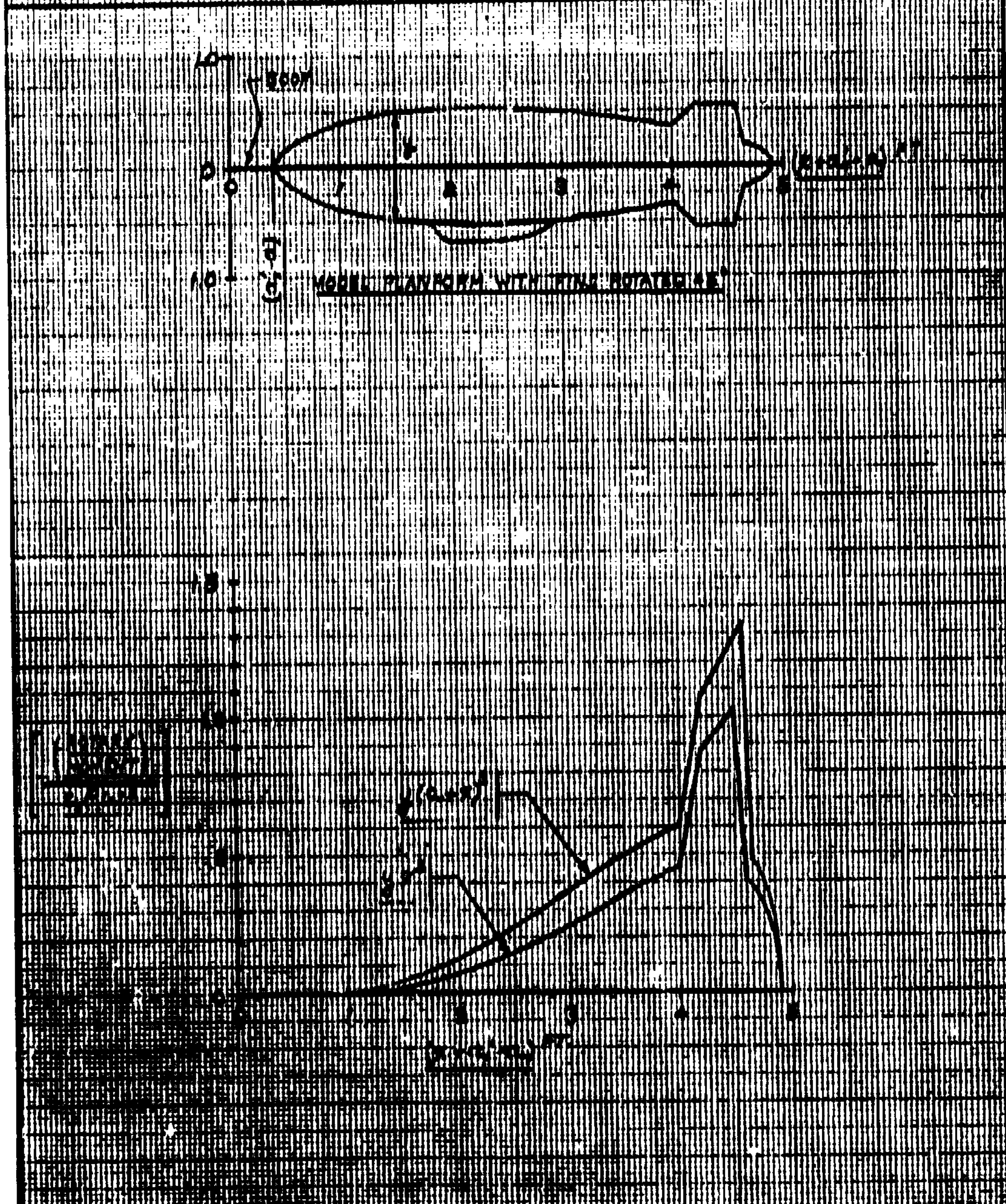

PREPARED BY J. D. M.
CHECKED BY J. W. B.
DATE May 1, 1961
REVISED

GOODYEAR AIRCRAFT

PAGE 56
MODEL ZPG-2/2W/3W
GER-10052
REF NO.

FIGURE 10
ZPG-2/2W/3W AIRSHIPS
AERODYNAMIC DAMPING MOMENT COEFFICIENTS

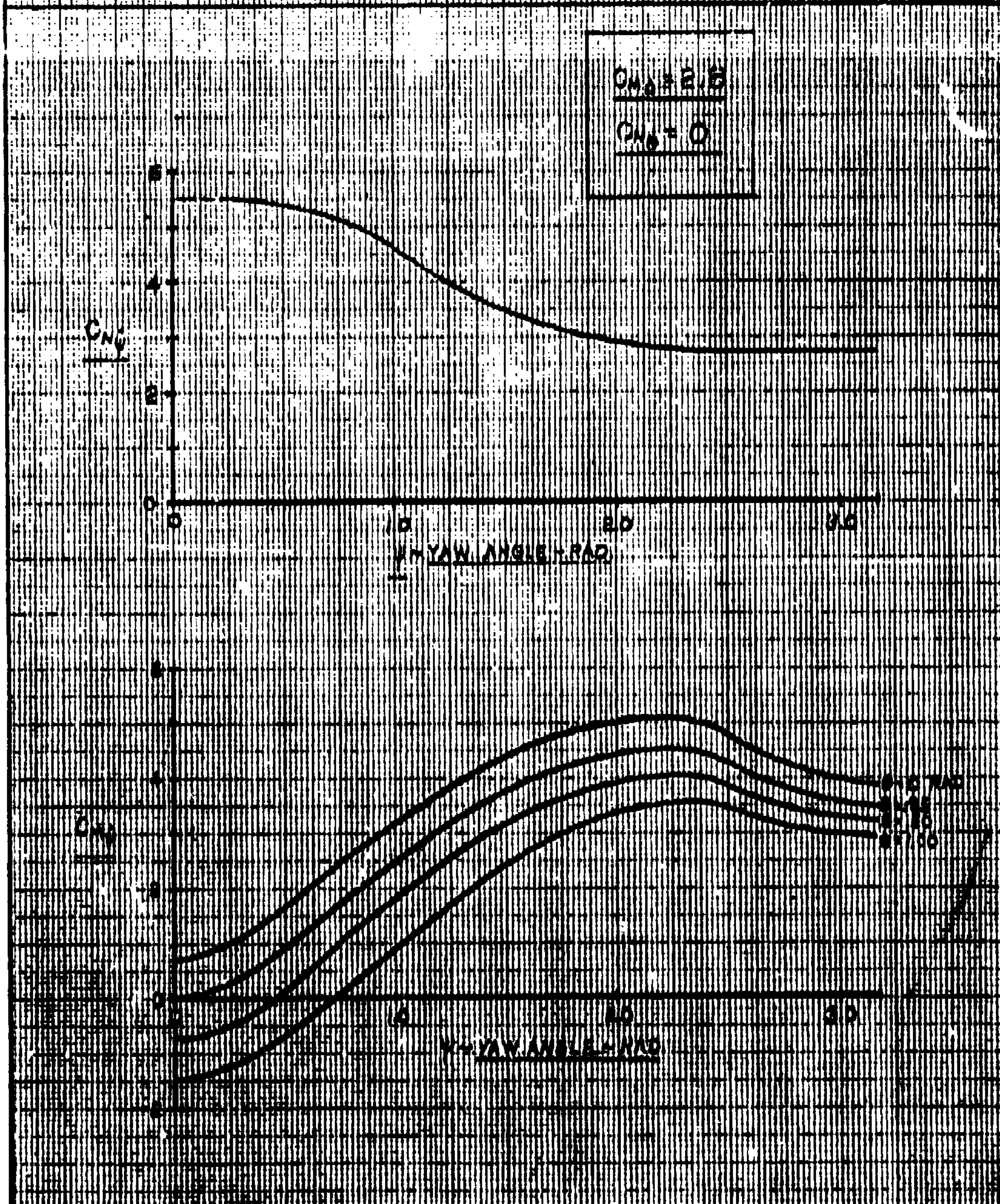

PREPAR
CHECKE
DATE
REVISE

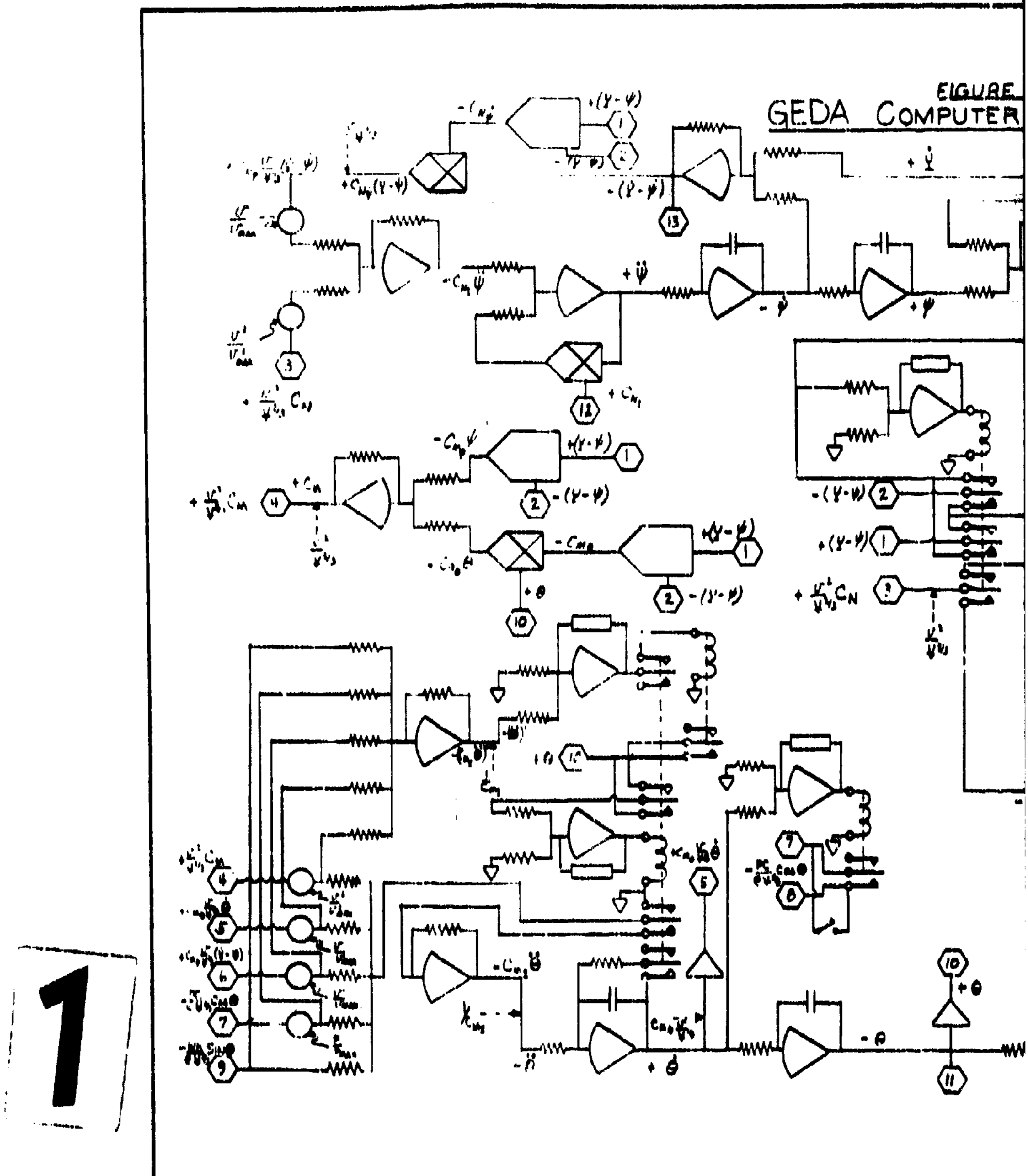

FIGURE 11
GEDA COMPUTER SCHEMATIC

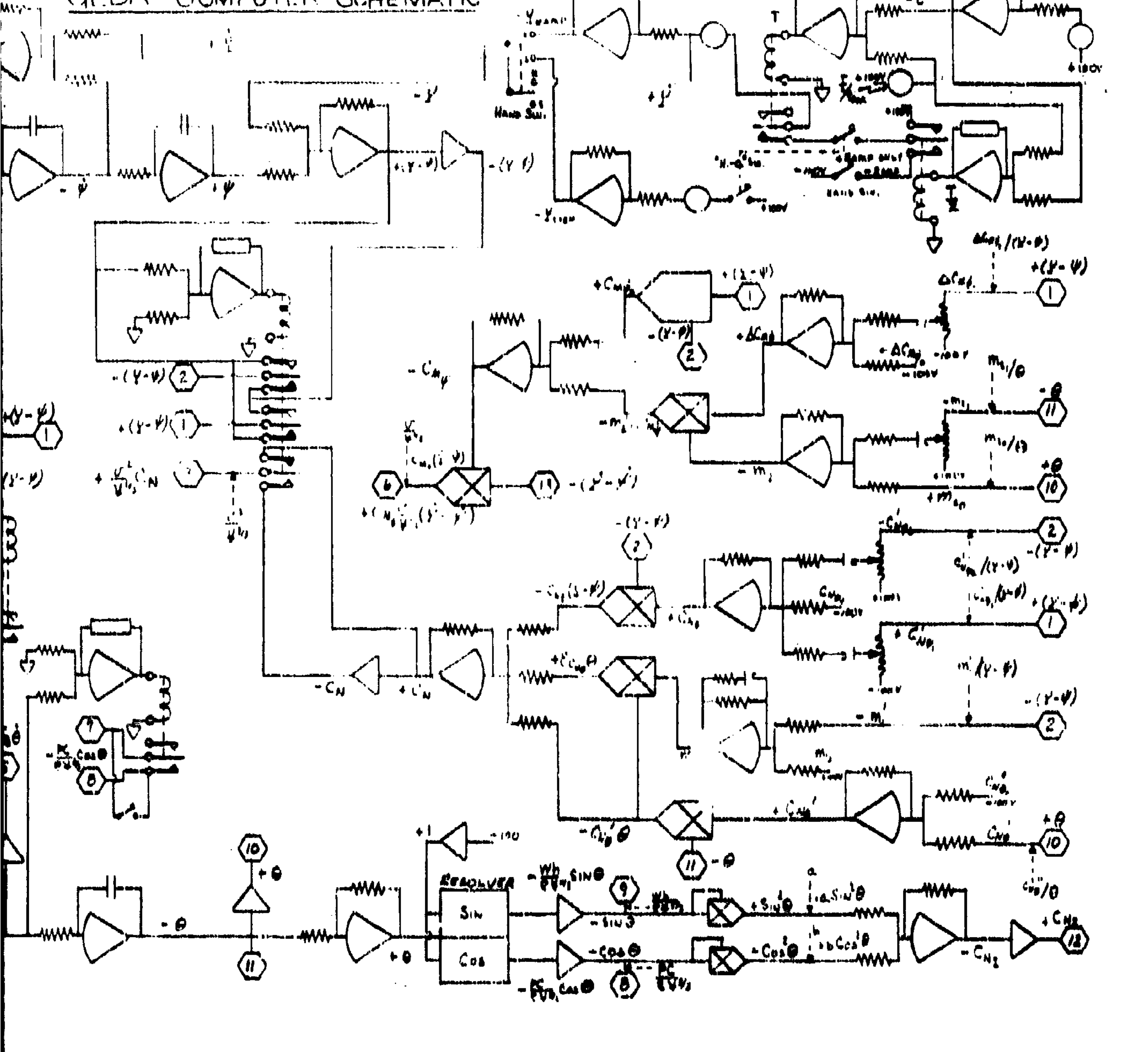

PREPARED BY J.D...
J.W...
CHECKED BY
DATE May 1, 1...
REVISED

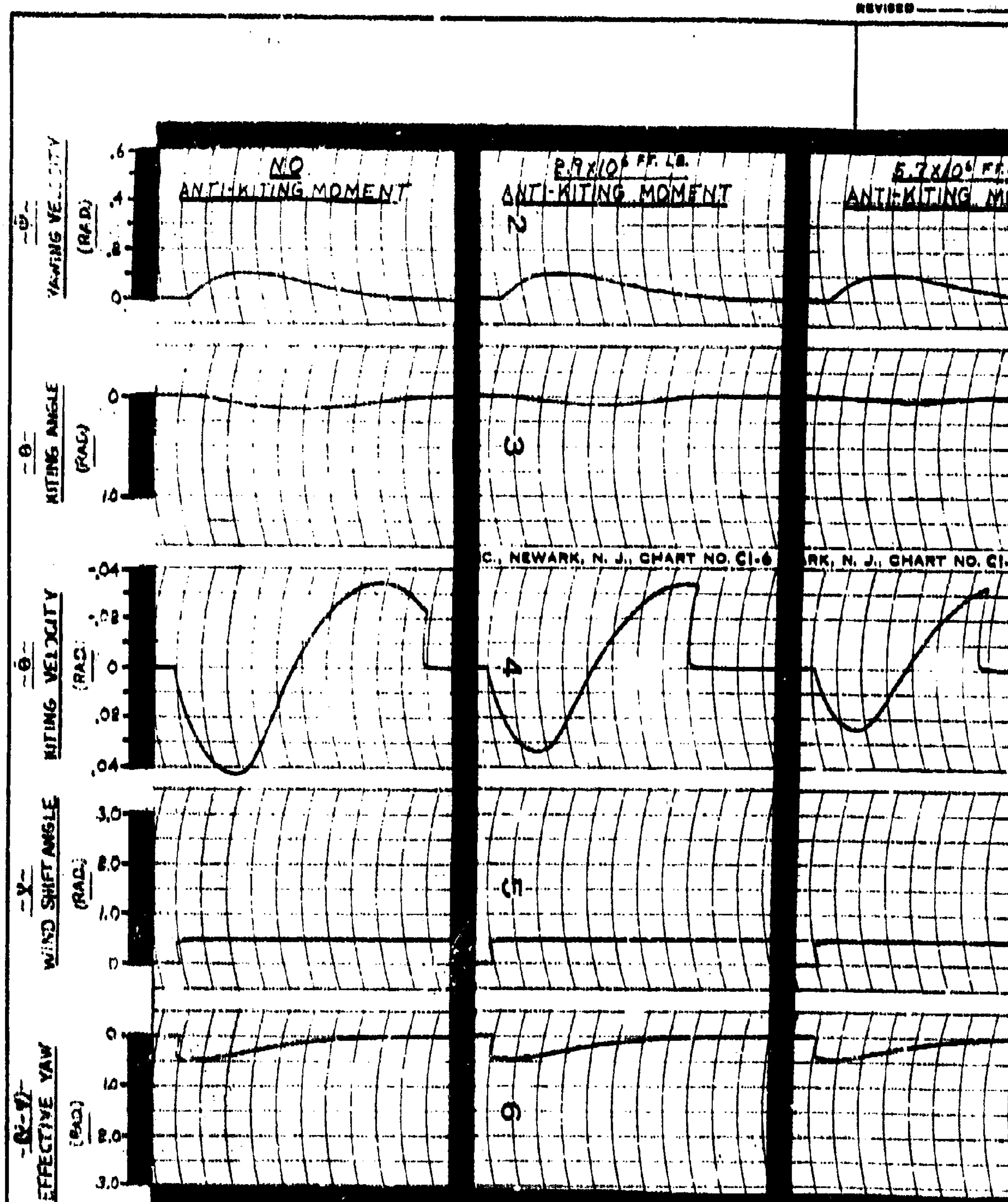

1

FIGURE 12

ZPG-3W AIRSHIP ANTI-KITING STUDY

$\psi = .5$ RAD ~ CONVENTIONAL ANTI-KITER ~ $V_{TS} = 55$ KN.

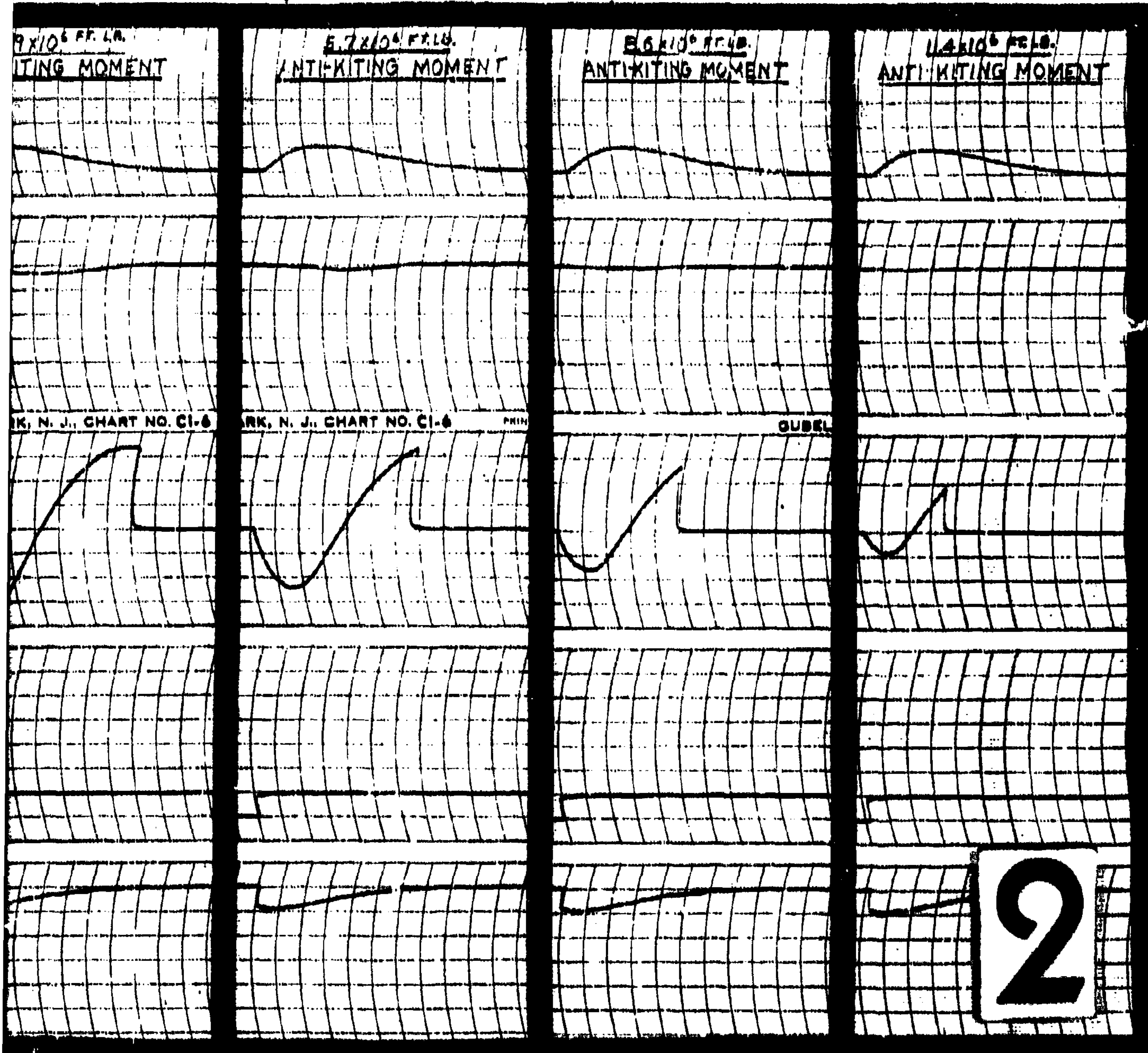

PREPARED	J. D. M.	PAGE	61
CHECKED	J. J. R.	MODEL	ZPG-2/2W/3W
DATE	May 1, 1961	GER-	10052
REV DATE		CODE	25500

GOODYEAR
GOODYEAR AIRCRAFT CORPORATION
AKRON OHIO

FIGURE 12 (CON'T)

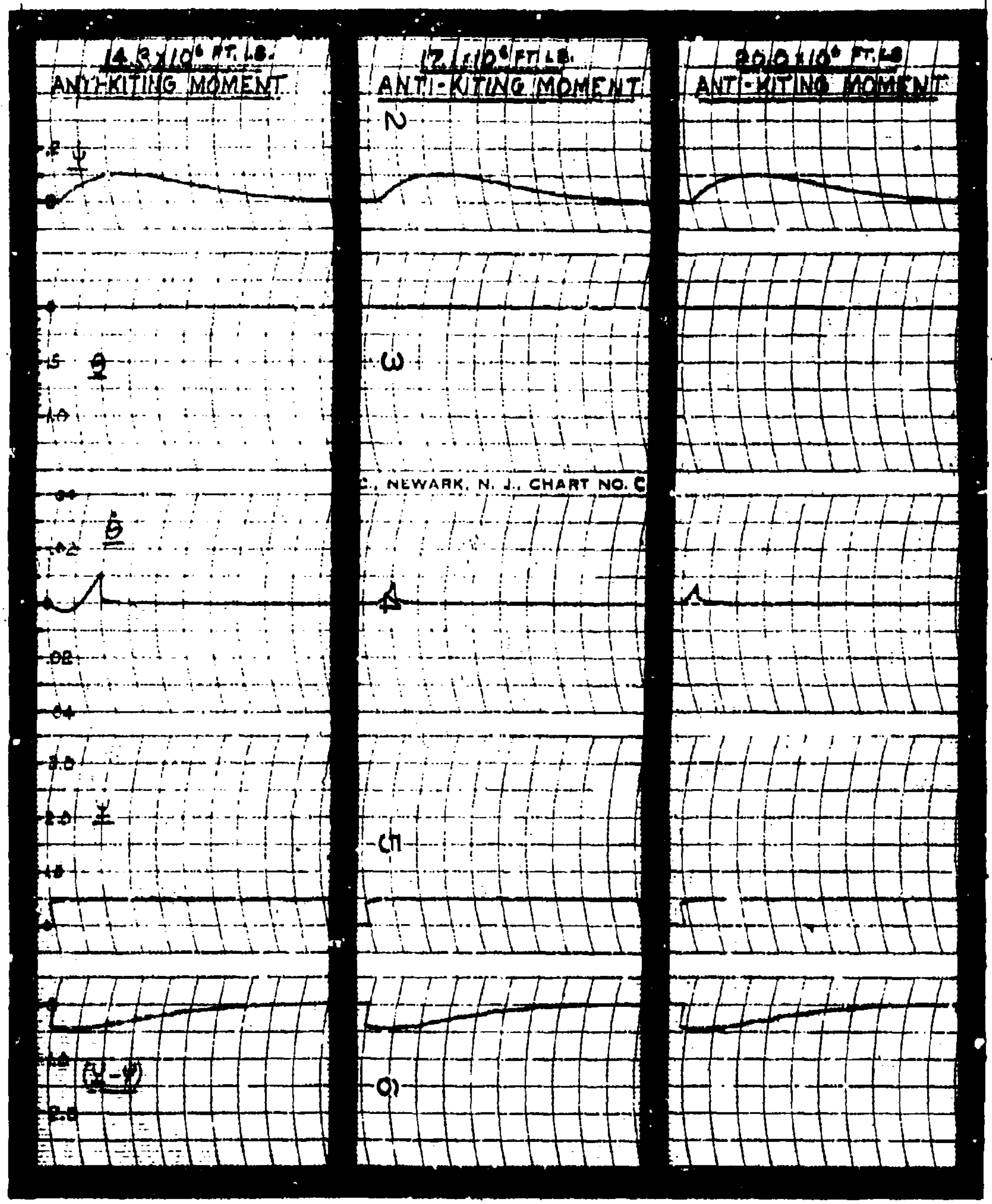

PREPARED BY J.D.M.
CHECKED BY J.W.B.
DATE May 1, 1961
REVISED

GOODYEAR AIRCRAFT

PAGE 62 63
MODEL ZPG-2/2W/3W
SER 10052
REP. NO. Code 25500

FIGURE 13
ZPG-3W AIRSHIP WITH CONVENTIONAL ANTI-KITER
MAXIMUM KITING ANGLES & CONTACT VELOCITIES
30° EQUIVALENT SUDDEN WINDSHIFT

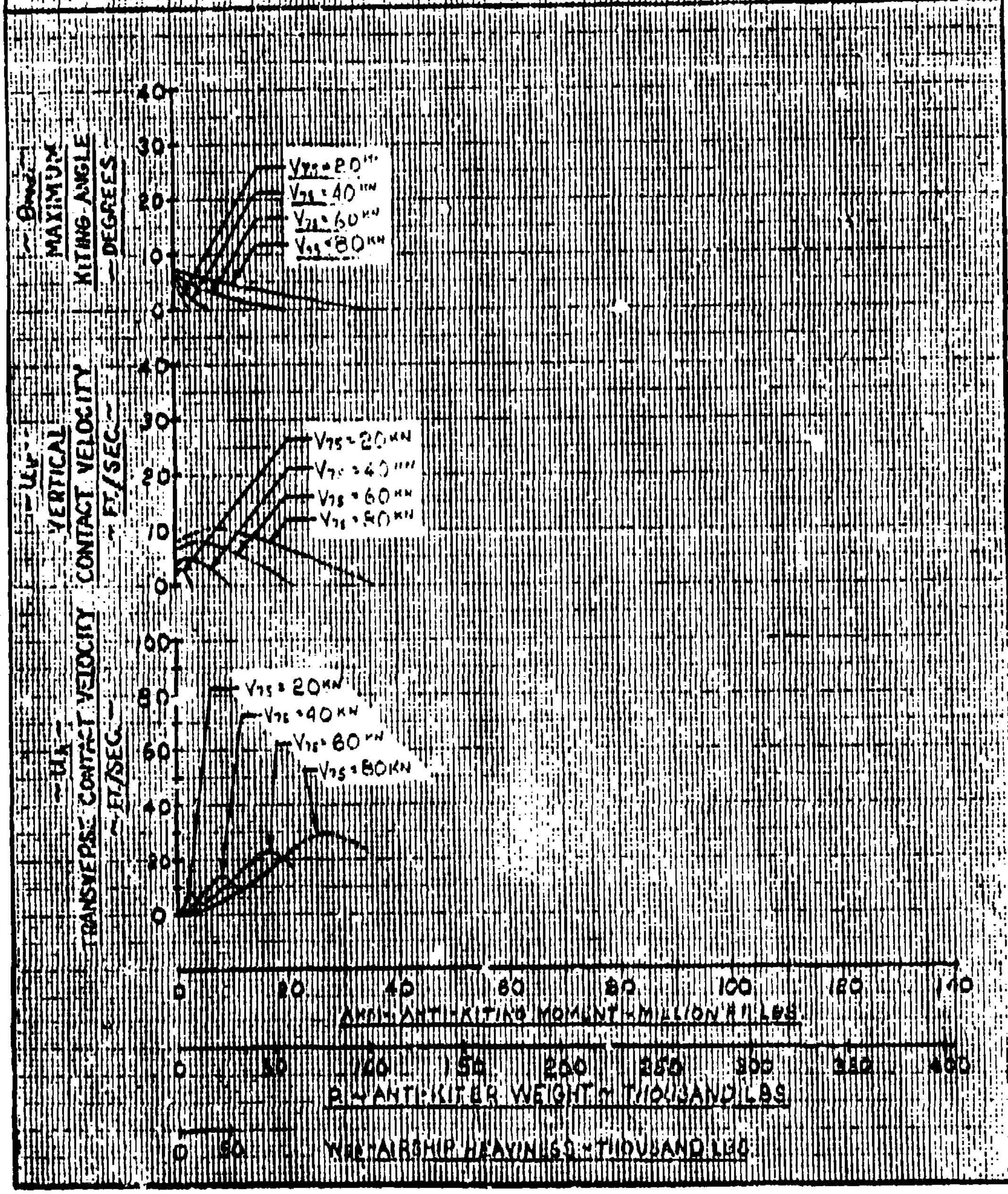

FIGURE 14
ZPG-3W AIRSHIP WITH CONVENTIONAL ANTI-KITER
MAXIMUM KITING ANGLES & CONTACT VELOCITIES
20° EQUIVALENT SUDDEN WINDSHIFT

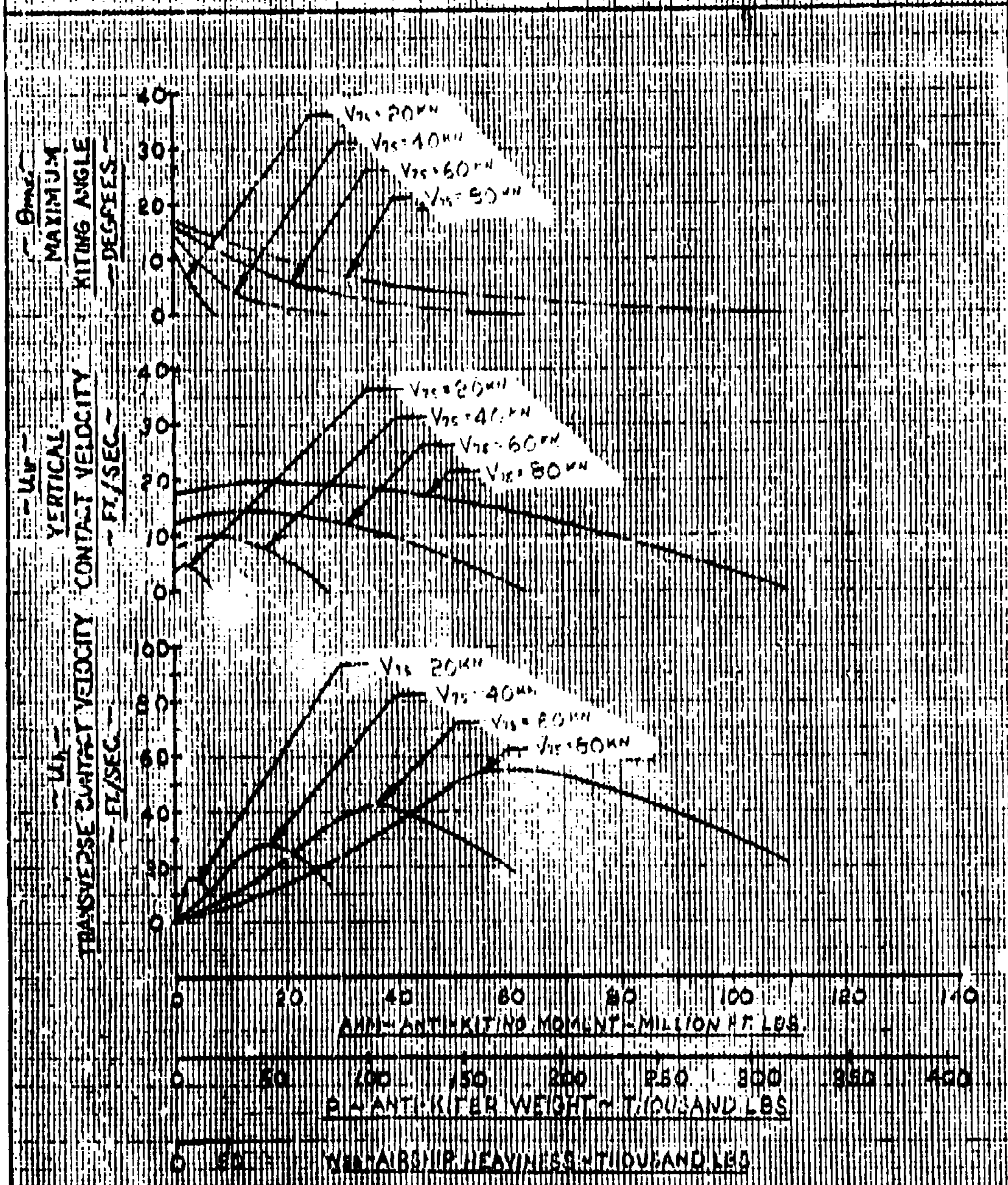

PREPARED BY J. D. M.
CHECKED BY J. W. R.
DATE May 1, 1961
REVISED

GOODYEAR AIRCRAFT

MODEL ZPG-2/2W/3W
10052
SER
REF NO. Code 25500

FIGURE 15
ZPG-3W AIRSHIP WITH CONVENTIONAL ANTI-KITER
MAXIMUM KITING ANGLES & CONTACT VELOCITIES
90° EQUIVALENT SUDDEN WINDSHIFT

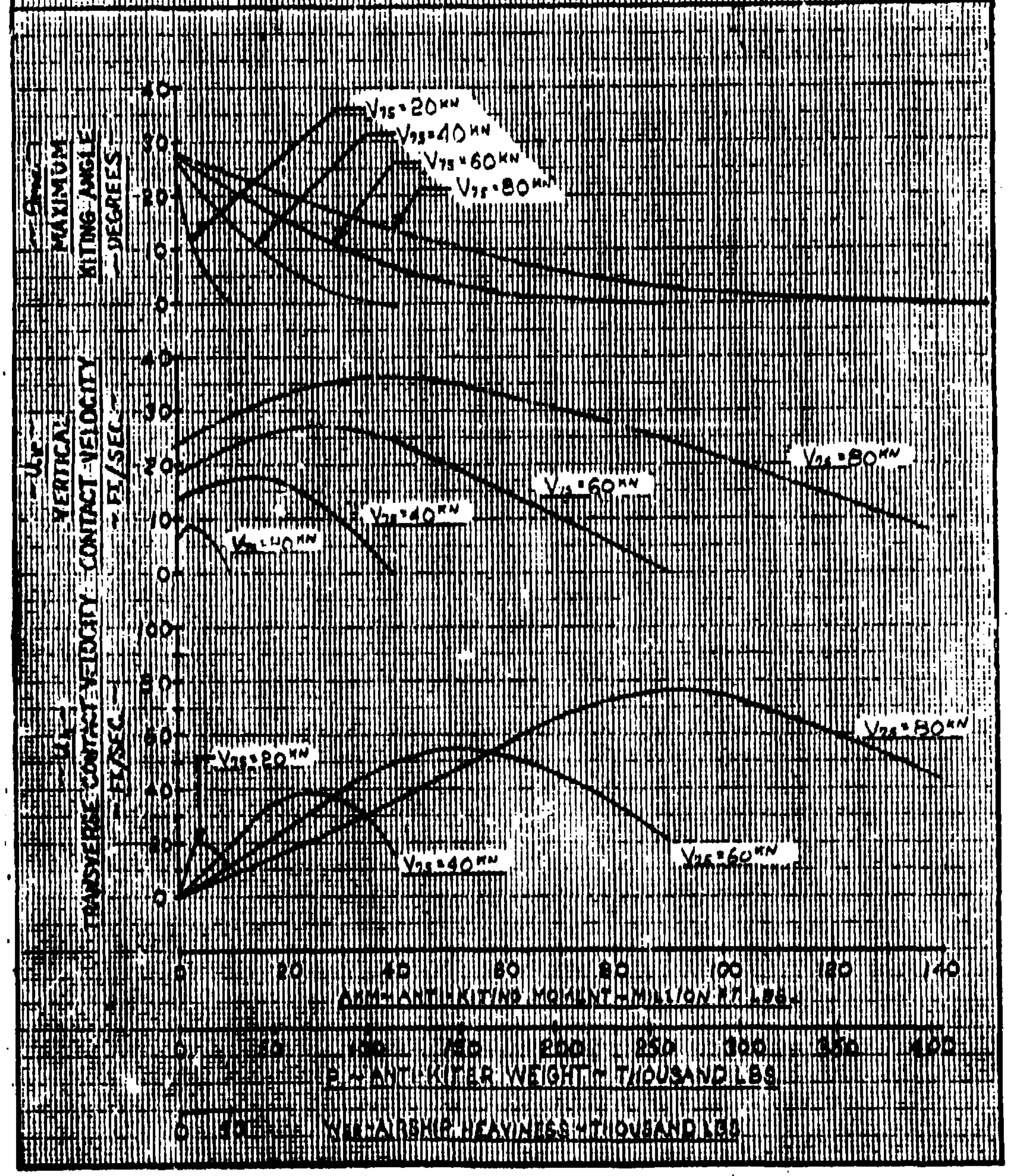

PREPARED BY J.D.M.
CHECKED BY J.W.B.
DATE May 1, 1961
REVISED

GOODYEAR AIRCRAFT

PAGE 65
MODEL ZPO-2/2W/3W
GER- 10052
REF NO. Code 25500

FIGURE 16
ZPG-3W AIRSHIP WITH CONVENTIONAL ANTI-KITER
MAXIMUM KITING ANGLES & CONTACT VELOCITIES
180° EQUIVALENT SUDDEN WINDSHIFT

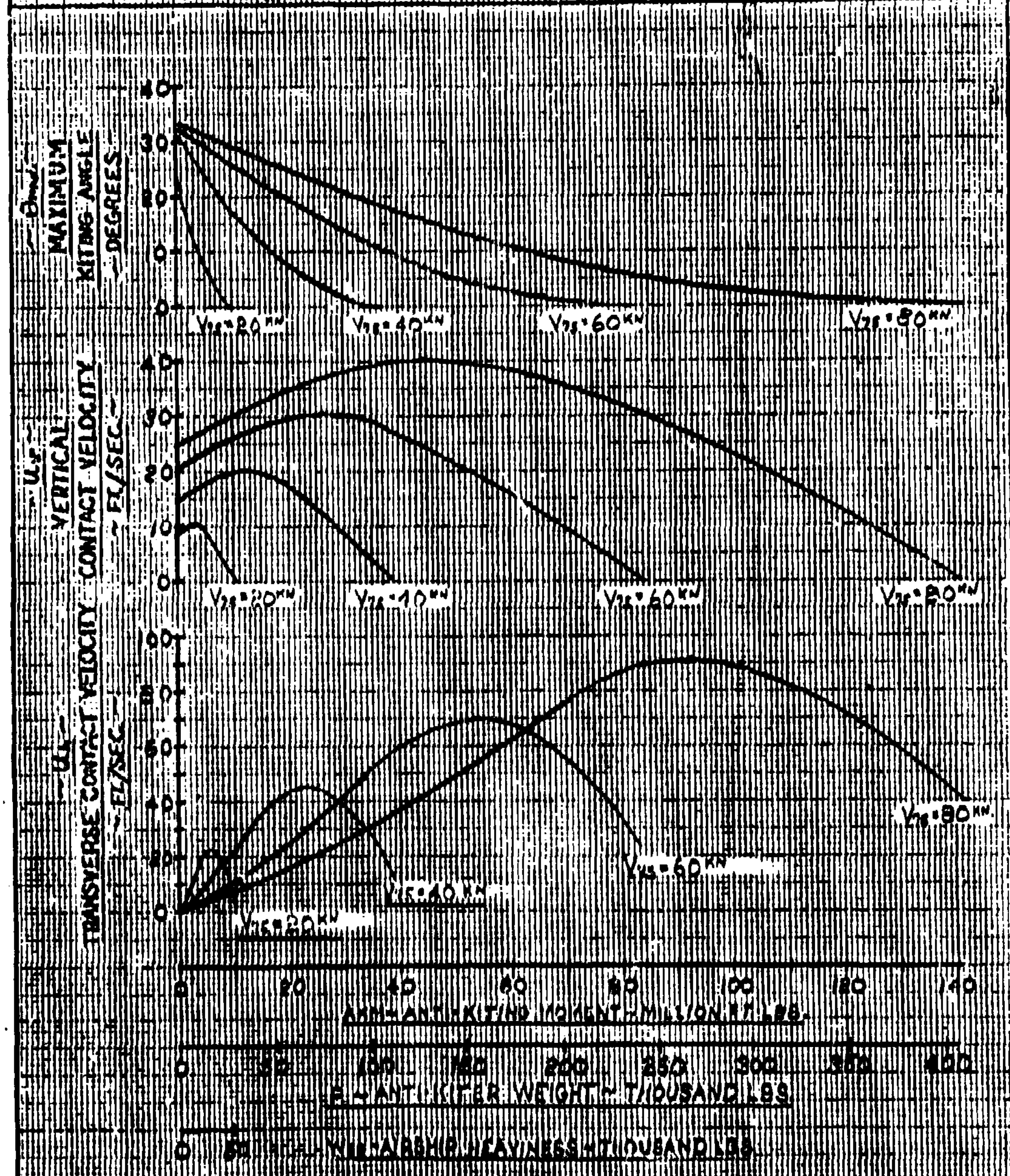

PREPARED BY J.D.M.
CHECKED BY J.W.B.
DATE May 1, 1961
REVISED

GOODYEAR AIRCRAFT

PAGE 66
MODEL ZPG-2/2W/3W
GER 10052
REF NO. Code 25500

FIGURE 17
ZPG-2W AIRSHIP WITH CONVENTIONAL ANTI-KITER
MAXIMUM KITING ANGLES & CONTACT VELOCITIES
150° EQUIVALENT SUDDEN WINDSHIFT

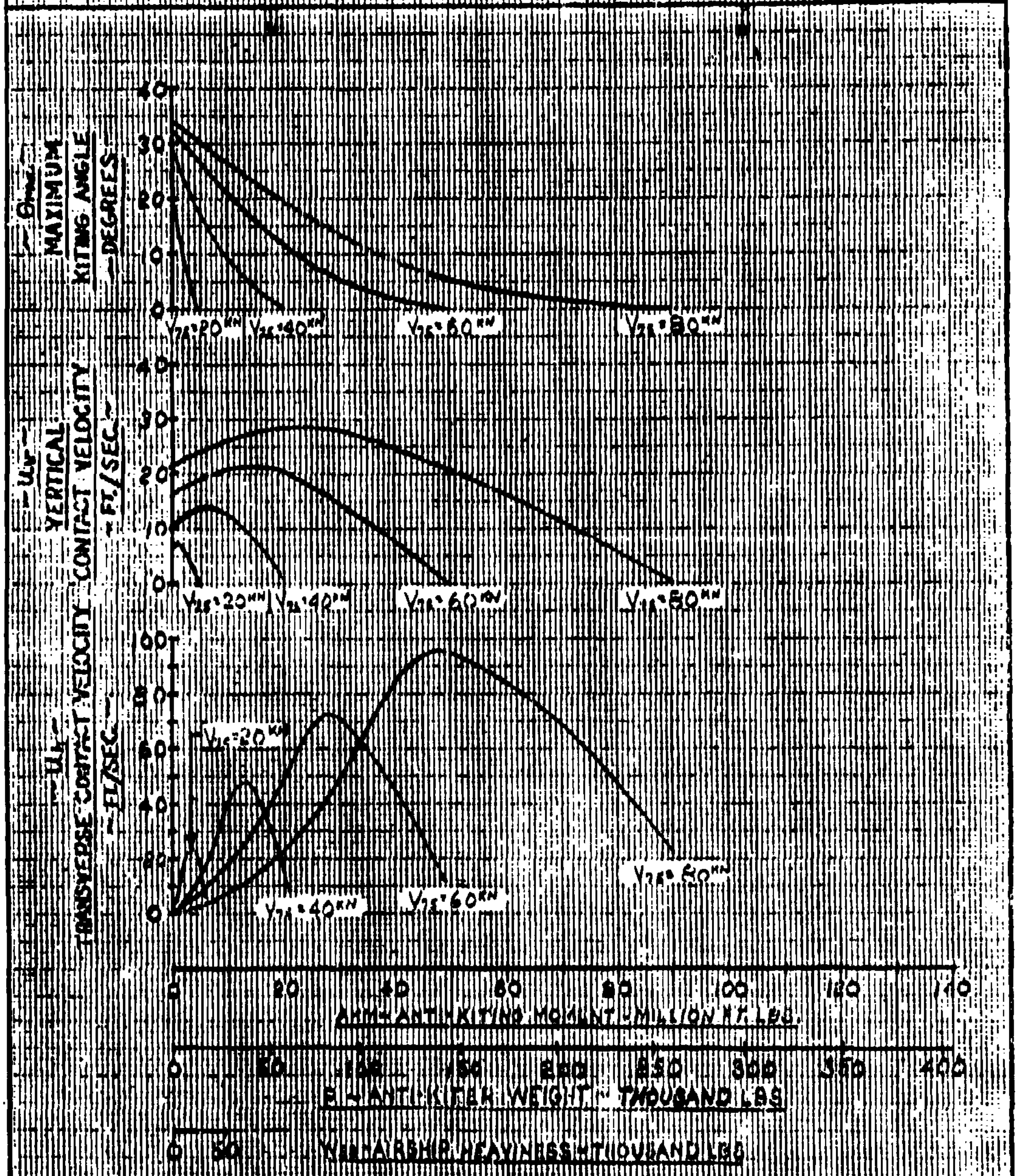

PREPARED BY J.D.M.
CHECKED BY J.W.B.
DATE May 1, 1961
REVISED

GOODYEAR AIRCRAFT

PAGE 67
MODEL ZPG-2/2W/3W
GER- 10052
REF NO. Code 25500

FIGURE 18

ZPG-3W AIRSHIP WITH CONVENTIONAL ANTI-KITER
MAXIMUM KITING ANGLES & CONTACT VELOCITIES
60° EQUIVALENT SUDDEN WINDSHIFT

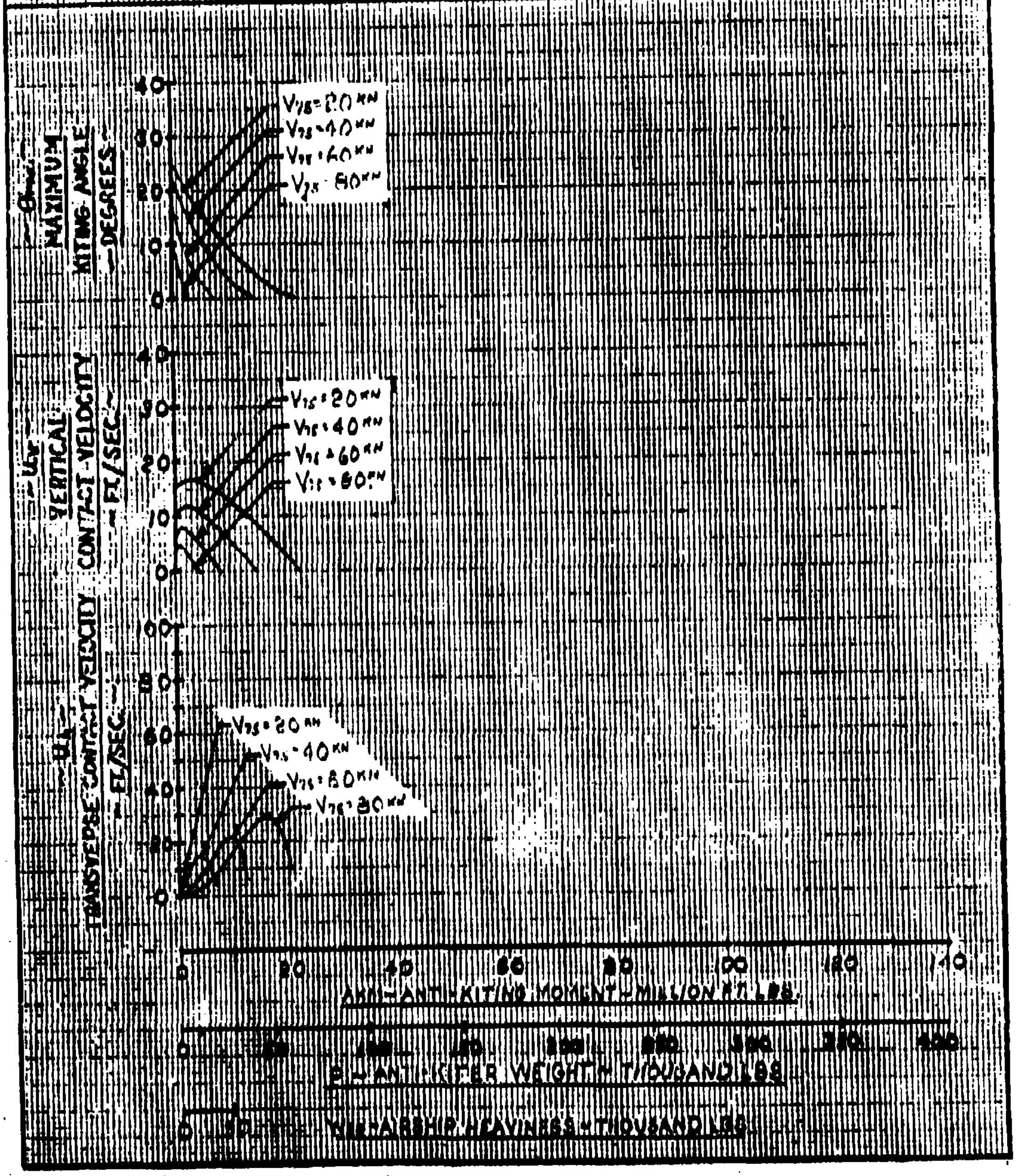

PREPARED BY
CHECKED BY
DATE
REVISED

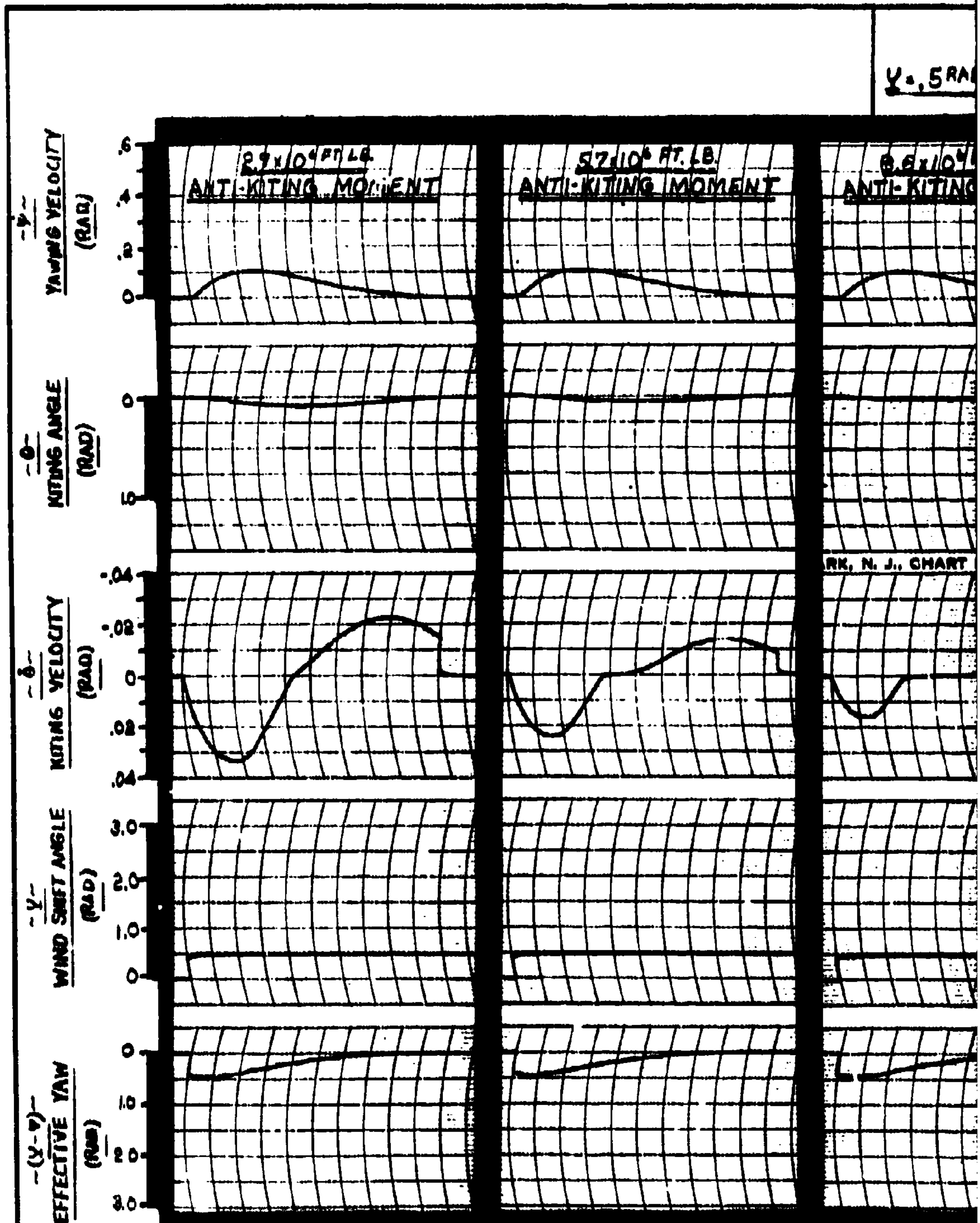

1

PREPARED BY J.D.M.
CHECKED BY J.W.B.
DATE May 1, 1962
REVISED

GOODYEAR AIRCRAFT

PAGE 68
MODEL ZPG-2/2W/3W
GER 10052
REP NO. Code 25500

FIGURE 19
ZPG-3W AIRSHIP ANTI-KITING STUDY
γ = .5 RAD. ~ ANTI-KITER WITH IMPROVED ATTACHMENT SYSTEM ~ V_{IS} = 55 KN

PREPARED J.D.M.
CHECKED J.W.B.
DATE May 1, 1961
REV DATE

GOODYEAR
GOODYEAR AIRCRAFT CORPORATION
AKRON OHIO

PAGE 69
MODEL ZPG-2/2W/3W
SER- 10052
CODE

FIGURE 19 (CON'T)

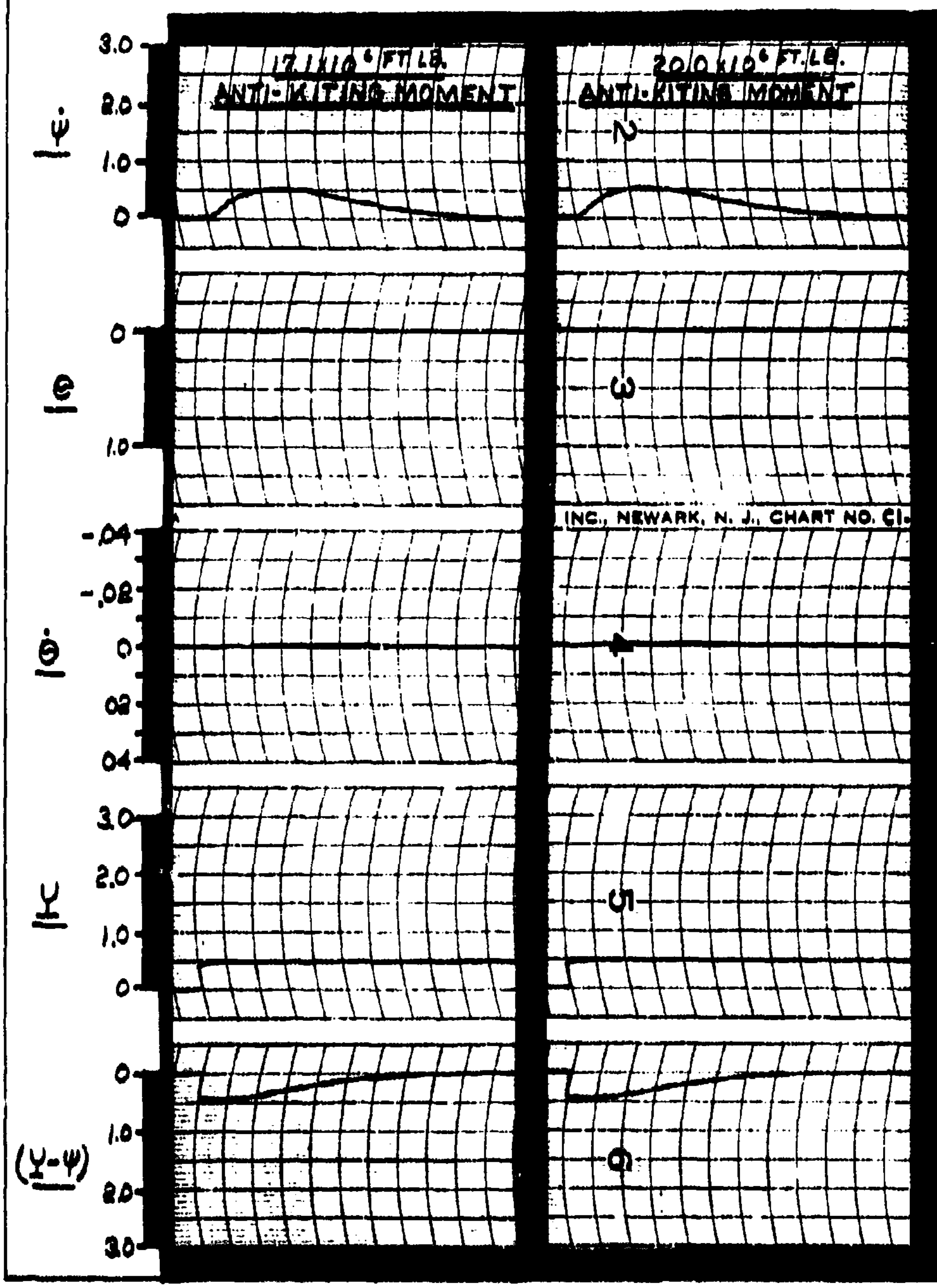

PREPARED J.D.M.
CHECKED J.W.B.
DATE May 1, 1961
REV DATE

GOODYEAR
GOODYEAR AIRCRAFT CORPORATION

PAGE 70
MODEL ZPG-2/3W/3W
GER- 10092
CODE 25500

FIGURE 20
ZPG-3W AIRSHIP WITH IMPROVED ANTI-KITER ATTACHMENT SYSTEM
MAXIMUM KITING ANGLES & CONTACT VELOCITIES
30° EQUIVALENT SUDDEN WINDSHIFT

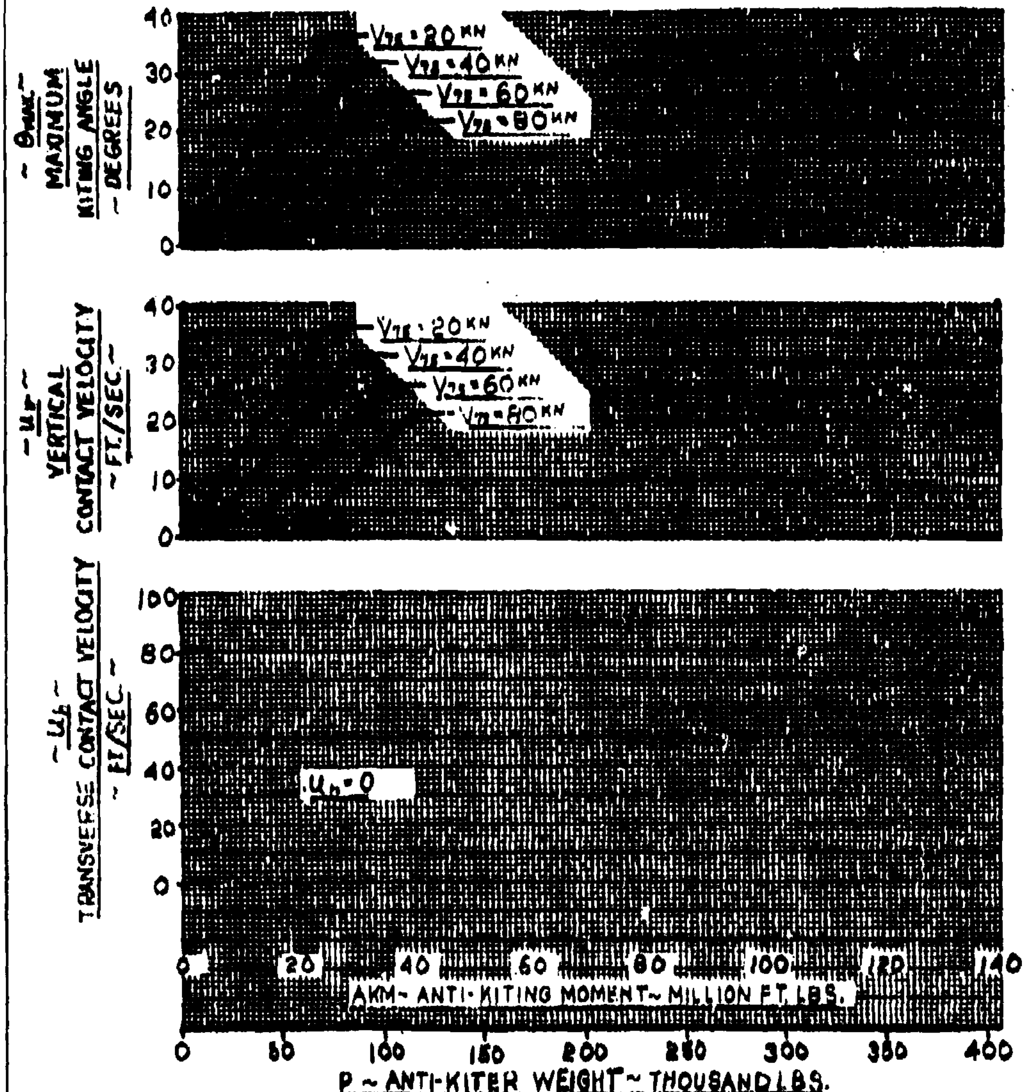

FIGURE 21

ZPG-3W AIRSHIP WITH IMPROVED ANTI-KITER ATTACHMENT SYSTEM
MAXIMUM KITING ANGLES & CONTACT VELOCITIES
60° EQUIVALENT SUDDEN WINDSHIFT

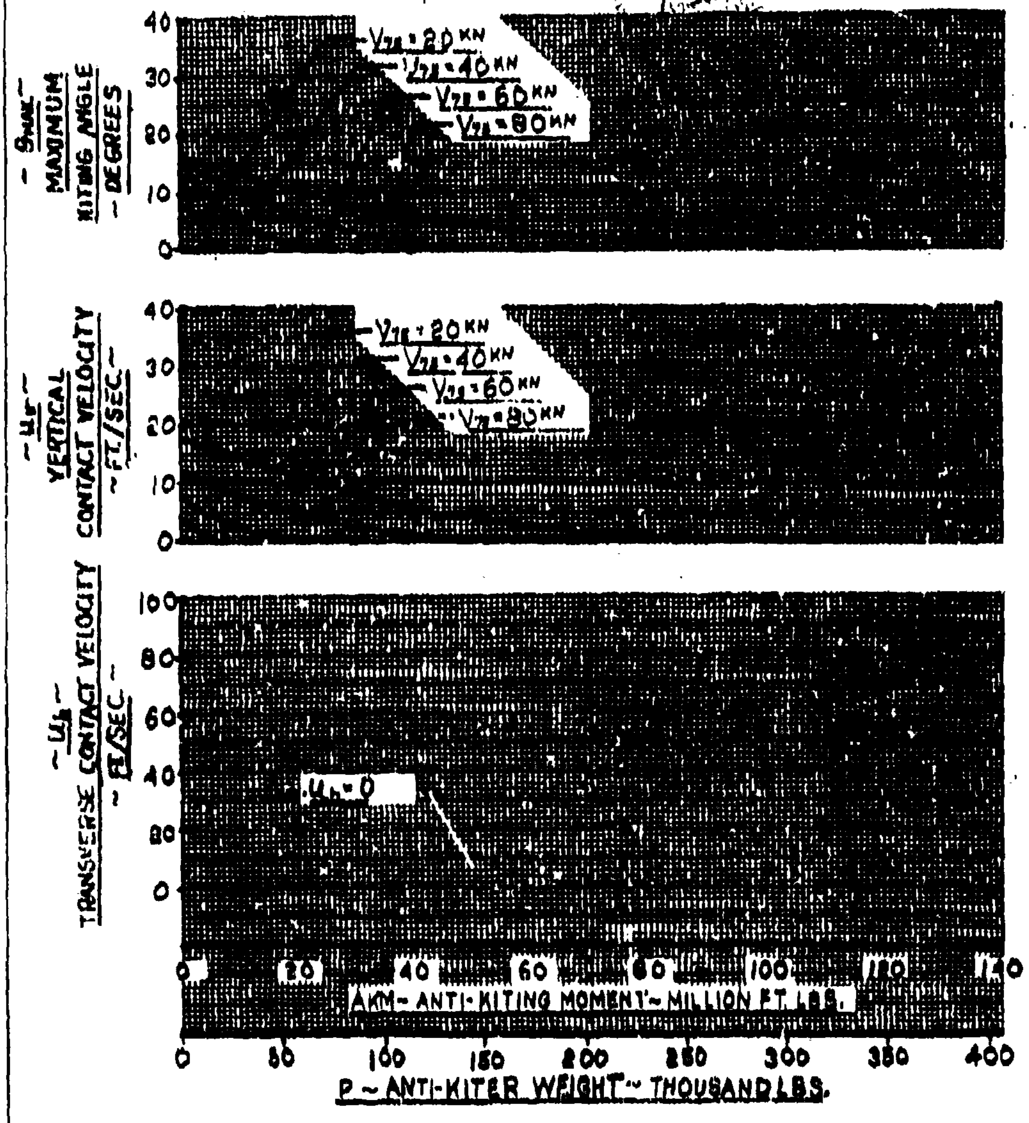

FIGURE 22
ZPG-3W AIRSHIP WITH IMPROVED ANTI-KITER ATTACHMENT SYSTEM
MAXIMUM KITING ANGLES & CONTACT VELOCITIES
70° EQUIVALENT SUDDEN WINDSHIFT

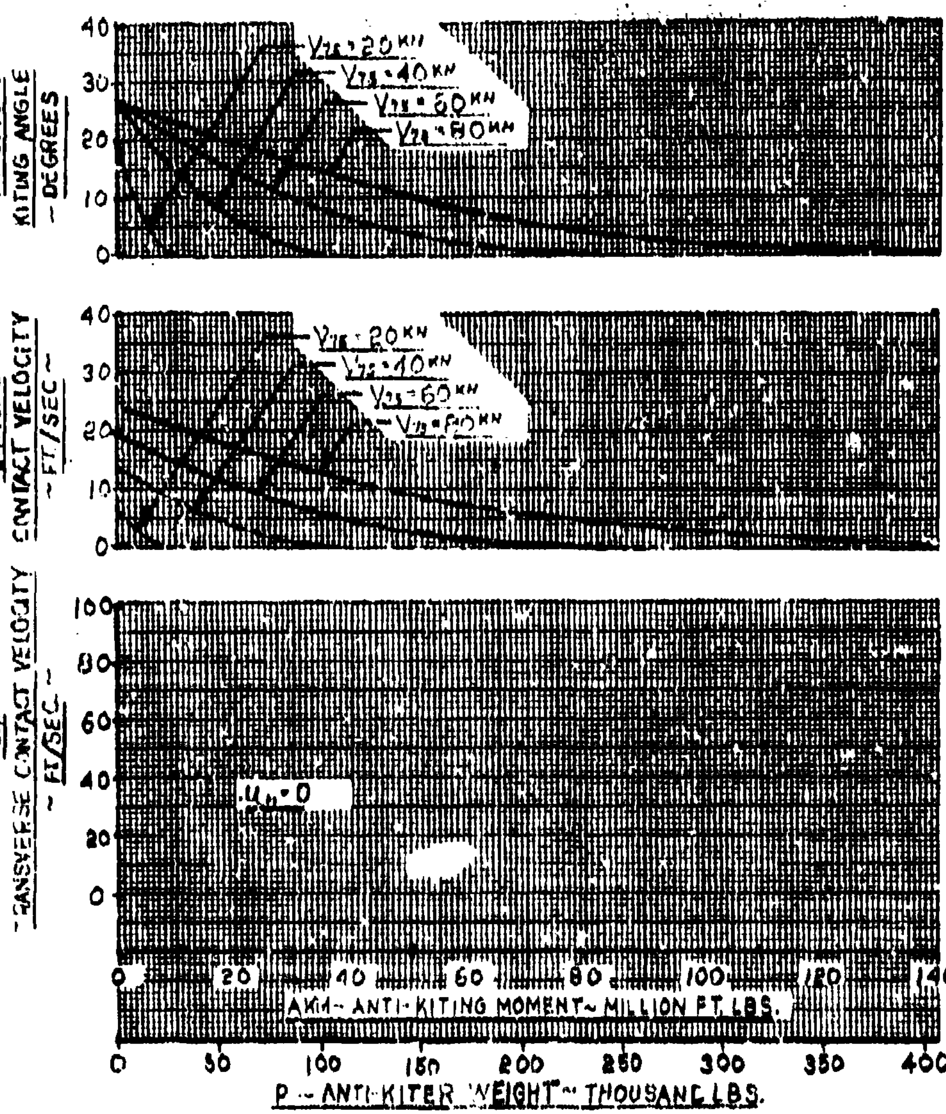

PREPARED J.D.M.
CHECKED J.W.B.
DATE May 1, 1961
REV DATE

GOODYEAR
GOODYEAR AIRCRAFT CORPORATION

PAGE 73
MODEL ZPG-2/2W/3W
GER- 10052
CODE 25500

FIGURE 23
ZPG-3W AIRSHIP WITH IMPROVED ANTI-KITER ATTACHMENT SYSTEM
MAXIMUM KITING ANGLES & CONTACT VELOCITIES
180° EQUIVALENT SUDDEN WINDSHIFT

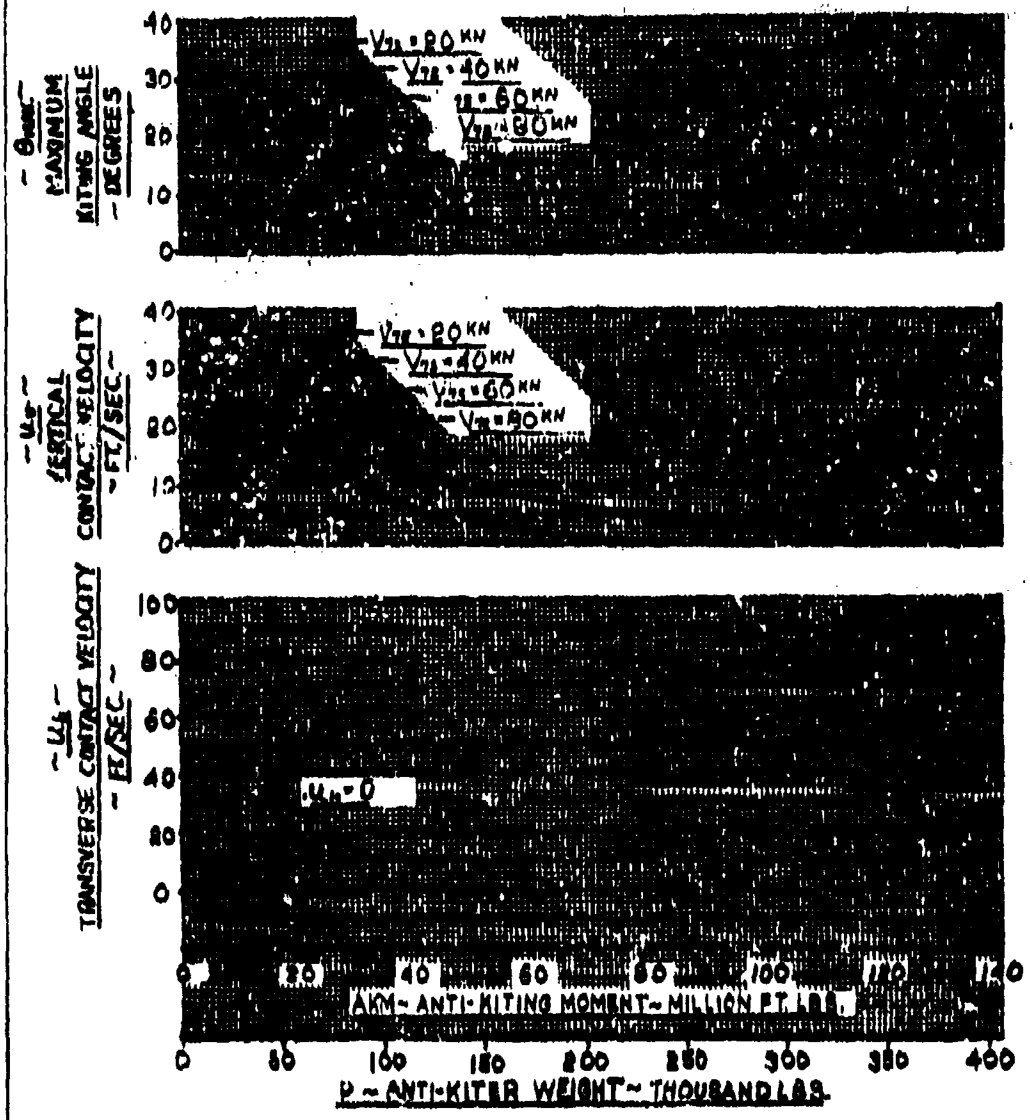

FIGURE 24

ZPG-3W AIRSHIP WITH IMPROVED ANTI-KITER ATTACHMENT SYSTEM
M[illegible]MUM KITING ANGLES & CONTACT VELOCITIES
15° EQUIVALENT SUDDEN WINDSHIFT

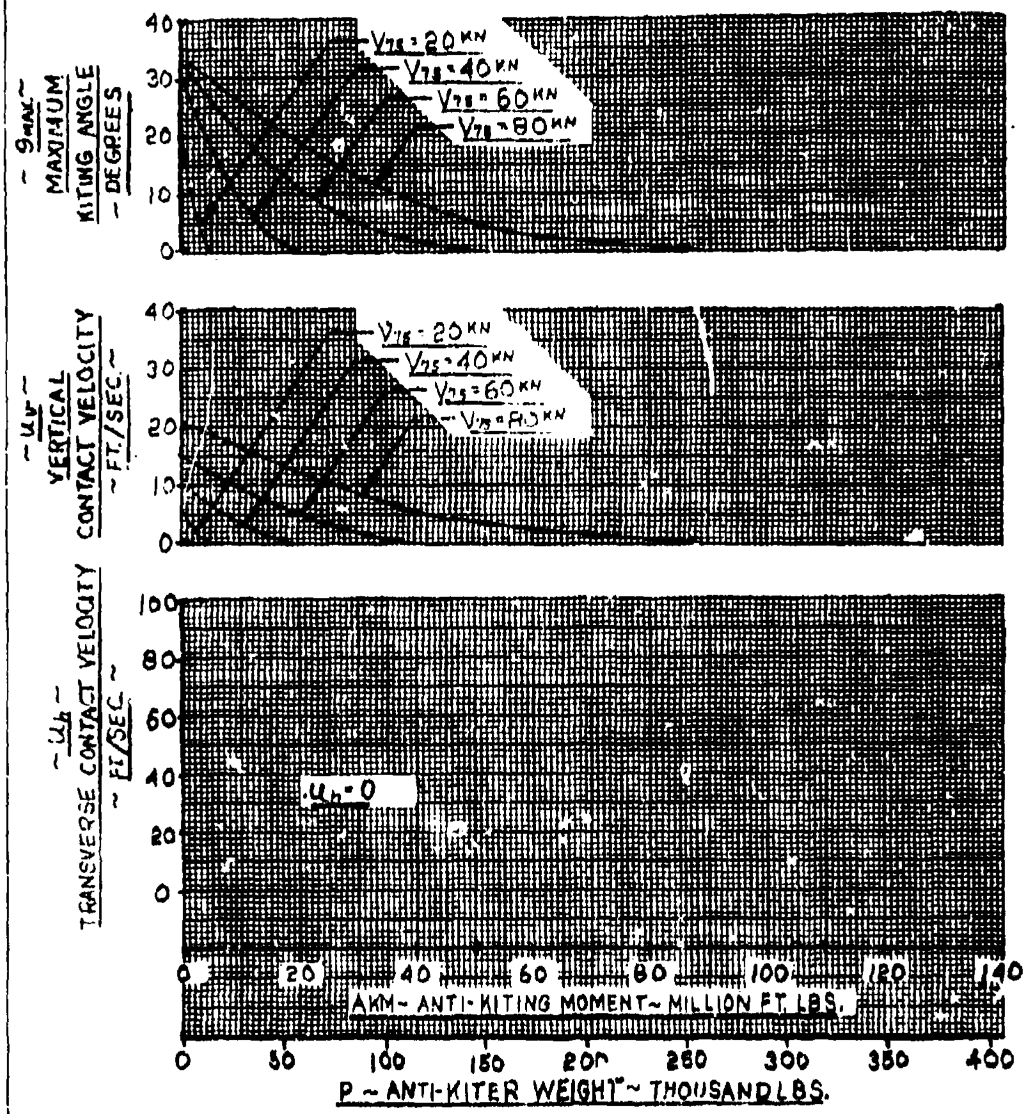

FIGURE 25
ZPG-3W AIRSHIP WITH IMPROVED ANTI-KITER ATTACHMENT SYSTEM
MAXIMUM KITING ANGLES & CONTACT VELOCITIES
180° EQUIVALENT SUDDEN WINDSHIFT

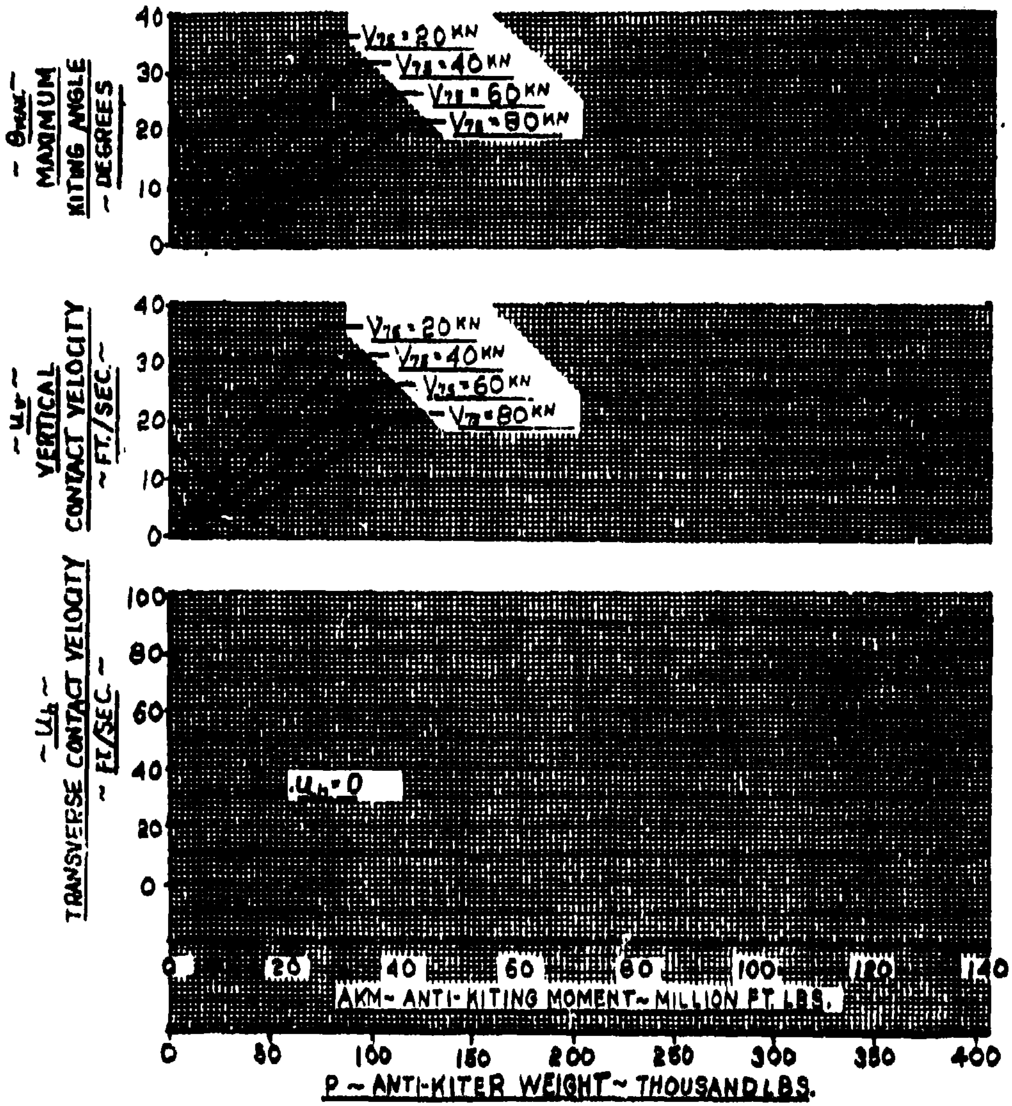

FIGURE 26
ZPG-2/2W AIRSHIP WITH CONVENTIONAL ANTI-KITER
MAXIMUM KITING ANGLES & CONTACT VELOCITIES
30° EQUIVALENT SUDDEN WINDSHIFT

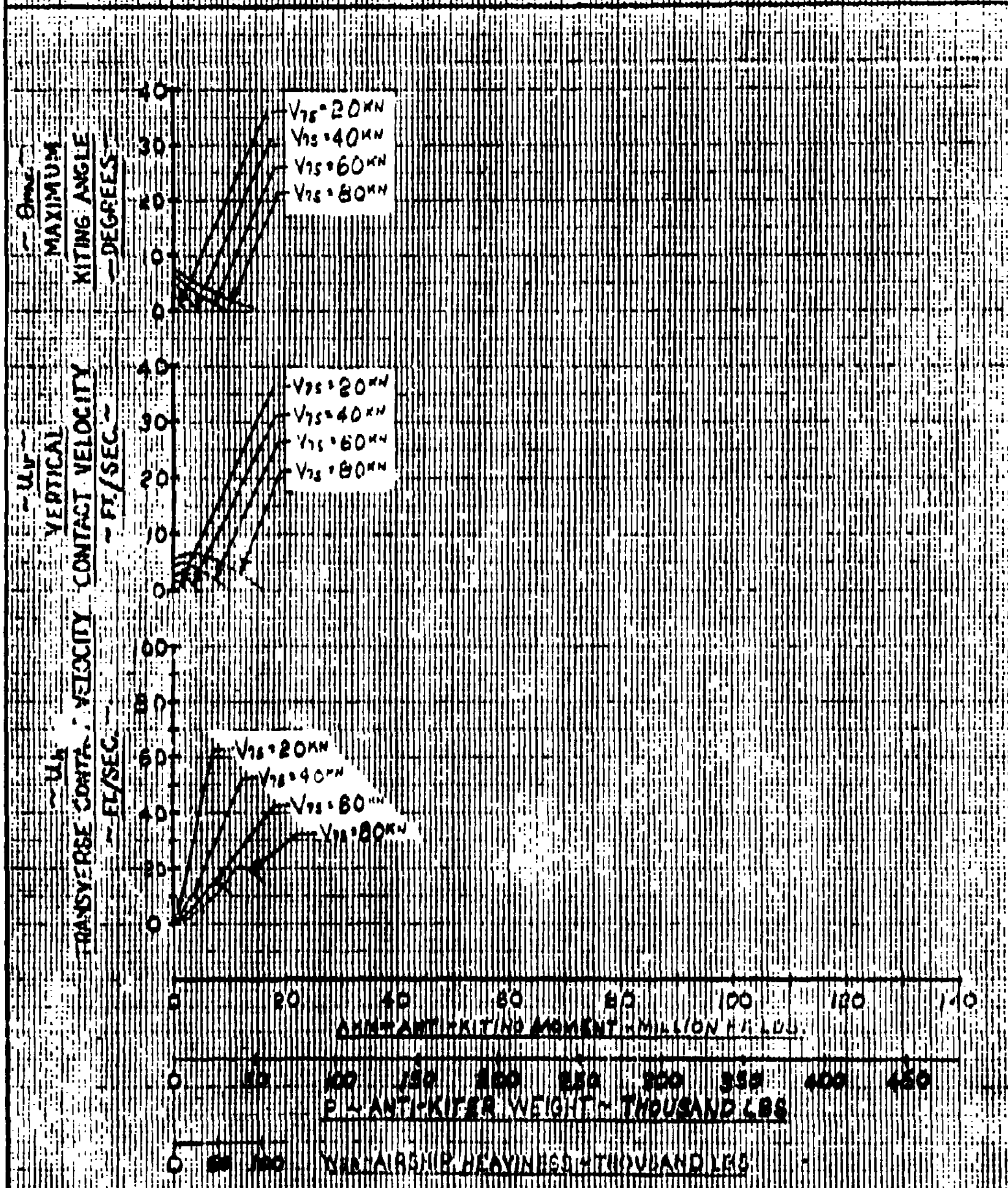

PREPARED BY J.D.M.
CHECKED BY J.W.H.
DATE May 1, 19
REVISED

GOODYEAR AIRCRAFT

PAGE 72
MODEL ZPG-2 ... 3/3W
REF. NO. ... 500

FIGURE 27
ZPG-2/2W AIRSHIP WITH CONVENTIONAL ANTI-KITER
MAXIMUM KITING ANGLES & CONTACT VELOCITIES
80° EQUIVALENT SUDDEN WINDSHIFT

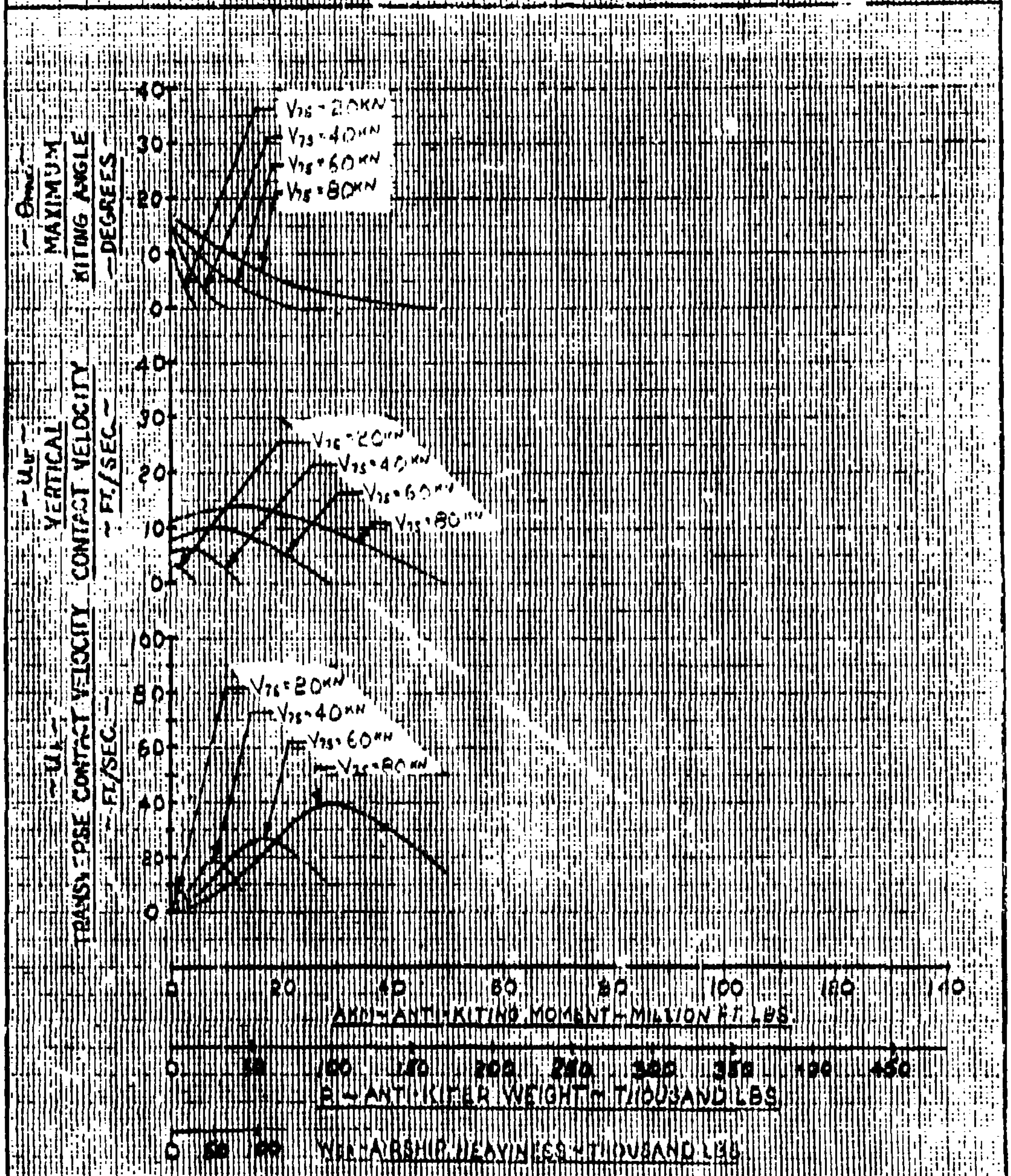

FIGURE 28
ZPG-2/2W AIRSHIP WITH CONVENTIONAL ANTI-KITER
MAXIMUM KITING ANGLES & CONTACT VELOCITIES
VS. EQUIVALENT SUDDEN WINDSHIFT

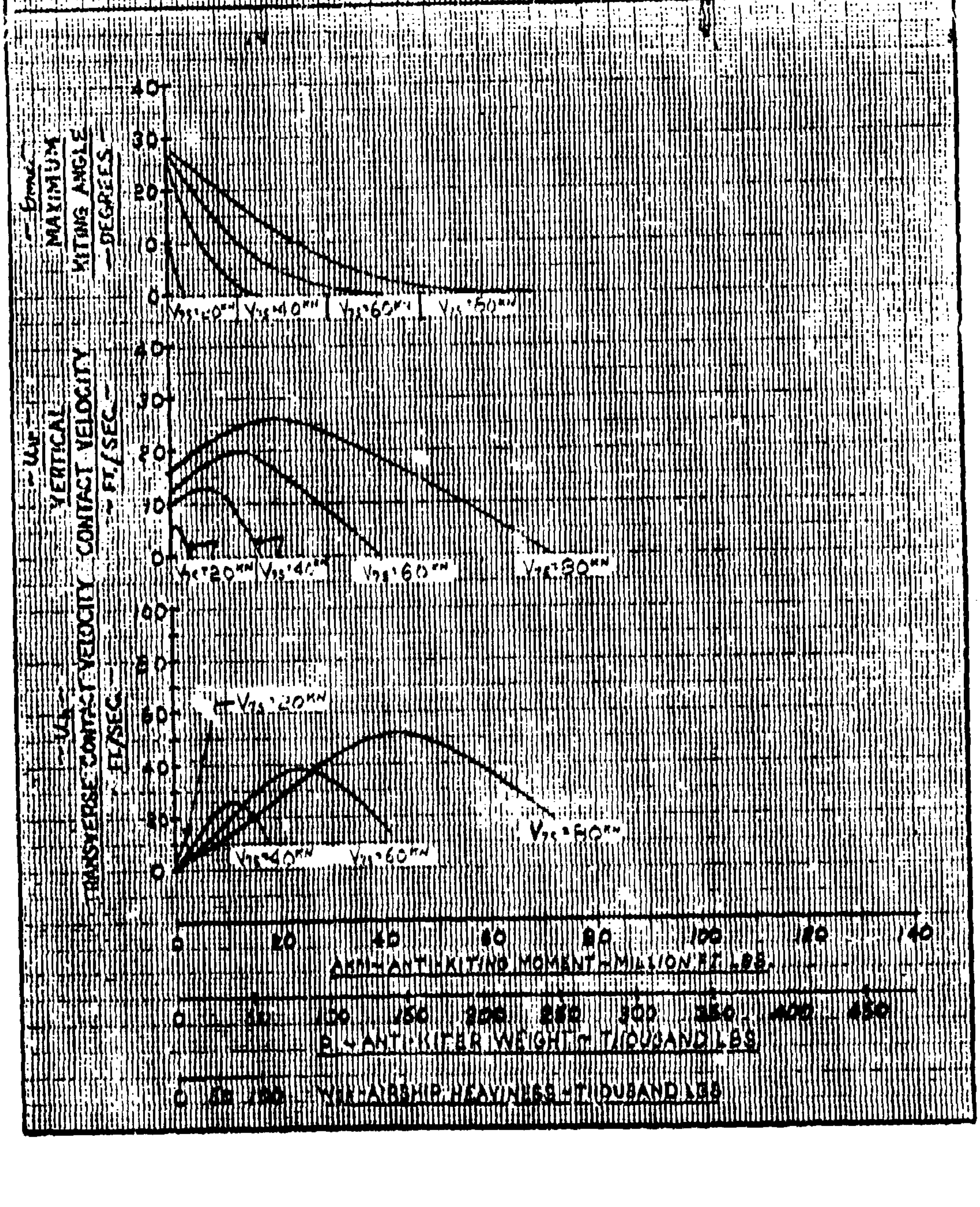

FIGURE 29
ZPG-2/2W AIRSHIP WITH CONVENTIONAL ANTI-KITER
MAXIMUM KITING ANGLES & CONTACT VELOCITIES
120° EQUIVALENT SUDDEN WINDSHIFT

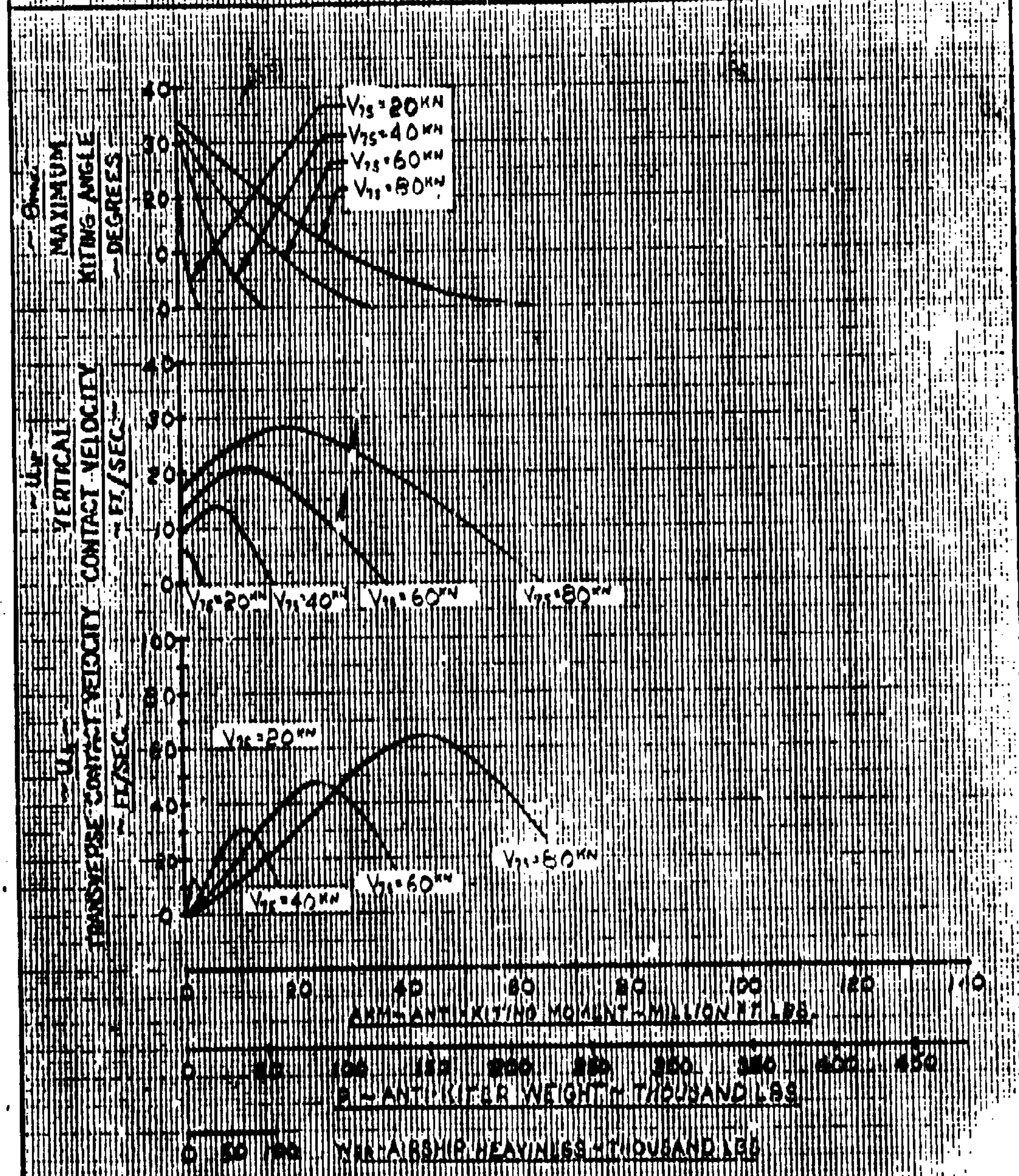

PREPARED BY J. D. M.
CHECKED BY J. W. B.
DATE May 1, 1961
REVISED

GOODYEAR AIRCRAFT

PAGE 80
MODEL ZPG-2/2W/3W
SER 10052
REF NO. Code 25500

FIGURE 30
ZPG-2/2W AIRSHIP WITH CONVENTIONAL ANTI-KITER
MAXIMUM KITING ANGLES & CONTACT VELOCITIES
(60° EQUIVALENT SUDDEN WINDSHIFT)

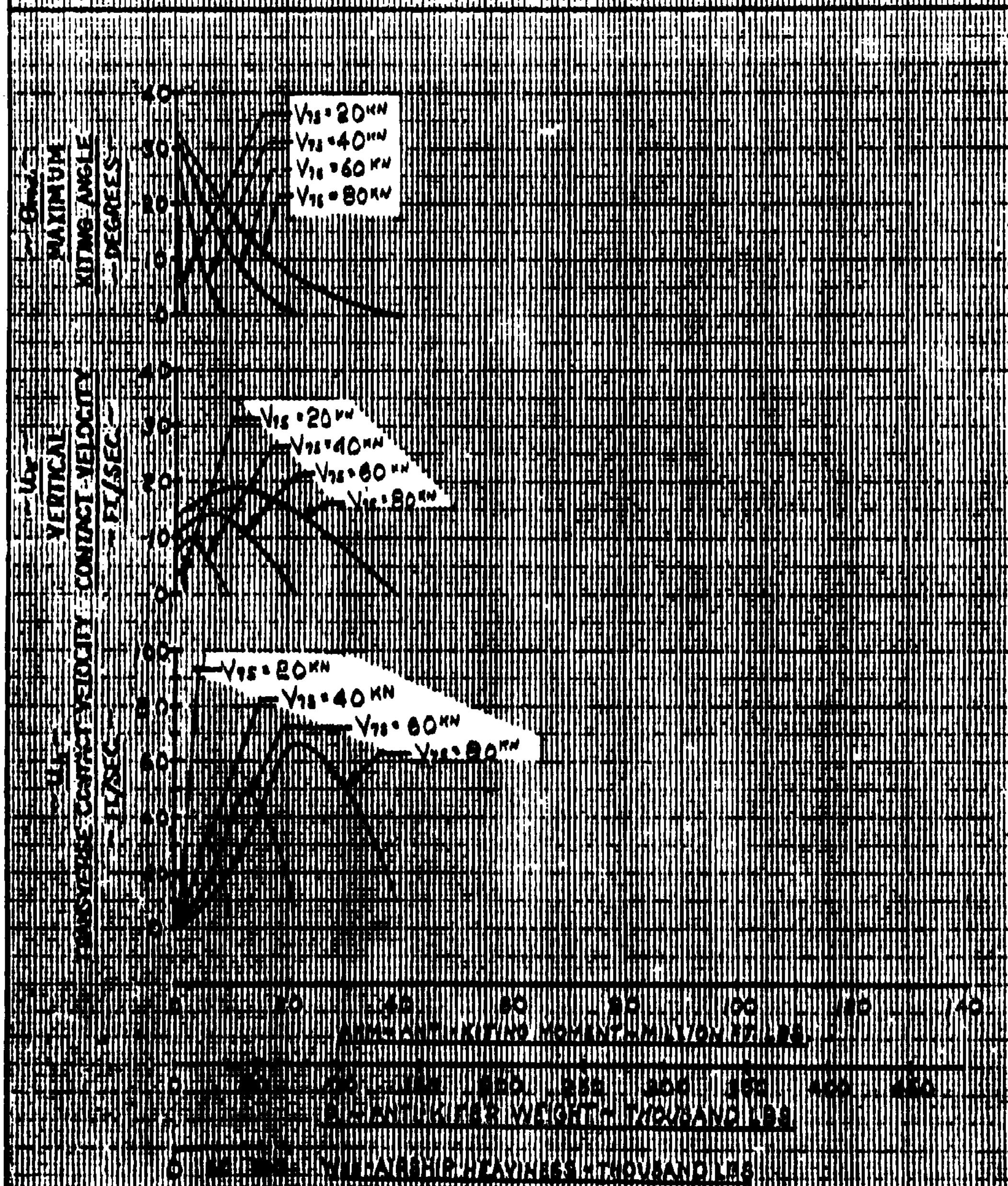

PREPARED BY J.D.M.
CHECKED BY J.W.B.
DATE May 1, 1961
REVISED

GOODYEAR AIRCRAFT

PAGE 81
MODEL ZPG-2/2W/3W
GER- 10052
REF NO. Code 25500

FIGURE 31
ZP3-2/2W AIRSHIP WITH CONVENTIONAL ANTI-KITER
MAXIMUM KITING ANGLES & CONTACT VELOCITIES
180° EQUIVALENT SUDDEN WINDSHIFT

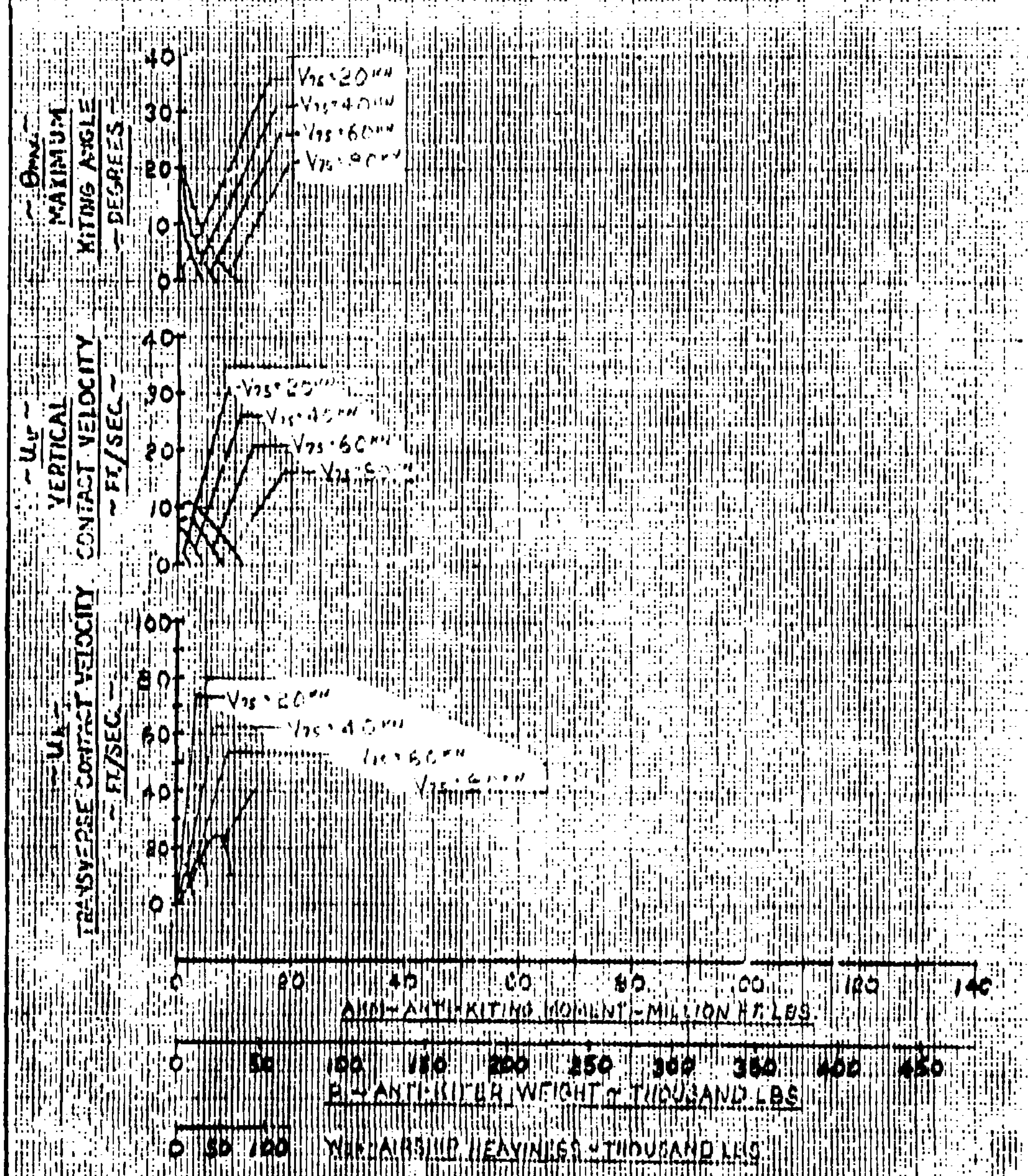

PREPARED J.D.M. | GOODYEAR | PAGE 82
CHECKED J.W.B. | GOODYEAR AIRCRAFT CORPORATION | MODEL ZPG-2/2W/3W
DATE May 1, 1961 | | GER- 10052
REV DATE | | CODE 25500

FIGURE 32
ZPG-2/2W AIRSHIP WITH IMPROVED ANTI-KITER ATTACHMENT SYSTEM
MAXIMUM KITING ANGLE AND CONTACT VELOCITIES
30° EQUIVALENT SUDDEN WIND SHIFT

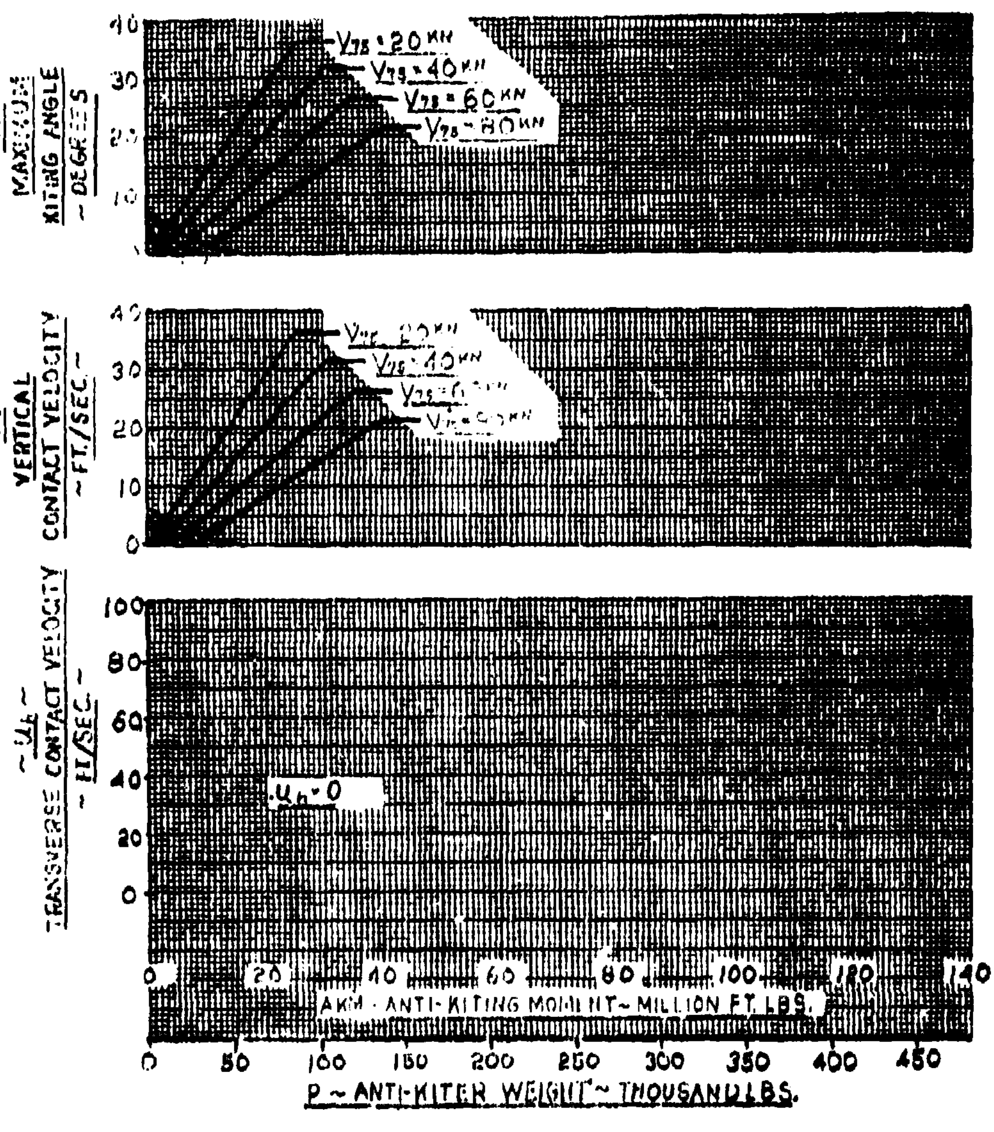

PREPARED J. D. K.
CHECKED J. W. B.
DATE May 1, 1961
REV DATE

GOODYEAR
GOODYEAR AIRCRAFT CORPORATION

PAGE 89
MODEL ZPG-2/2W/3W
GER- 10452
CODE 25500

FIGURE 33

ZPG-2/2W AIRSHIP WITH IMPROVED ANTI-KITER ATTACHMENT SYSTEM
MAXIMUM KITING ANGLES & CONTACT VELOCITIES
60° EQUIVALENT SUDDEN WINDSHIFT

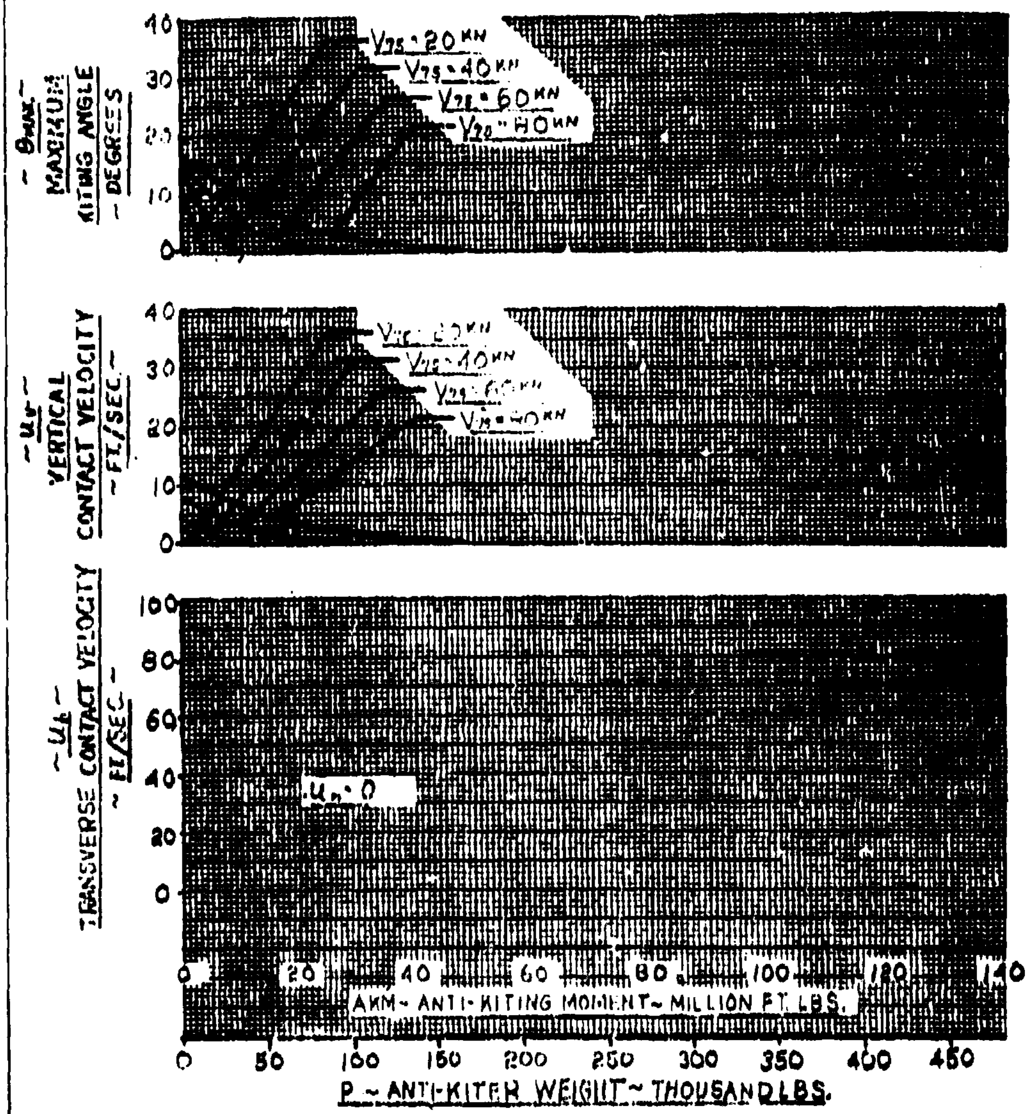

FIG. E-34
ZPG-2/2W AIRSHIP WITH IMPROVED ANTIKITER ATTACHMENT SYSTEM

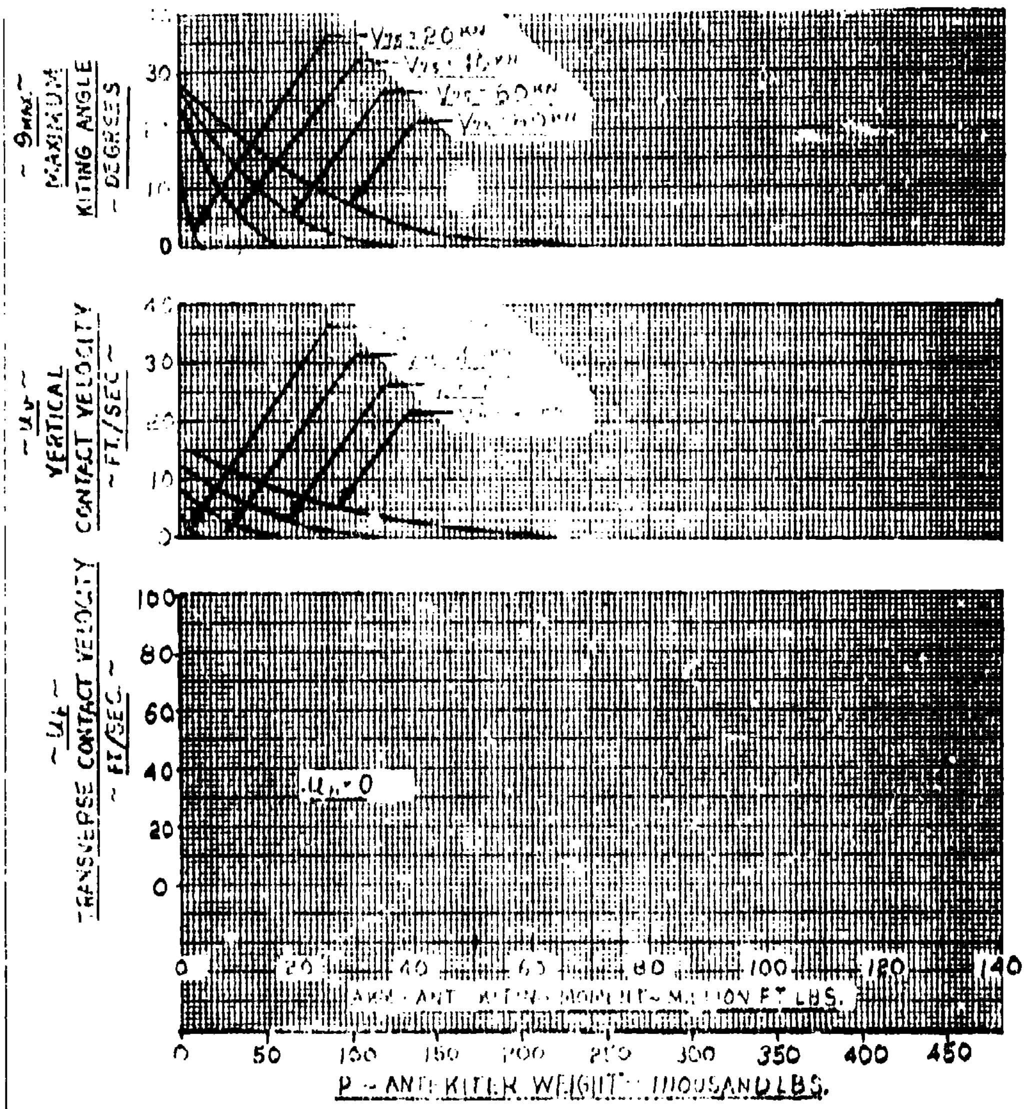

FIGURE 35

ZPG-2/2W GROUP WITH IMPROVED ANTI-KITER ATTACHMENT SYSTEM

MAXIMUM KITING ANGLES & CONTACT VELOCITIES

[illegible]

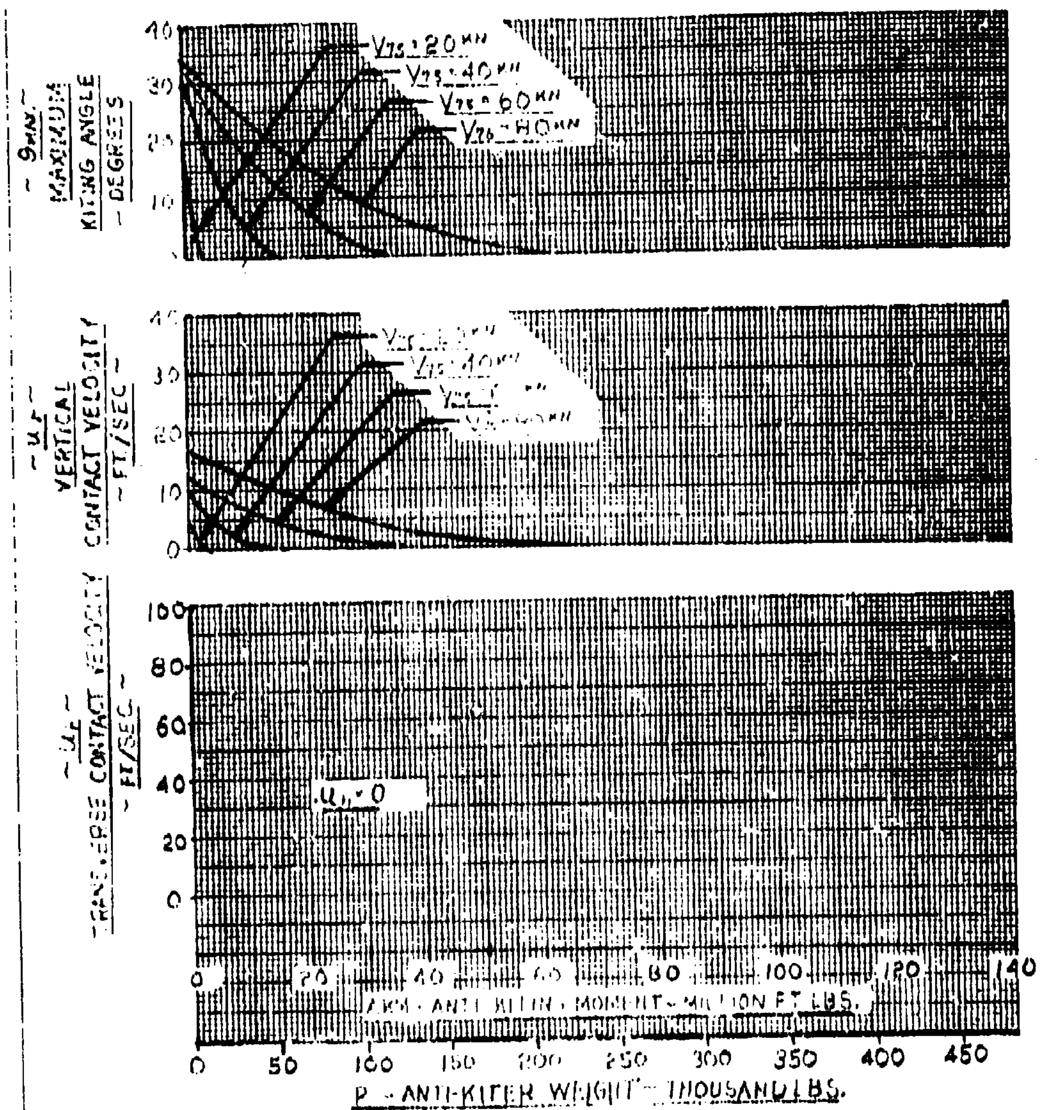

FIGURE 36
ZPG-2/2W AIRSHIP WITH IMPROVED ANTI-KITER ATTACHMENT SYSTEM
MAXIMUM KITING ANGLES & CONTACT VELOCITIES
150° EQUIVALENT SUDDEN WINDSHIFT

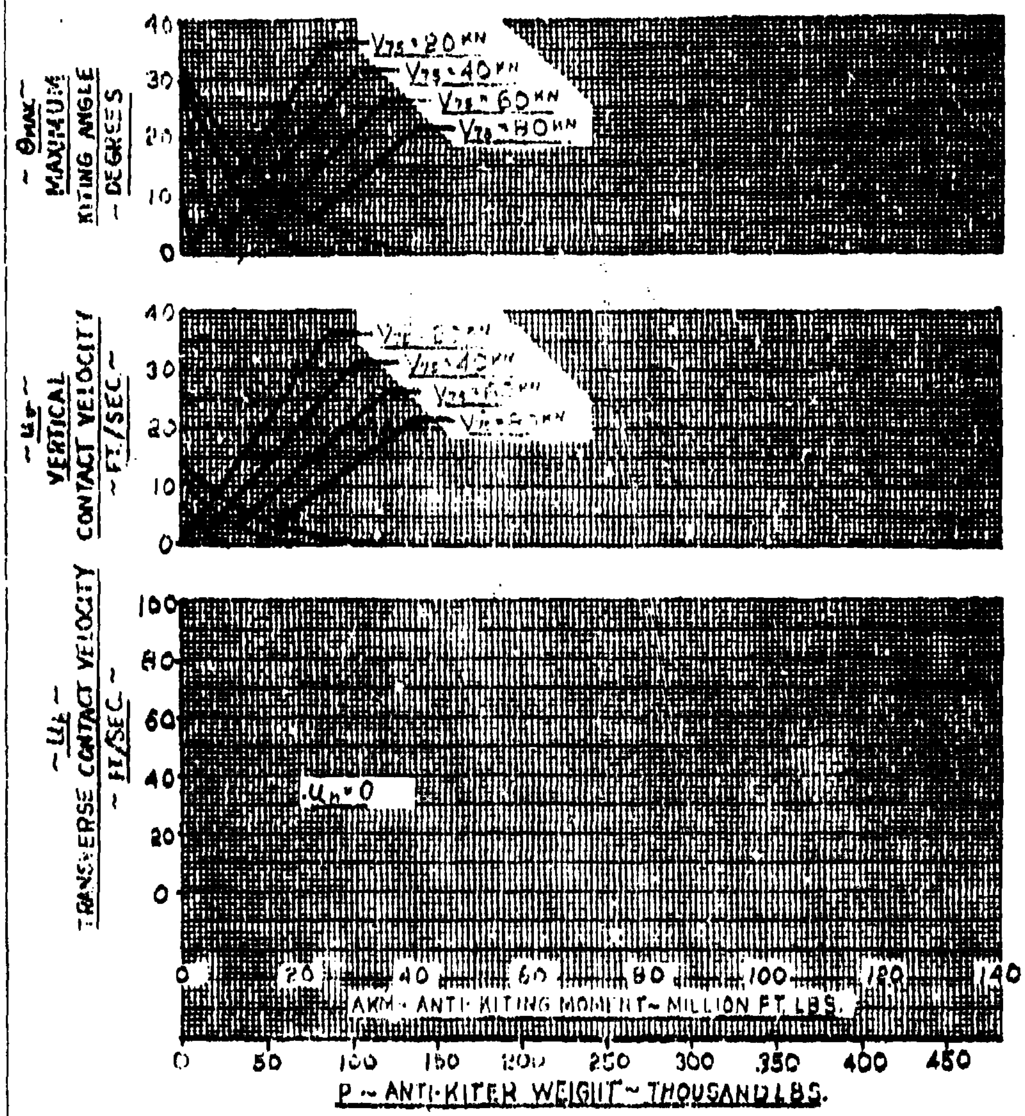

FIGURE 37
ZPG-2/2W AIRSHIP WITH IMPROVED ANTI-KITER ATTACHMENT SYSTEM
MAXIMUM KITING ANGLES & CONTACT VELOCITIES
180° EQUIVALENT SUDDEN WINDSHIFT

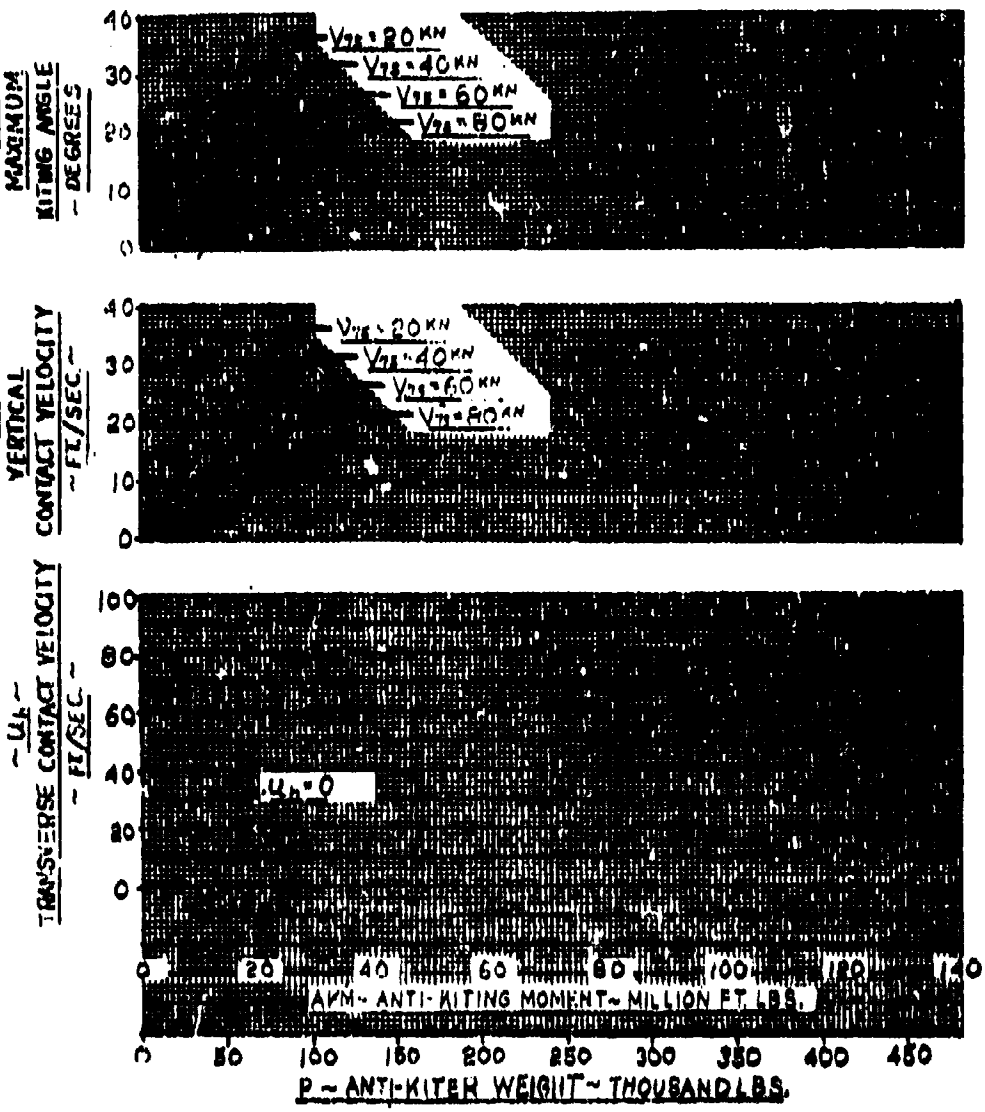

UNCLASSIFIED

UNCLASSIFIED